Scottish Universities Research and Reactor Centre

An Airborne Gamma-Ray Spectrometry Survey of Nuclear Sites in Belgium

D.C.W. Sanderson, A.J. Cresswell, S. Murphy, J.J. McLeod

January 2001

SUMMARY

An Airborne Gamma Spectrometry (AGS) survey was conducted to establish the contemporary radiation environment of the Belgian nuclear sites of Mol-Dessel and Fleurus. The project was commissioned jointly by the Belgian Nuclear Research Centre (SCK-CEN) near Mol, and the National Institute for Radioelements (IRE Fleurus) as part of a contract under NIRAS/ONDRAF, the authority responsible for the management of radioactive wastes arising from nuclear sites. The survey was conducted in May 2000 by the SURRC AGS team using a twin-engined AS355 aircraft equipped and tested in the UK and transferred to Belgium for the survey.

The site near Mol in northern Belgium incorporates a complex of nuclear facilities operated by the Belgian Nuclear Research Centre (SCK-CEN), Belgoprocess, Belgonucléaire, and FBFC International. The complex also includes a non-nuclear technical research centre, VITO, operated by the Flemish authorities. The European Commission's Joint Research Centre - Institute for Reference Materials and Measurements (IRMM) is located south-west of SCK-CEN, near Geel. The Institut National des Radioelements (IRE) is located at Fleurus near Charleroi, south of Brussels. The aircraft arrived on the 9th May and completed the survey of the Mol-Dessel area on the 10th-11th May. The IRE site at Fleurus was surveyed on the 12th May and the aircraft returned to the UK the following day.

More than 12000 spectra were recorded using a 16 litre NaI(Tl) and approximately 6000 spectra were recorded with a 50% efficiency Ge (GMX) spectrometer during the survey together with positional information from GPS and ground clearance data from radar altimetry. The results were used to prepare radiometric maps of ^{137}Cs, ^{60}Co, ^{40}K, ^{214}Bi and ^{208}Tl activity, along with the total gamma-ray dose rate for each of the survey areas, which together with spectral information can be used to evaluate the radiometric impact of each site. The natural radiation background levels observed in the areas are typical of radiometric surveys, the Mol-Dessel area having generally lower levels than the Fleurus area. The data sets reveal a variety of signals associated with the nuclear sites, representing known sources of radioactivity or radiation from materials contained onsite, varying in response to the type of operation and radioactivity on each site. Small signals observed at IRMM are characteristic of machine sources, with high energy components and annihilation radiation present. Those at FBFC are associated with uranium and MOX fuel materials, which give rise to signals from ^{234m}Pa, ^{214}Bi and 662keV radiation. The SCK-CEN complex produced a range of signals including ^{41}Ar from the BR1 reactor, and ^{134}Cs from agricultural research plots to the west of the site. The Belgoprocess sites produced a range of signals including ^{137}Cs and ^{60}Co from stored materials on both sites, and ^{214}Bi signals, mainly from ^{226}Ra. At the IRE site small anomalies associated with ^{99}Mo and ^{131}I were observed. The gamma dose rate maps show the relative importance of the anthropogenic radiation fields on the nuclear sites and their surroundings. The spatial distribution and nature of these signals is highly consistent with expectations based on the types of operation taking place within the sites.

The data sets serve as a reference against which future changes can be measured. Whether in response to an internal or external event, or simply as part of a regular series of campaigns to document the changing environments of the sites, as new construction and decommissioning of old plant, or development of new waste-management approaches take place, it would be possible to repeat this survey rapidly to document change.

ACKNOWLEDGEMENTS

The survey was commissioned jointly by the Belgian Nuclear Research Centre (SCK-CEN) near Mol, and the National Institute for Radioelements (IRE Fleurus) as part of a contract with NIPAS/ONDRAF. We are grateful for the support given by Ir Mark Loos, Dr Frank Hardeman, and Dr Carlos Rojas-Palma of SCK-CEN and by Dr Antoine Debauche of IRE for initiating and coordinating the project, and for their support in general. We are also grateful for the support and cooperation given to the survey by Dr Walter Blommaert of Belgoprocess, Freddy Goens of FBFC, and Dr Luc Peeters of IRMM and Ir Mark Van Reusel of VITO. We appreciate the practical support support given by SCK-CEN and IRE for provision of office accommodation and for facilitating the airborne operations.

We are also greateful to PDG Helicopters for their support with aircraft engineering, operations support and especially Dominic Lawlor for making arrangements for transfer of the aircraft and systems to Belgium with appropriate permissions from the Belgian aviation authorities to conduct the low level operations in the survey areas. We are particularly grateful to John Constable for his expert contribution to the project, which resulted in a safe, highly efficient and accurate survey operation.

CONTENTS

APPENDICES

FIGURES

APPENDIX C

TABLES

APPENDIX A

1. INTRODUCTION

This report documents the results of an airborne gamma-ray survey conducted by the Scottish Universities Research and Reactor Centre (SURRC) on behalf of the Belgian Nuclear Research Centre (SCK-CEN), located near Mol in the north of Belgium and the National Institute for Radioelement (IRE), located further south near Fleurus. The project was financed by NIRAS-ONDRAF. The objective of the study was to establish the contemporary radiation environment of nuclear sites of Mol-Dessel and Fleurus, using airborne gamma ray techniques. In particular the specific activities of naturally occurring isotopes (^{40}K, ^{214}Bi, ^{208}Tl), anthropogenic ^{137}Cs and ^{60}Co, and the dose rate at ground level were to be mapped using AGS techniques, and the results related to established calibration sites.

The survey was conducted using a UK helicopter deployed between the 8th and 13th of May 2000. The system was installed, tested and pre-calibrated prior to routing to Belgium on the 8th May, arriving on the 9th May. The survey was conducted between 10th and 12th May, the aircraft returning directly thereafter. This report gives details of the AGS method, the survey areas, deployment, calibration and field work together with a presentation of the radiometric maps produced for the nuclides specified above. Further technical information is provided in appendices, including details of individual sites.

1.1 Airborne Gamma Spectrometry (AGS)

The airborne gamma spectrometry (AGS) method is highly appropriate for large scale environmental surveys of areas of potentially contaminated ground. The methodology for aerial surveys is well established (Sanderson *et al*, 1994a, 1994b), and has been used by the SURRC team for a variety of purposes including environmental assessments of contamination (Sanderson *et al*, 1990a, 1990b); Chernobyl fallout mapping (Sanderson *et al*, 1989a, 1989b, 1990c, 1994c); baseline mapping around nuclear establishments (Sanderson *et al*, 1990d, 1992, 1993b, 1994d); the effects of marine discharges on coastal environments (Sanderson *et al*, 1994c); epidemiological studies (Sanderson *et al*, 1993a); and radioactive source searches (Sanderson *et al*, 1988b, 1991). In addition, the technique has been used by airborne survey teams from Scandinavia, Germany and France and other countries.

By operating suitable spectrometers from low flying aircraft, in this case a helicopter, it is possible to map the distribution of gamma-ray emitting radionuclides at ground level. This has a number of advantages when compared with conventional methods. High sensitivity gamma-ray detectors installed in the aircraft are capable of making environmental radioactivity measurements every few seconds, thus providing a sampling rate some 10^2-10^3 times greater than other approaches. The radiation detector averages signals over fields of view (Tyler *et al,* 1996a) of several hundred metre dimensions, resulting in area sampling rates some 10^6-10^7 times greater than ground based methods. Sequences of gamma-ray spectra, geographic positioning information and ground clearance data are recorded, and are used to quantify levels of individual radionuclides and the general gamma-dose rate. The high mobility of the aircraft is also advantageous, as is its ability to operate over varied terrain, unimpeded by ground level obstacles or natural boundaries. Moreover, the remote sensing nature of the measurements minimises exposure of survey teams to contamination or radiation hazards. This results in a practical means of conducting surveys with total effective coverage, which can be used for rapid location of point sources or areas of radioactive contamination. This has important implications for environmental radioactivity studies, especially where there are time constraints, and is highly significant in emergency response situations.

The SURRC team has also utilised a combined detector system, utilising both a 16 litre NaI(Tl) detector and one or two cryogenically cooled germanium (Ge) semiconductor detectors, for airborne radionuclide monitoring. Whilst the use of NaI(Tl) detectors is well established and used frequently in airborne surveys, the use of Ge detectors is relatively new. Ge detectors have a much higher energy resolution than the NaI(Tl) scintillator detector, and so are better able to identify the nuclides contributing to the gamma ray spectrum, particularly where complex fission product sources are present. However, they are considerably less sensitive than NaI(Tl) requiring the use of longer integration times with a resulting loss of spatial resolution in all but the most active environments. In the current work a single 50% efficiency Ge (GMX) detector mounted inside the aircraft was used.

1.2 The Survey Areas

The survey area comprised the nuclear site complex near Mol, and the environment of the IRE site near Fleurus. Figure 1.1 indicates the location of these sites, showing some of the facilities and institutes at each site.

The site near Mol, approximately 80km north east of Brussels, is a complex of several nuclear facilities. The site is occupied by a number of institutes: (i) the Belgian Nuclear Research Centre (SCK-CEN) is primarily concerned with research into nuclear safety, waste management and radiation protection, and its facilities include research reactors and laboratories handling radioactive materials; (ii) Belgoprocess specialises in radioactive waste management and decommissioning of nuclear facilities; (iii) Belgonucléaire produces mixed oxide (MOX) fuel material; and (iv) FBFC International is a fuel fabrication plant making uranium fuel elements and assembling MOX fuel elements. The European Commission's Joint Research Centre - Institute for Reference Materials and Measurements (IRMM) is located approximately 5km south west of the SCK-CEN site, and is a centre of excellence for measurement sciences with a number of nuclear facilities including accelerators. The location of the principal facilities and institutes within the Mol area are included in figure 1.1. Permission was granted to over-fly all areas, with the exception of the Belgonucléaire site, subject to constraints agreed with individual site safety officers.

The facilities of SCK-CEN which could be expected to have radiometric signals include three research reactors: BR1, a 700kW air-cooled graphite moderated reactor which discharges gaseous ^{41}Ar while operating; BR2, a high flux materials research reactor, which is licensed to operate at approximately 100 MWt; and BR3, a PWR in process of decommissioning. Other facilities include various laboratories handling radioactive materials, and several small plots of land deliberately contaminated with ^{137}Cs, ^{134}Cs and ^{85}Sr (which has subsequently decayed to very low levels) to investigate radionuclide uptake by plants.

Belgoprocess occupies two sites in the complex, handling and storing a wide variety of radioactive materials including those derived from the nuclear fuel cycle and from decommissioning. There is a considerable quantity of waste material stored on these sites in well shielded buildings, although there is some discharge of ^{222}Rn gas from ^{226}Ra and uranium-series wastes through filtration systems.

The FBFC International site is concerned with nuclear fuel fabrication, based on uranium in oxide forms, and on MOX. Materials on site include depleted, natural and enriched uranium. MOX-fuel elements are assembled in one building, starting from fuel rods. Other buildings, containing fissile material, are associated with storage and/or production of nuclear fuel based on uranium.

The IRMM site has both electron LINAC and Van de Graaff accelerators, as well as a range of radiochemical laboratories, stores and other non-active buildings. The 150 MeV linear accelerator incorporates a Bremsstrahlung target resulting in neutron production from subthermal energies to 20 MeV. The two Van de Graaff accelerators produce mainly charged particle beams, which are mostly used for neutron production by interaction with low atomic number targets. Thus, in addition to the high energy photons associated with these machines, there is potential for production of a wide range of activation products, some of which may be detectable, depending on the configuration of local shielding to radiation directed upwards.

The VITO laboratories are located both in the same complex as SCK-CEN, and in the vicinity of IRMM.

The Institut National des Radioelements (IRE) is situated at Fleurus near Charleroi. The site includes a number of irradiation and radiochemical facilities. A large ^{60}Co irradiator on the north east side of the complex is used for medical sterilisation and, irradiation of materials and foodstuffs. Two cyclotrons of 100 MeV and 30 MeV are used for radioisotope production. Radiochemical laboratories and associated waste storage facilities are used to prepare a range of
isotopic products including radio-pharmaceutical tracers, mainly ^{99}Mo for which IRE is the second producer in the world (first in Europe). The location of some of these facilities is also included in figure 1.1.

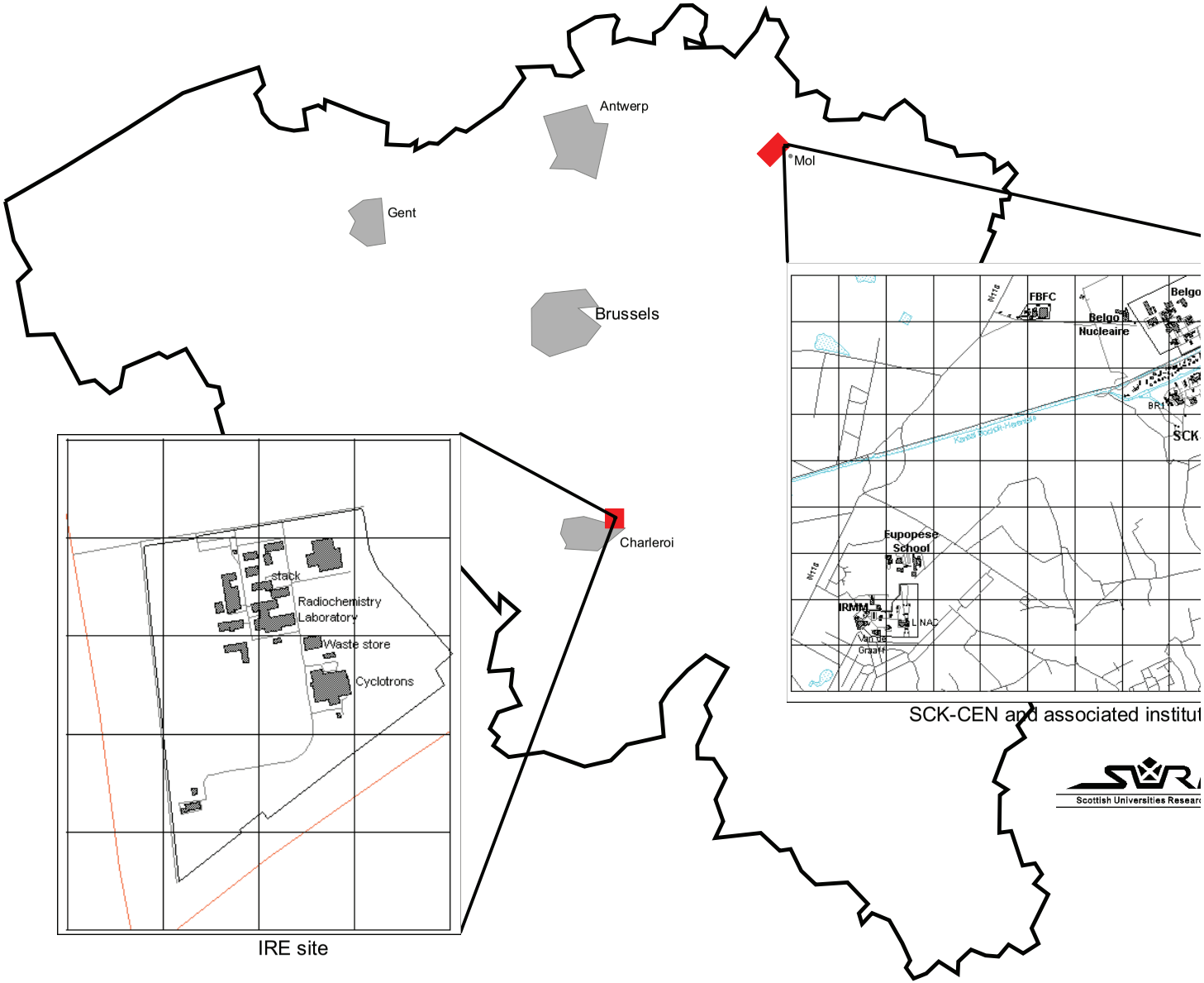

Figure 1.1 Map showing the location of the institutes and facilities surveyed in this work.

2. METHODOLOGY

2.1 Instrumentation

The AGS system used consisted of a high volume 16 litre thallium doped sodium iodide (NaI(Tl)) spectrometer, a single 50% efficiency Ge semiconductor (GMX) detector, an electronics rack containing power supplies, nucleonics and computer, and two GPS systems consisting of a Navstar DGPS4 unit and a Garmin unit. Both were differentially corrected using an FM carrier wave DGPS correction service (based on an RDS 3000 receiver). The local DGPS service was provided by Geometius NV from The Netherlands. The Navstar unit, which was attached to the electronic rack and connected to the logging computer, was used to log aircraft position at the start and end of each spectrum recorded. The Garmin unit was programmed with waypoints for the survey grids and used by the pilot for navigation. The aircraft used was a twin engine AS355 Squirrel helicopter, supplied by PDG Helicopters, and fitted with a radar altimeter, and appropriate auxiliary power supplies. All equipment was mounted on custom built base plates approved by the appropriate aviation authority. A video camera was fitted on the inside of the aircraft, looking downward through the front window bubble in front of the electronics rack. This records a continuous record of each flight, from which a total video track or images of selected features could be extracted.

2.2 Installation, Testing and Deployment for Survey

The equipment consisting of the combined system of NaI(Tl) and Ge detector and associated instrumentation was installed in the helicopter at Cumbernauld airport, Scotland on the 8th May, and tested prior to deployment for the survey. An initial test flight at Cumbernauld confirmed the correct functioning of all components, the radar altimeter calibration, and working values for the aircraft background. The aircraft routed to the Solway Firth for calibration manoeuvres early in the afternoon of the 8th May, the remainder of the technical team travelling by car to the calibration site.

Calibration manoeuvres were conducted on route to Belgium and again during the return flight over the salt marshes at Caerlaverock on the Solway Firth in SW Scotland. These consisted of measurements recorded while hovering at a series of altitudes above a calibration pattern consisting of concentric hexagons at 8, 32, 128 and 256m from the central point. Cores were collected from this site in February 1992 (Sanderson *et al*, 1992) and April 1999 (Sanderson *et al*, 2000). Data from these manoeuvres was used to determine altitude correction and sensitivity calibration factors before the start of survey.

Having verified the calibration, the aircraft together with one operator continued to route towards Belgium, overnighting in Kent, clearing customs in the UK on the morning of the 9th May, and in Antwerp in the middle of the day, arriving at the SCK-CEN site in the afternoon. The remaining two team members travelled by air to Brussels on the 8th May, and established the data processing facilities at SCK-CEN on the morning of the 9th May prior to aircraft arrival.

In this manner, a fully functional AGS system and ground station was established at SCK-CEN one day after deployment from SURRC. The DGPS service used in the UK was supplied by a different operator than that available in Belgium. Minor difficulties were experienced in getting the RDS3000 unit to transfer from the UK operator to the network managed by Geometius. This turned out to be due to the presence of a high sided metal building directly adjacent to the landing site, which was blocking the registration transmissions from being received on site. Having substituted antennae, and an alternative RDS unit, this was overcome in time for the Charleroi survey. Fortunately, however, the quality of GPS location achieved at Mol (typically 5-15 m depending on satellite configuration) was comparable with that achieved near Charleroi (typically 4-12 m depending on satellite configuration), since the US Department of Defence had in any case discontinued the Selective Availability function approximately two weeks prior to start of survey.

Prior to start of survey, a safety briefing was held to allow the pilot, Captain John Constable, and the safety representatives of the nuclear sites to discuss specific areas of concern within the nuclear sites, and how best to conduct the surveys. It was decided at this meeting to conduct reconnaissance flights early on the 10th May with the safety representatives on board the aircraft to identify hazardous areas to the pilot. Data were collected over the individual sites during these flights, and the rest of the survey conducted according to pre-planned navigational routes thereafter. The area surveys in Mol were successfully completed on the 10th and 11th May, despite a severe electrical storm in the afternoon and evening of the 10th May. Initial survey results, including a demonstration of the spectral analysis, and maps were presented to sponsors on the 11th May.

The aircraft was transferred to IRE Fleurus on the morning of the 12th May, with the ground support team travelling by car. Following initial briefings at IRE, the survey was conducted in the evening of the 12th May, with short demonstration flights being concluded on the 13th. The aircraft cleared Belgium customs at midday at Charleroi, and returned to Cumbernauld the same day, repeating calibration measurements at the Caerlaverock site en-route.

2.3 Measurement Procedure

The procedures specified and used for this survey work were based on normal practice in environmental airborne gamma spectrometry (Sanderson *et al* 1994a,b). The NaI(Tl) spectra were initially reduced into standard energy windows corresponding to nuclides which are frequently encountered in environmental surveys. The calibration procedures are based on standard models for the response (Allyson *et al* 1998), and traced to spatially representative calibration sites (Tyler *et al* 1996a, Sanderson *et al* 1997a,b) of known mass depth (Tyler *et al* 1996b). It should be realised however that in the vicinity of nuclear sites and similar facilities there may be other isotopic or radiation features present, and local deviations from open field geometries. The effects of spectral interferences to isotope identification, and of finite or collimated geometries, and local shielding, on quantitative estimates need to be considered in interpreting data and maps generated in this way.

The detector system performance (gain, resolution and sensitivity) was checked at the start of each day, and trimmed as necessary. Background measurements were made over open water at least once each day. During flight the NaI(Tl) detector gain was monitored by using the ^{40}K peak at 1462 keV. Spectra were recorded from the NaI(Tl) spectrometer with a 2s integration time, and 4s for the GMX detector. Files containing 2 NaI(Tl) spectra and one GMX spectrum were written to disk, together with timing information, GPS positioning data and time-averaged radar altimetry data.

Summary files, consisting of gross count rates for 6 windows (corresponding to energies normally associated with ^{137}Cs, ^{60}Co, ^{40}K, ^{214}Bi, ^{208}Tl and total gamma-dose rate) were produced from the data after each survey flight. The windows used for these measurements are given in Appendix A, Table A.1. All data were backed up onto duplicated ZIP disks at the end of each day, and restored to a separate computer for verification. Spectral data were examined, using software to "replay" the flight, to verify that restored data could be read, prior to deletion of primary data from the logging computer in the aircraft. The combination of the duplicate backup and verification procedures was designed to minimise the probability of data loss through media failure.

Initial analysis was conducted on site to check the quality of the data from each flight, and to identify any lines requiring re-surveying while the aircraft was available. This included using the spectral replay facility to confirm the continuity of data streams, the energy calibration and resolution, and the presence of spectral anomalies such as strong radiometric signals, time-varying components (for example due to the noble gas ^{41}Ar), or noise contributions such as the presence of small microphonic signals from the semiconductor detector during aircraft turns. Initial flight maps were produced, and updated after each flight, to verify the aircraft flight paths, and to visualise the distribution of radiometric features.

2.4 Data Analysis

The sequence of data reduction conducted both in the field, and retrospectively, proceeds by firstly subtracting an appropriate background from each observation, separating spectral interferences using matrix stripping procedures, standardising the data to constant ground clearance based on radar altimetry results, and conversion to activity concentration or dose rate using linear calibration functions. These procedures have been described elsewhere (Sanderson *et al* 1994b). During initial data processing the complete data streams were analysed using working values for necessary calibration constants. After the survey was complete the final data set was extracted, removing transit flight legs or data which were outside the working range of ground clearance. Calibration factors were reviewed and the final maps produced.

The daily backgrounds recorded over water, as given in Appendix A, Table A.2, were subtracted from the data in the summary files. For the Mol-Dessel survey these were conducted over large lagoons just to the east of the survey area, and for the Fleurus survey a lake to the south of Charleroi was used. The background includes contributions from cosmic rays, activity within the aircraft, and may also include contamination with uranium series daughters as a result of radon gas disequilibrium. Spectral interferences were stripped out using stripping factors determined from measurements conducted in November 2000 with the NaI(Tl) detector pack placed over a series of calibration pads doped in U, Th and K along with an undoped pad and sheets doped in ^{137}Cs and a ^{60}Co point source. Seven sheets of perspex, equivalent to approximately 70m of air, were placed between the pads and the detector.

The sensitivity and altitude normalisation constants for ^{137}Cs and the naturally occurring ^{40}K, ^{214}Bi and ^{208}Tl were determined from data collected over the Caerlaverock site (Tyler *et al*, 1996b), which has a mean mass depth for ^{137}Cs of 15.7±1.2 g cm^{-2} with uniform depth distributions for the naturals. Because of the lack of measurable levels of ^{60}Co activity on the Caerlaverock site a calibration constant for this isotope could not be determined experimentally, and the activity is given as an altitude-corrected count rate. It has been estimated that an equivalent surface activity of 1 kBq m^{-2} would give a count rate of approximately 14cps in the 16 litre NaI(Tl) spectrometer at a ground clearance of 100m (Sanderson *et al*, 1994e). These altitude and sensitivity calibration factors were then applied to the net stripped data.

The resulting calibrated data for ^{137}Cs (in kBq m^{-2}), ^{60}Co (count rate normalized to 100 m ground clearance), ^{40}K, ^{214}Bi, ^{208}Tl (all Bq kg^{-1}) and the gamma-dose rate (mGy a^{-1}) were mapped for each of the survey areas. The calibrated data were mapped onto the Belgium National Grid, using an algorithm derived from IGN 1989 following a transformation from WGS84 to the Belgium projection as outlined in Appendix B, and a distance weighted smoothing algorithm applied to the data (Sanderson *et al* 1994b). The numerical data set contains more detail than can be expected to be seen in these maps.

The calibration factors were determined assuming a planar source with fairly simple depth profiles. This calibration will not be exact for source distributions which differ significantly from this, for example highly localised or well shielded sources. It should therefore be recognised that the working calibrations are a guide to the locations and variations of radiometric features within the survey area, but do not predict quantitative levels to high accuracy where field conditions differ markedly from the open field geometries and associated activity distribution of the calibration sites. Within this survey area such conditions occur in the built environment of the nuclear sites. Moreover, the area surrounding Mol contain areas of woodland which themselves present the potential for biomass attenuation of natural and anthropogenic nuclides. The approach taken here is to geo-locate the radiometric data so that the radiometric features can be interpreted in their topographic and cartographic contexts.

In addition, 33 cores were taken from a field at the IRE site by IRE staff. These cores were divided into 5cm thick slices, and all the slices from the same depth homogenized. Samples from each depth were put in open marinelli beakers, placed in a shielded geometry and long counting time spectra recorded using Ge detectors. This field has been regularly ploughed, resulting in a uniform depth distribution to a depth of 30cm. A hover manoeuvre was also conducted over this field, and the activity concentration determined using the parameters calculated from the Caerlaverock data. The results for these measurements are given in table 2.1. The agreement between the activities measured by core sampling and the airborne technique is very good, except for the U-series ^{214}Bi which may have been affected by disequilibrium due to Rn migration.

Nuclide	Activity Concentration	
	Core Samples	Airborne Measurement
^{137}Cs (kBq m^{-2})	3.8±0.2	3.2±0.5
^{40}K (Bq kg^{-1})	364±26	373±9
^{214}Bi (Bq kg^{-1})	17.2±1.2	27.7±1.2
^{208}Tl (Bq kg^{-1})	12.8±0.8	11.8±0.3

Table 2.1 Summary of measurements taken from the field at the IRE site

3. RESULTS

The survey of the Mol sites and surrounding areas was conducted during the 10th-11th May. Some 7500 NaI(Tl) and 3750 GMX spectra were recorded over 5½ hours. Figure 3.1 shows the flight track recorded at 15s intervals during these survey flights by the Garmin GPS.

The survey of the IRE site and surrounding areas at Fleurus was conducted on the 12th May. Some 5400 NaI(Tl) and 2700 GMX spectra were recorded over 4 hours. Figure 3.2 shows the flight track recorded at 15s intervals during these survey flights by the Garmin GPS.

The calibration used is based on comparison between altitude corrected stripped counts from the survey area and the calibration response of the system determined in open area conditions on calibration sites. In addition to being sensitive to variations in the mass depth distribution of any sources of deposited activity, there are potential geometrical effects particularly in the built environment of nuclear sites which may affect quantitative response. Where the spatial extent of a radiometric feature is significantly smaller than the field of view of the AGS detector, which is frequently the case in the vicinity of nuclear sites, the AGS system is expected to underestimate equivalent activity. Local shielding compounds this effect but can also lead to changes in the amount of scattered radiation observed and therefore influence spectral stripping. In the case of radioactive gases, including ^{41}Ar and ^{222}Rn, the relationship between airborne and ground based dose rates may be expected to differ markedly from open field conditions; in addition to dependence on local meteorological conditions. For these reasons, the maps themselves should be taken as an indication of the location of sources of enhanced radioactivity or radiation and only used in combination with other information for the purposes of radiological assessments. Bearing in mind that radiation fields can extend for up to a few hundred metres from the source, site specific investigations are helpful to determine whether features observed at or close to site perimeters are associated with local contamination, or with radiation fields projecting from the site. Moreover, where spectral components not considered in the standard model are evident the possibility of uncorrected interferences resulting in anomalies appearing in more than one nuclide specific map should be borne in mind.

Despite these qualifications the maps reveal an interesting range of radiometric features which correlate well with the locations and characteristics of activity associated with the individual nuclear sites. The maps are especially effective as an aid to visualisation of the spatial extent of enhancement to the ambient radiation fields in the immediate surroundings of the nuclear sites. They permit a general assessment of the magnitude of the radiometric impact of the sites on their local environment, and provide a basis for assessing change as the inventories of materials used and stored develops, and as old facilities are subject to decommissioning and site restoration.

The radiometric maps presented here cover the full survey areas of both the Mol-Dessel and Fleurus areas. Radiometric maps of individual sites along with summed spectra for active areas in these sites are included in Appendix C.

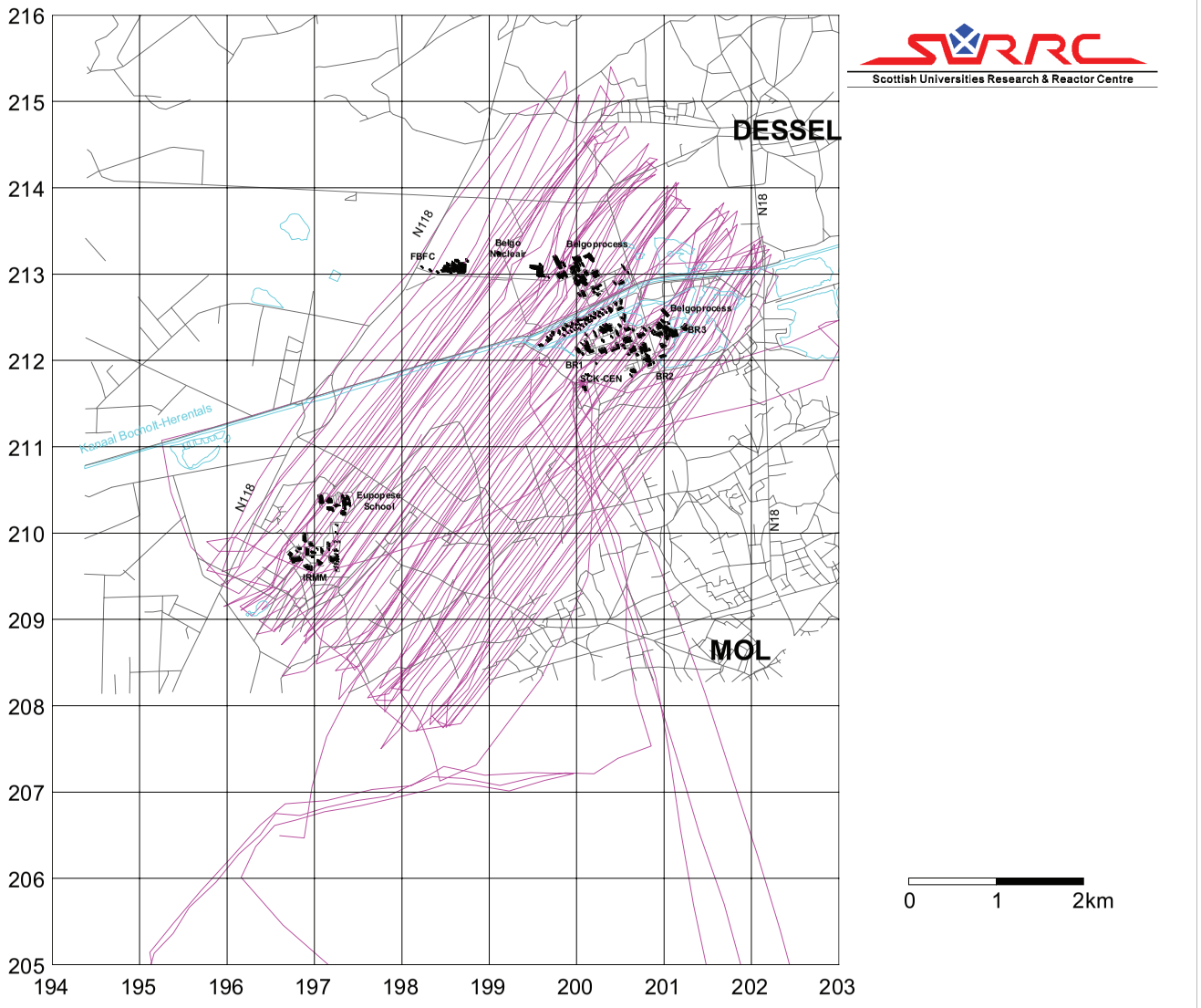

Figure 3.1 Flight track recorded by the Garmin GPS89 unit for the Mol survey.

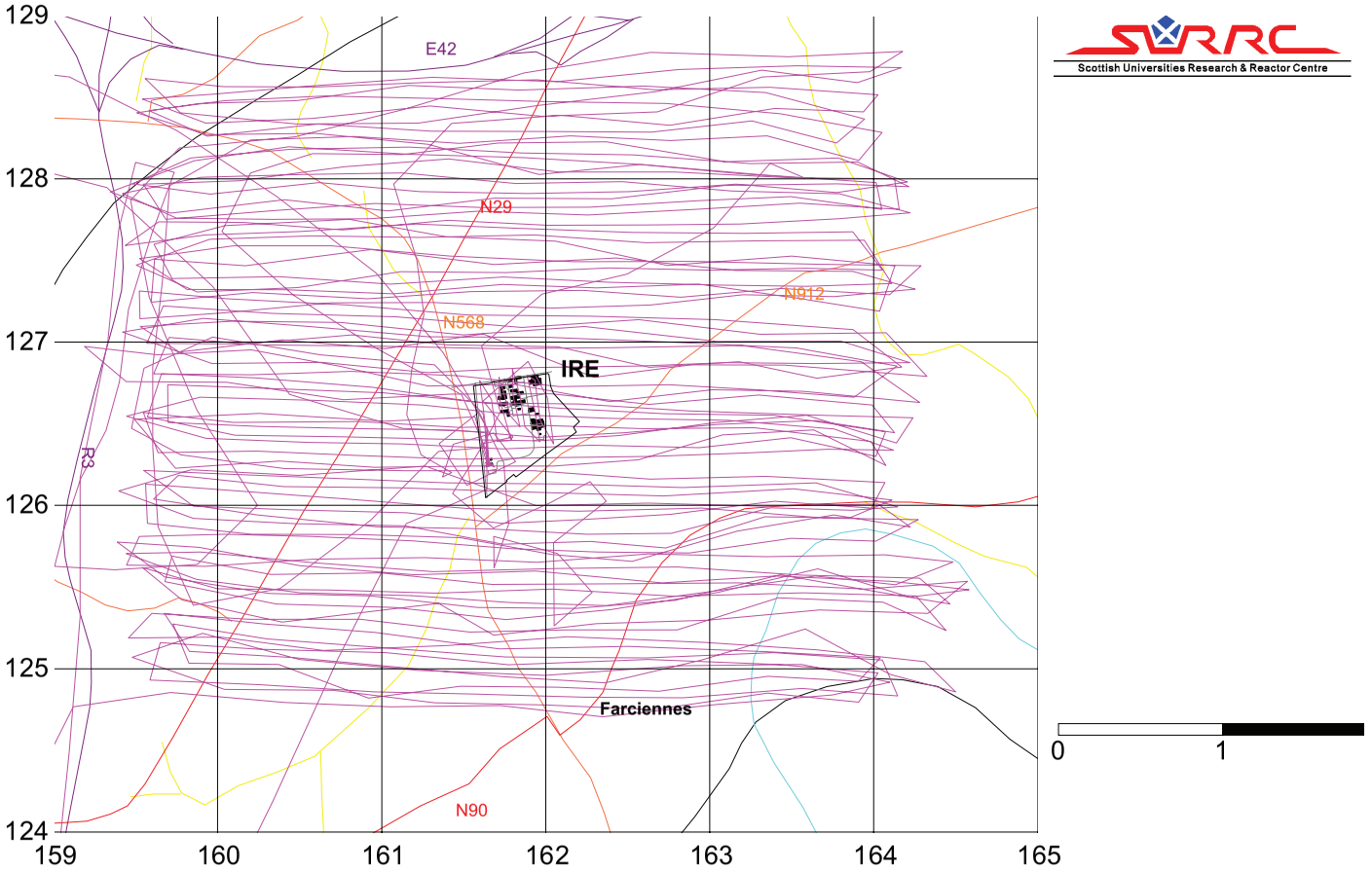

Figure 3.2 Flight track recorded by the Garmin GPS89 unit for the Fleurus survey.

3.1 Mol-Dessel area

The survey included flights over all the nuclear sites in the area, with the exception of the Belgonucléaire site. The data provides a complete record of the radiation environment of all the sites over flown, but only the radiation projected over the fence of the Belgonucléaire site.

The ^{137}Cs map, shown in figure 3.3, shows a number of features. Away from the nuclear sites the levels of ^{137}Cs are generally low reflecting the combination of deposition due to global fallout from the atmospheric testing of nuclear weapons, and the relatively low levels of Chernobyl deposition to the area. These levels typically range from below 2kBq m^{-2} to approximately 5-10 kBq m^{-2}, the extent to which spatial variations correspond to land cover features being as yet undetermined. A negative feature which corresponds clearly to the path of the Bocholt-Herentals canal is evident at western and north eastern parts of the map. A small enhancement is evident in the vicinity of IRMM, although this is largely attributed to interference from high energy radiation of machine origin. Distinct radiometric features are also observed at the FBFC site, which are attributed to a combination of 662 keV radiation associated with MOX materials, and spectral interferences from ^{234m}Pa and to a lesser extent ^{214}Bi associated with uranium derived materials. The large radiometric anomalies on the Belgoprocess sites 1 and 2 are associated with ^{137}Cs activity from stored radioactive materials on the sites, with some contributions from scattered radiation from other stored materials. The radiometric anomalies on and to the west of the SCK-CEN site are attributed to spectral interferences from ^{41}Ar discharged from the BR1 reactor, and its meandering plume, coupled to radiation fields around the site, and the Cs labelled cultivated plots to the west of the site.

The ^{60}Co map, shown in figure 3.4, shows a number of features. Outwith the nuclear sites the levels of ^{60}Co are, as expected, very low with activities less than 14 cps, corresponding to less than approximately 1kBq m^{-2}. A slight enhanced signal from the FBFC site is attributed to spectral interferences from ^{234m}Pa, which has a 1001 keV gamma-ray the peak of which slightly overlaps the ^{60}Co window. The large anomalies on the Belgoprocess sites 1 and 2 are associated with ^{60}Co activity from stored materials on the sites, with some contributions from scattered radiation from other stored materials. To the west of the SCK-CEN site a signal in the ^{60}Co channel results from the 1294keV ^{41}Ar gamma -ray which corresponds to the ^{60}Co window for 1173keV and 1332keV gamma-rays.

The ^{40}K map, shown in figure 3.5, shows a number of features. There is a large range of natural variation, with enhanced activity to the south and the far north of the region, reflecting the combination of geological and land cover variations. To the north and north west of the SCK-CEN the negative features associated with lagoons or lakes are clearly visible. There are small anomalies on Belgoprocess sites 1 and 2. The first of these is of relatively small extent, and may simply reflect the different natural radioelement content of the built environment of this site in contrast with its surrounding environment. On site 2 there are areas where the levels of radiation due to stored materials are sufficiently high to produce scattered radiation in the ^{40}K energy region and the onset of spectral distortion at high count rates. Interestingly, the anomaly present is on the north west side of the storage areas suggesting that scattered radiation from materials stored within the facilities is a substantial component. In the vicinity of BR1 and to the west there is a signal in the ^{40}K channel due to interference from ^{41}Ar emitted from the research reactor during its operations on the 10th May.

The ^{214}Bi map, shown in figure 3.6, shows a number of features. There is natural variation outwith the nuclear sites, with higher levels to the south of the survey area, and to the northwest of the SCK-CEN complex. Major anomalies associated with the nuclear sites is from Belgoprocess site 2, which is known to contain substantial stocks of ^{226}Ra, thus explaining the radiometric feature, which is observed in precisely the locations expected. A minor anomaly is also detected at the FBFC site. ^{214}Bi is not expected to be a major radiation contribution from purified uranium materials, and therefore the possibility that this signal indicates the presence of uranium ores on the site, perhaps associated with past activities, may merit further consideration.

The ^{208}Tl map, shown in figure 3.7, shows a number of features. There is natural variation outwith the nuclear sites, with higher activity in the southern side of the survey area and significantly higher activity to the north of the SCK-CEN site. There are reduced activity areas associated with the lagoons to the north and west of the SCK-CEN site. There is a slight anomaly on the IRMM site, as a result of interference from high energy photons generated by the LINAC accelerator. There is also an anomaly on Belgoprocess site 2, where there are areas where the levels of radiation due to stored materials are sufficiently high to produce scattered radiation in the ^{208}Tl energy region and the onset of spectral distortion at high count rates.

The gamma-dose rate map, shown in figure 3.8, shows a number of features. There are natural variations reflecting the variations in ^{40}K, ^{214}Bi and ^{208}Tl activities, with higher levels to the south of the survey area, and to the north west of the SCK-CEN site.

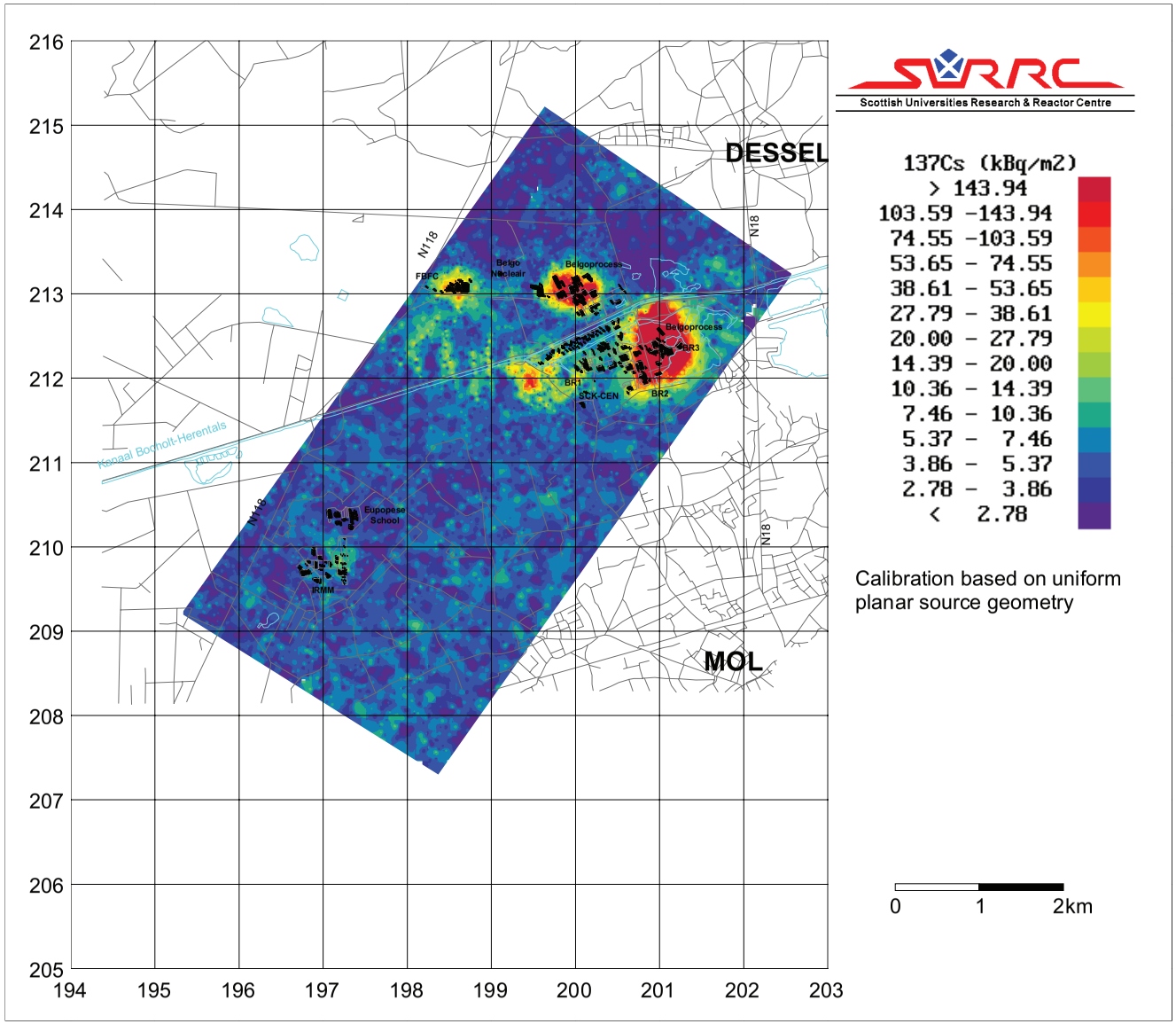

Figure 3.3 The distribution of ^{137}Cs signals (662 keV) in the Mol survey area.

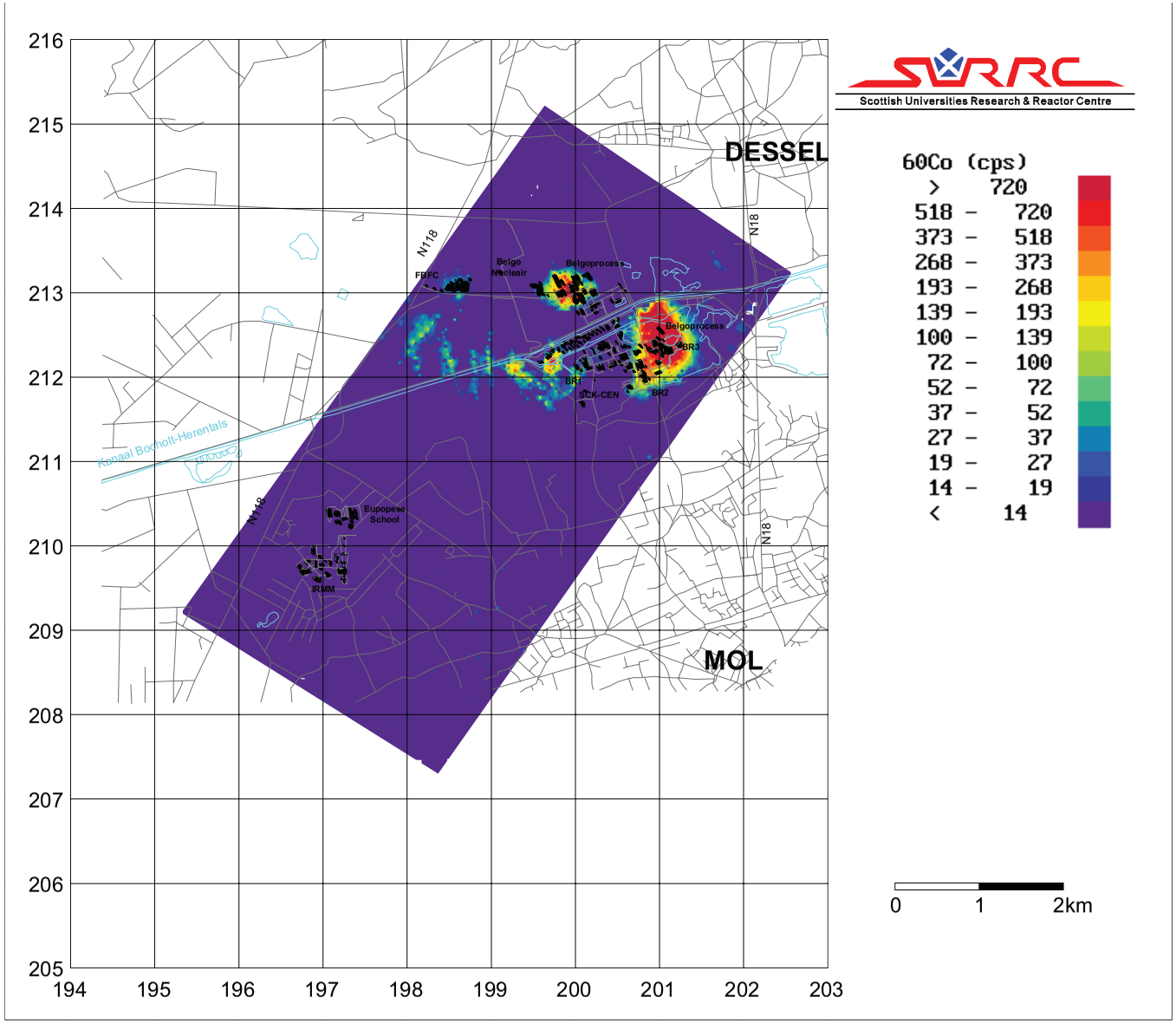

Figure 3.4 The distribution of ^{60}Co signals (1.1-1.3 MeV) in the Mol survey area.

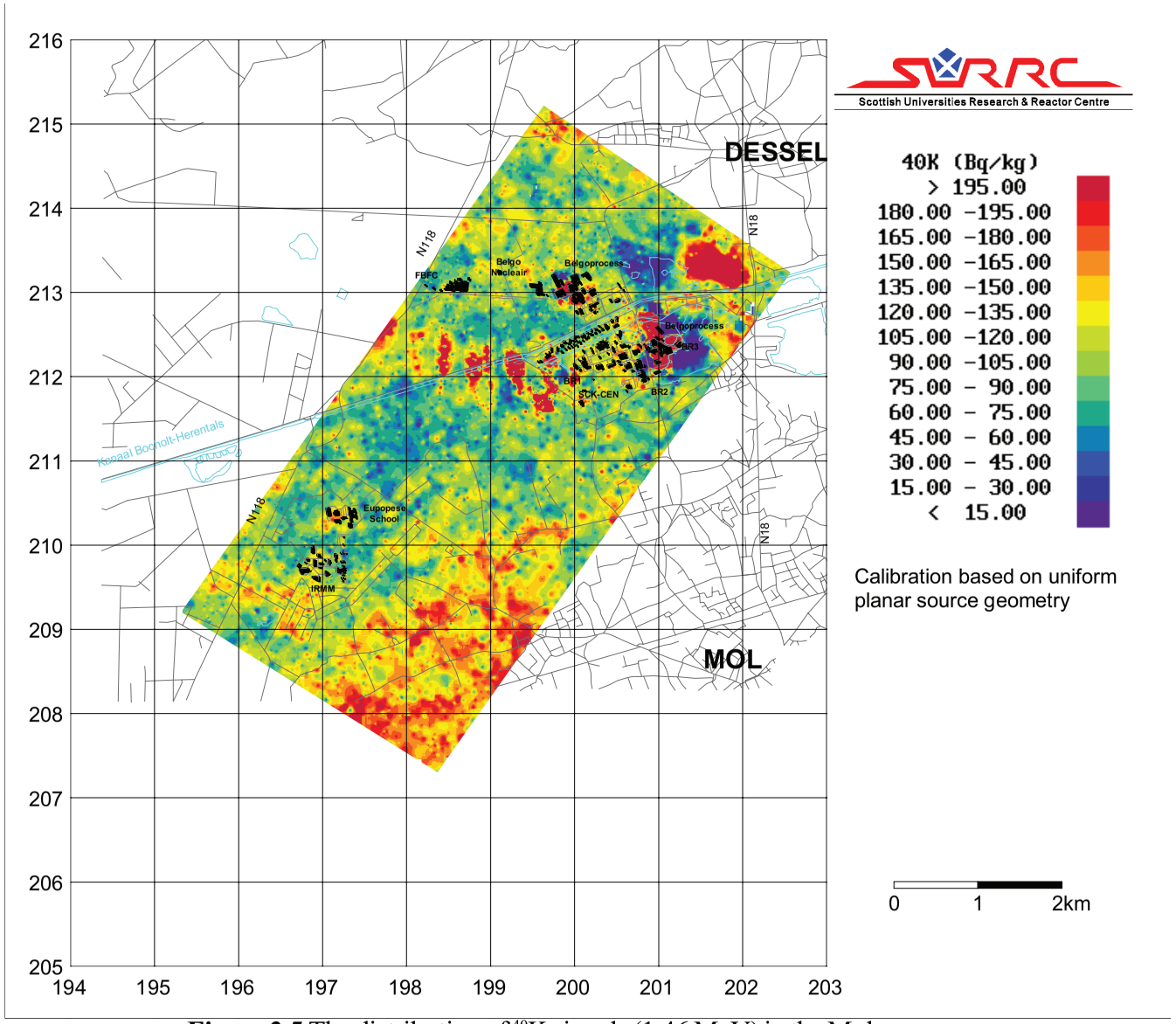

Figure 3.5 The distribution of ^{40}K signals (1.46 MeV) in the Mol survey area.

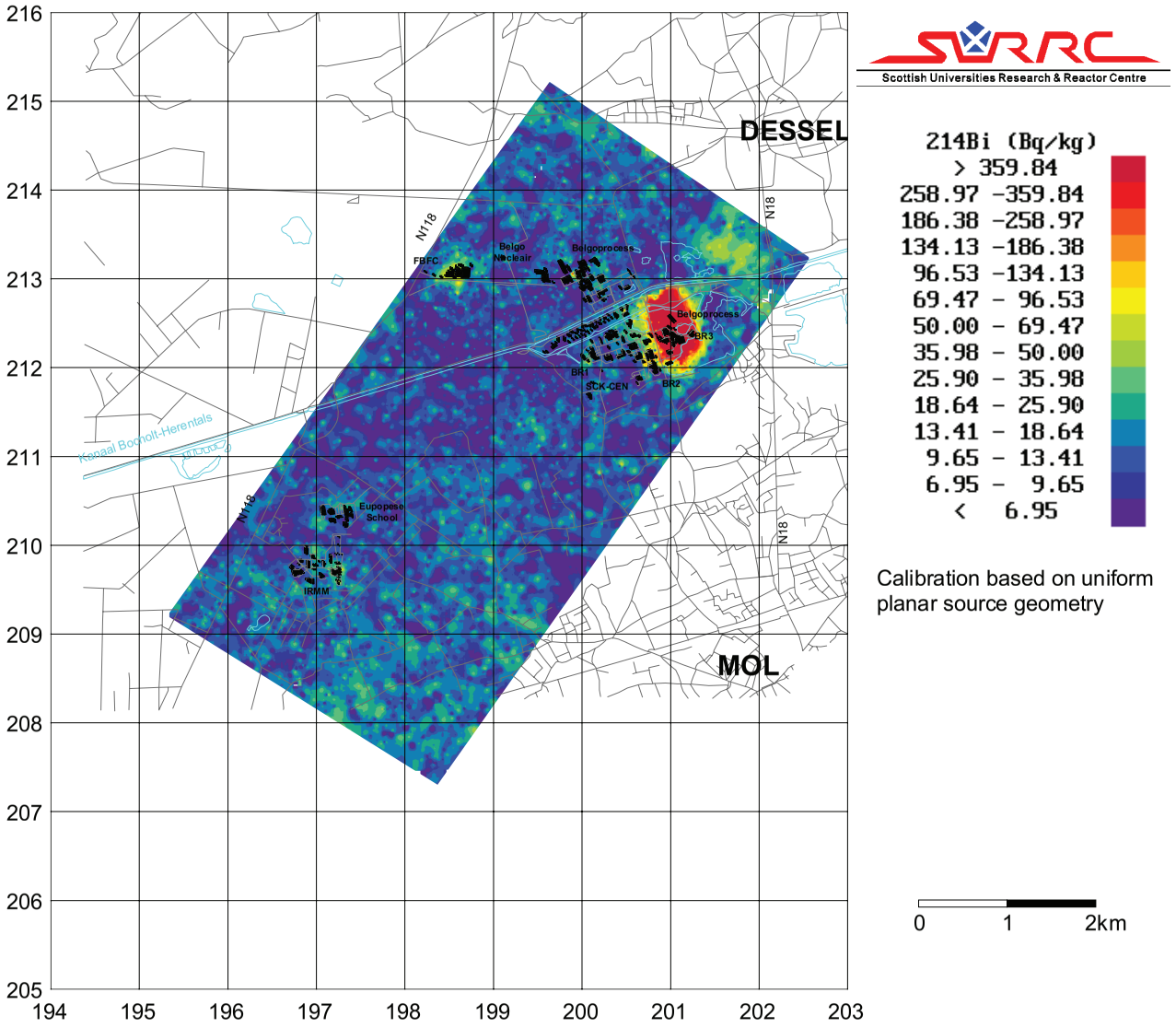

Figure 3.6 The distribution of ^{214}Bi signals (1.76 MeV) in the Mol survey area

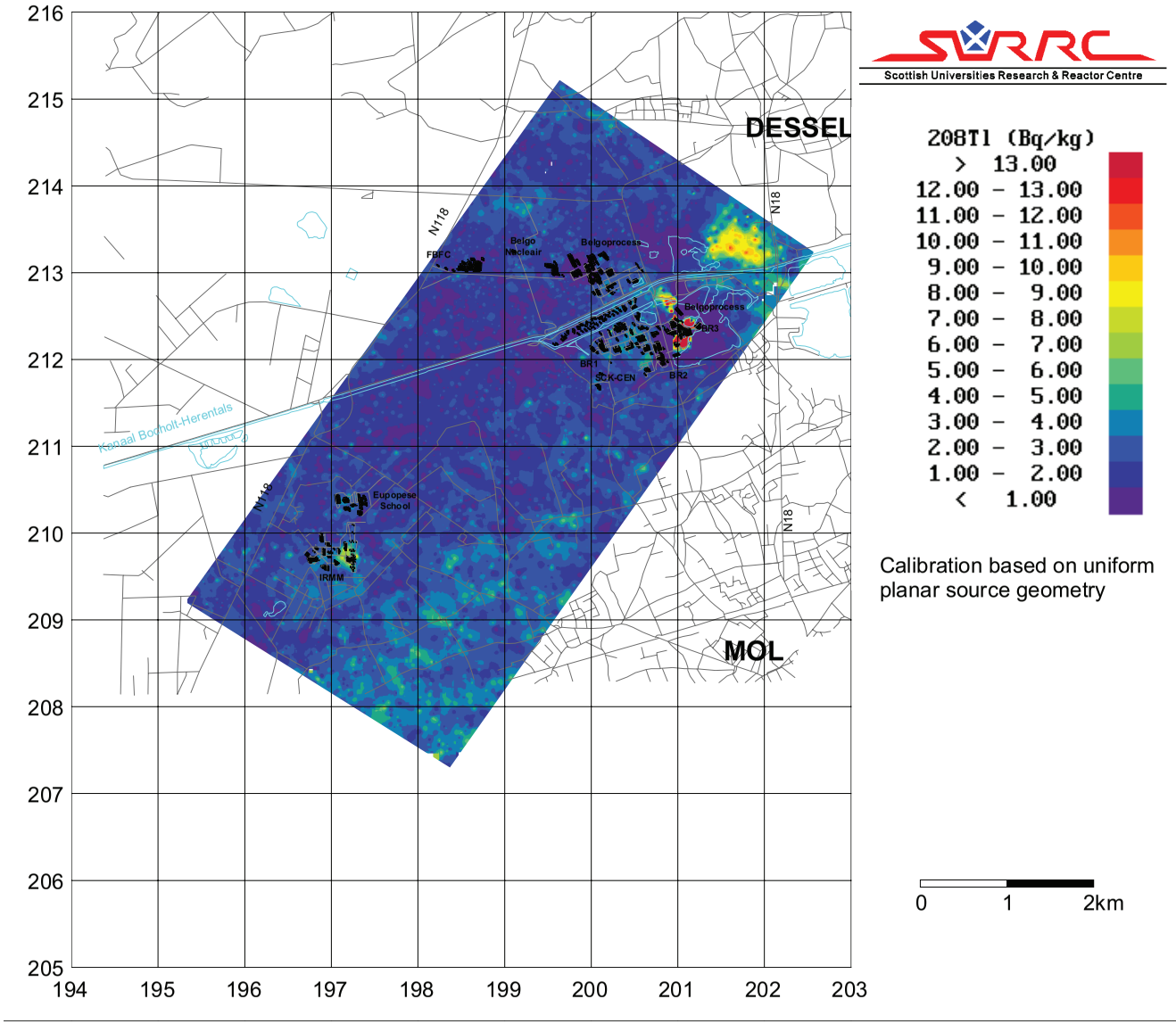

Figure 3.7 The distribution of ^{208}Tl signals (2.6 MeV) in the Mol survey area

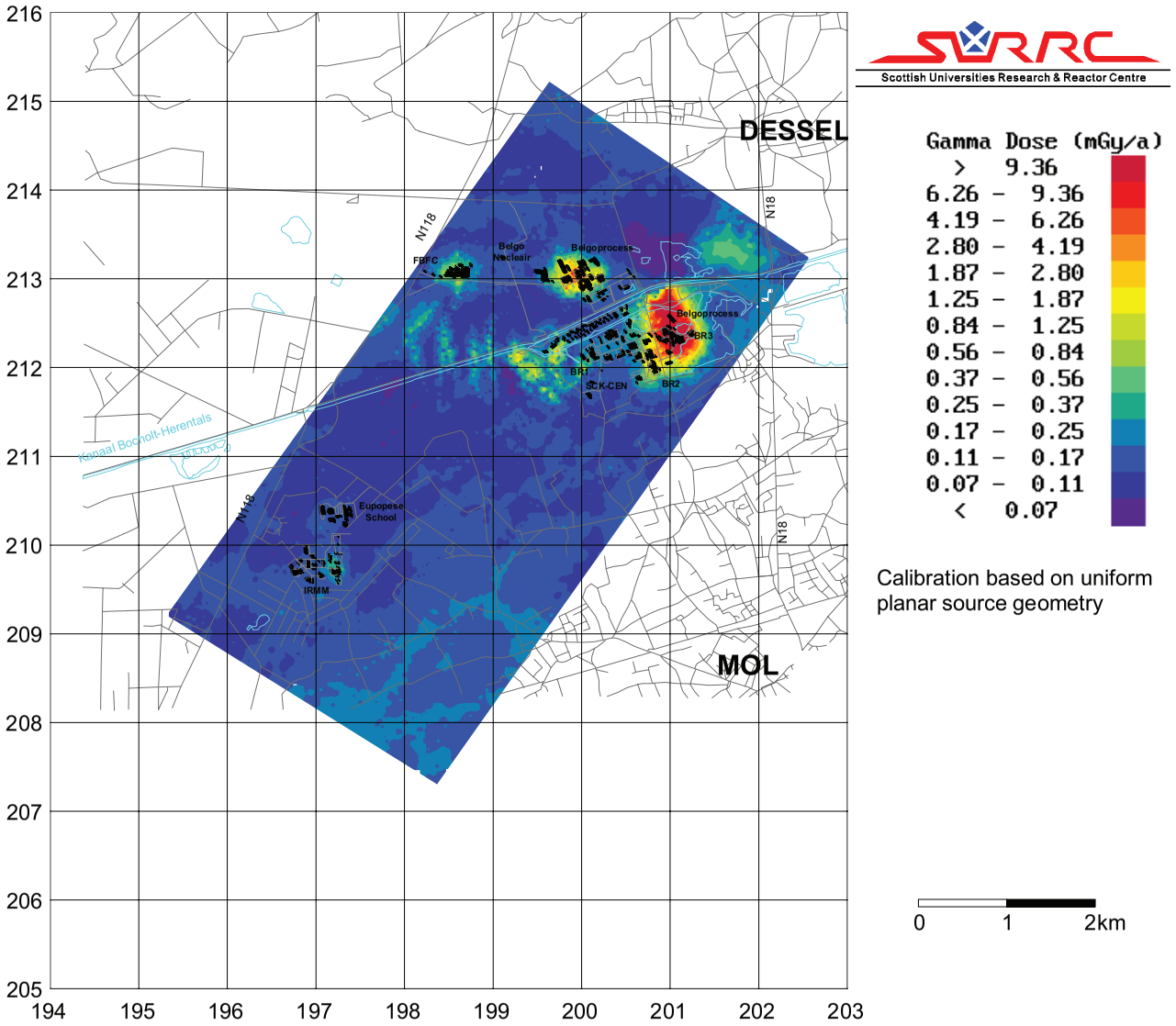

Figure 3.8 Ground level gamma-ray dose rates (mGy a^{-1}) in the Mol survey area. Net dose rates after subtraction of cosmic ray and detector background.

3.2 Fleurus site

The ^{137}Cs map, shown in figure 3.9, shows slightly higher levels of ^{137}Cs in the area outwith the nuclear site than was observed in the Mol-Dessel area, typically ranging from 1-2 kBq m^{-2} to 10-12 kBq m^{-2}, it was noted that the airborne survey data overestimated the ^{137}Cs activity on the sampled field at IRE suggesting a slight problem with the processing of this data. The higher of these levels are associated with higher levels of ^{40}K, suggesting that there may be some residual interferences in this data set due to incorrect stripping. There is an anomaly within the IRE site associated with materials in the vicinity of the radiochemical laboratories and waste store. In addition to small levels of ^{137}Cs, there are also gamma -rays from ^{214}Bi (609keV) and ^{99}Mo (739keV) which contribute to this channel. There is a highly localised signal of unknown origin to the north of the IRE site.

The ^{60}Co map, shown in figure 3.10, shows some activity outwith the nuclear site where no ^{60}Co would be expected. These correspond to areas with higher levels of ^{40}K and are almost certainly due to a problem with spectral stripping. There is an anomaly within the IRE site in the vicinity of the radiochemical laboratories and waste store. There are unidentified gamma -rays at 1236keV and 1333keV evident in the GMX spectrometer data which contribute to this channel.

The ^{40}K map, shown in figure 3.11, shows the natural variation within the survey area as a result of geological and land cover variation. The activity levels in the Fleurus area are higher than those observed in the Mol-Dessel area. There are higher activity areas to the east and south east of the IRE site, with low levels in areas to the west and south east of the IRE site associated with woodland. There is no enhancement in ^{40}K signals associated with the IRE site.

The ^{214}Bi map, shown in figure 3.12, shows the natural variation within the survey area. The activity levels in the Fleurus area are higher than those observed in the Mol-Dessel area. There are slightly higher levels to the northern and eastern sides of the survey area, with lower levels to the west of the IRE site. There is no enhancement in ^{214}Bi signals associated with the IRE site.

The ^{208}Tl map, shown in figure 3.13, shows the natural variation within the survey area, showing the same pattern as the other natural channels. The activity levels in the Fleurus area are higher than those observed in the Mol-Dessel area. There is no evidence of enhanced ^{208}Tl levels associated with the IRE site.

The gamma-ray dose map, shown in figure 3.14, shows the natural variation outwith the nuclear site, with higher levels to the east of the survey area and low levels to the west and south east of the IRE site. There are enhanced dose rate levels associated with the previously noted anthropogenic signals in the vicinity of the radiochemical laboratories and waste stores.

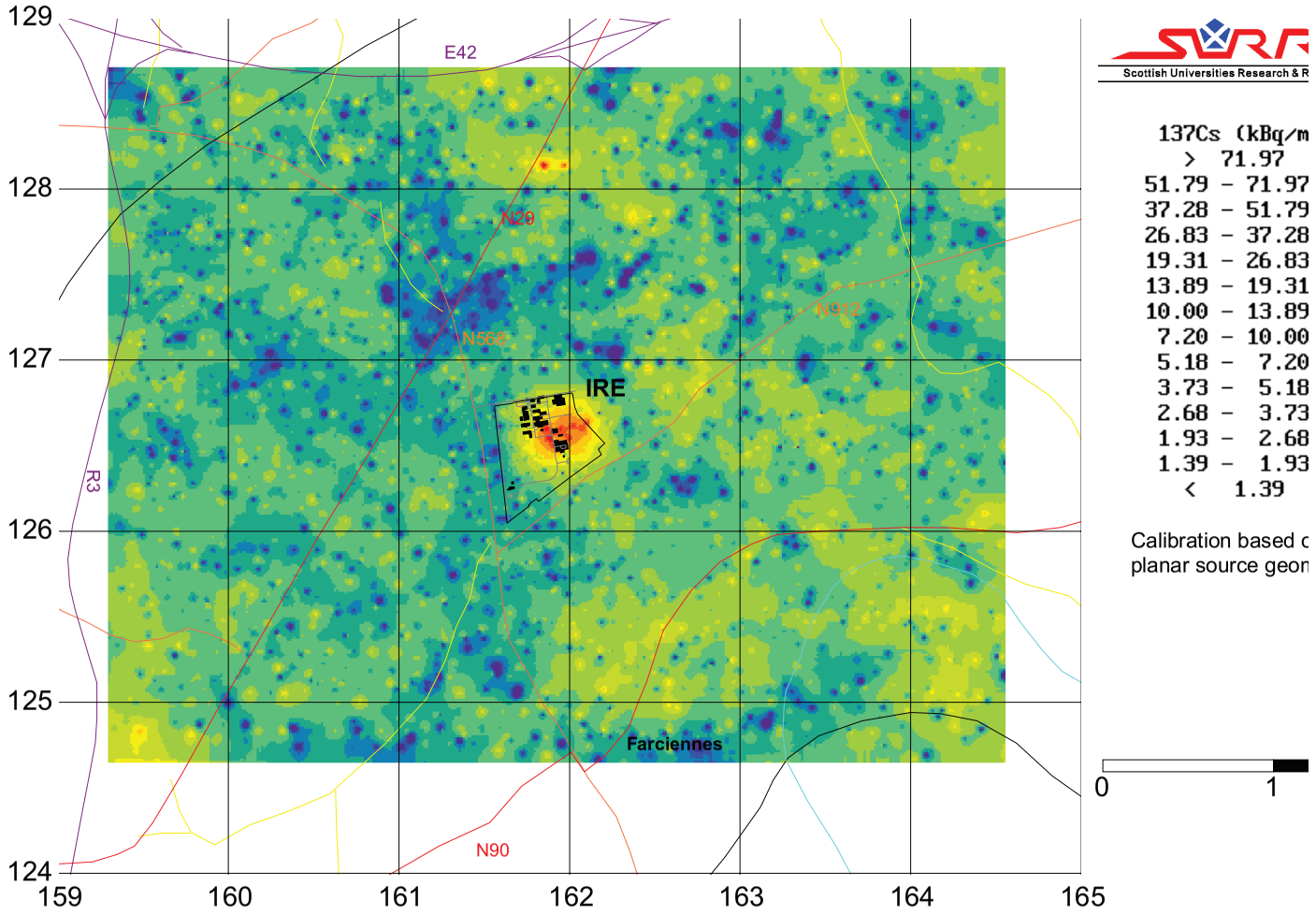

Figure 3.9 The distribution of ^{137}Cs signals (662 keV) un the vicinity of the IRE site.

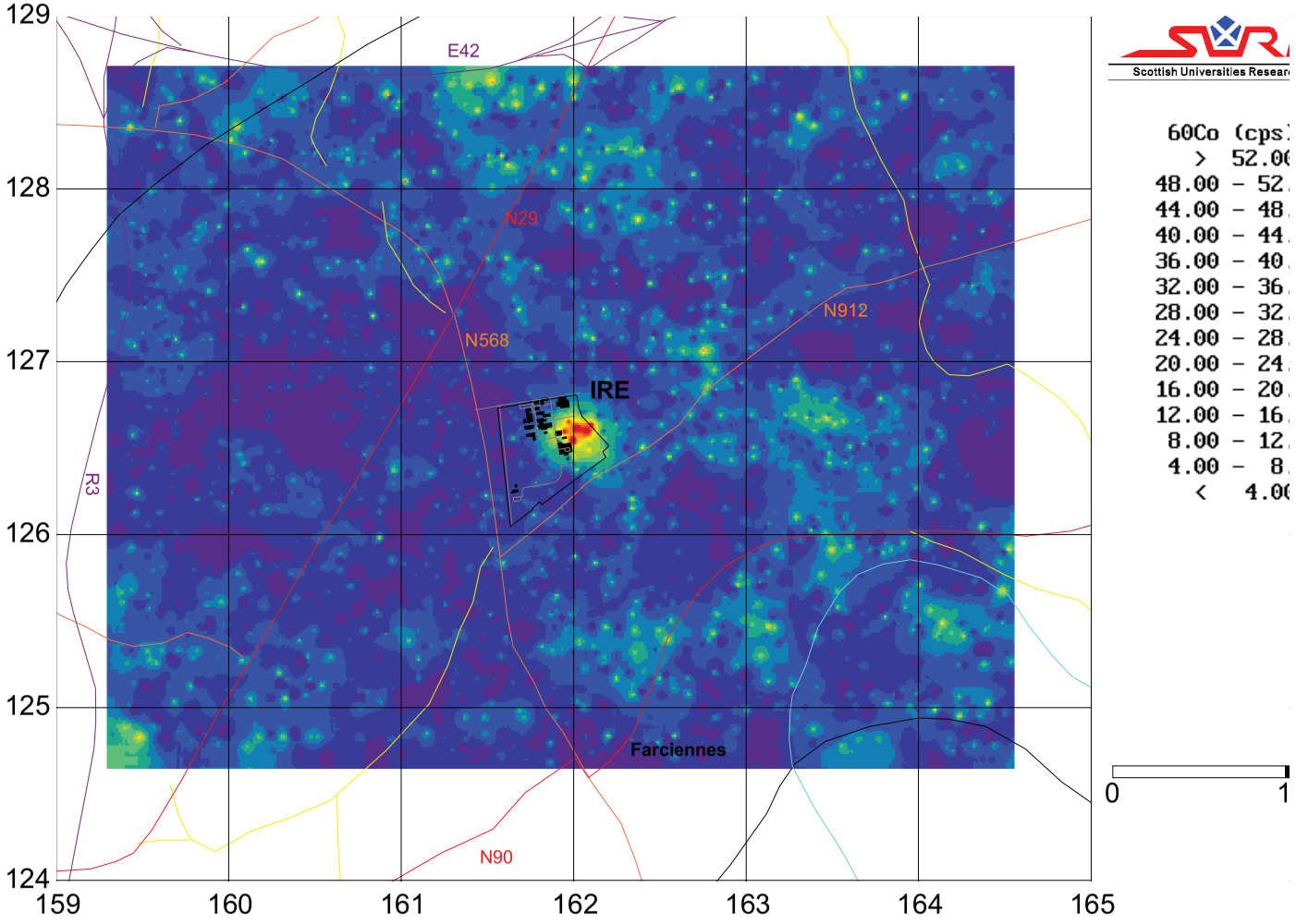

Figure 3.10 The distribution of ^{60}Co signals (1.1-1.3 MeV) in the vicinity of the IRE site

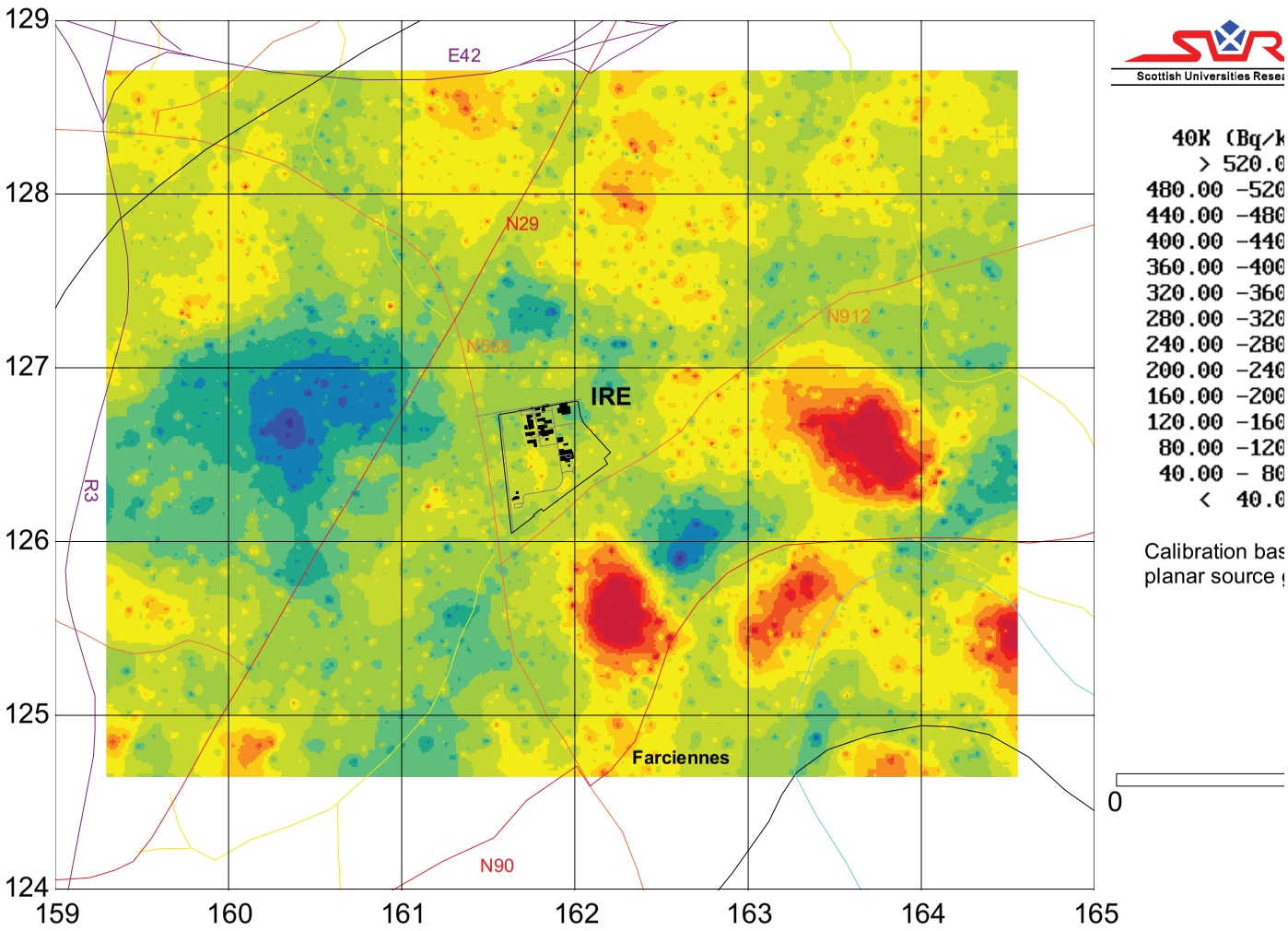

Figure 3.11 The distribution of ^{40}K signals (1.46 MeV) in the vicinity of the IRE site.

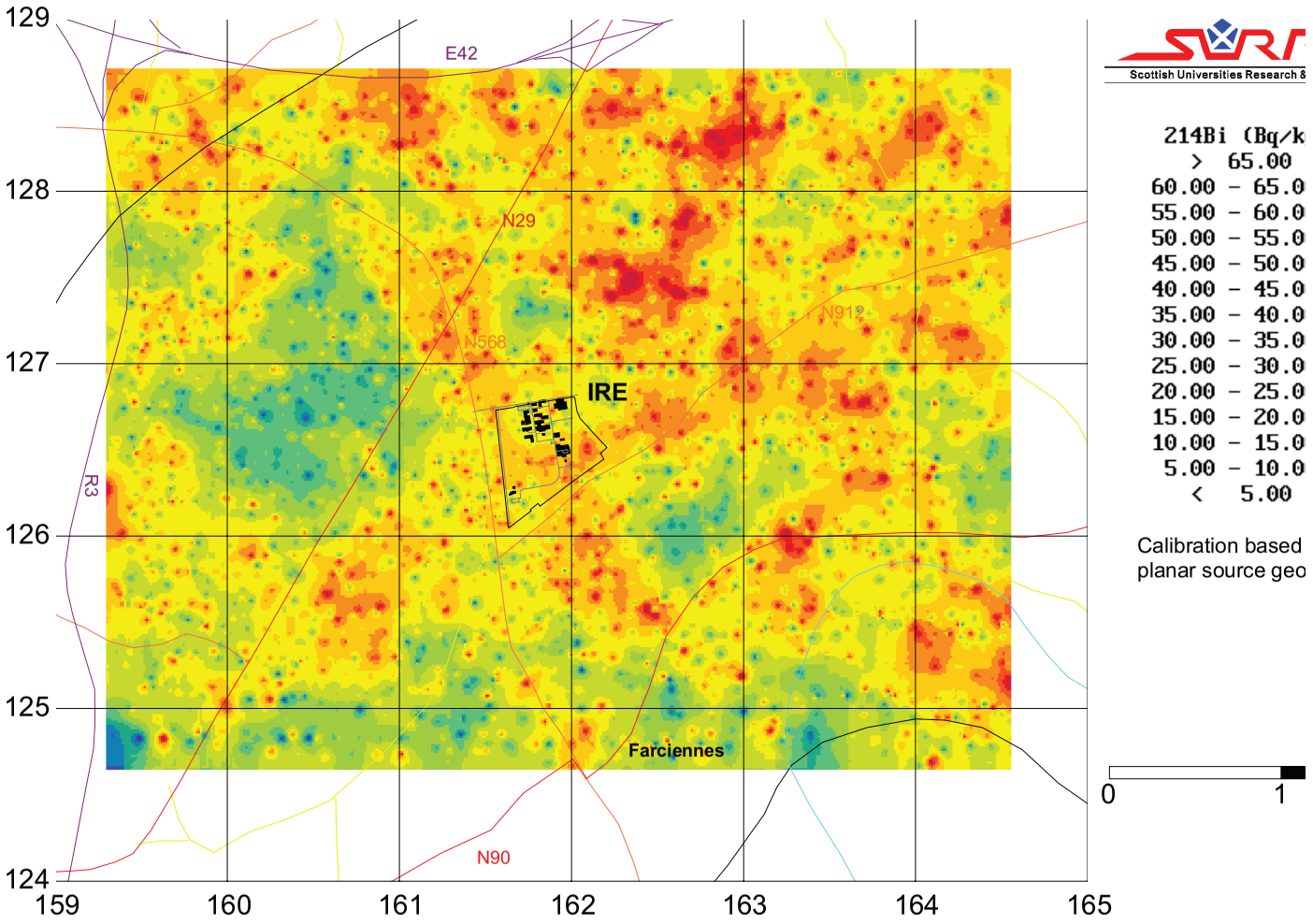

Figure 3.12 The distribution of ^{214}Bi signals (1.76 MeV) in the vicinity of the IRE site.

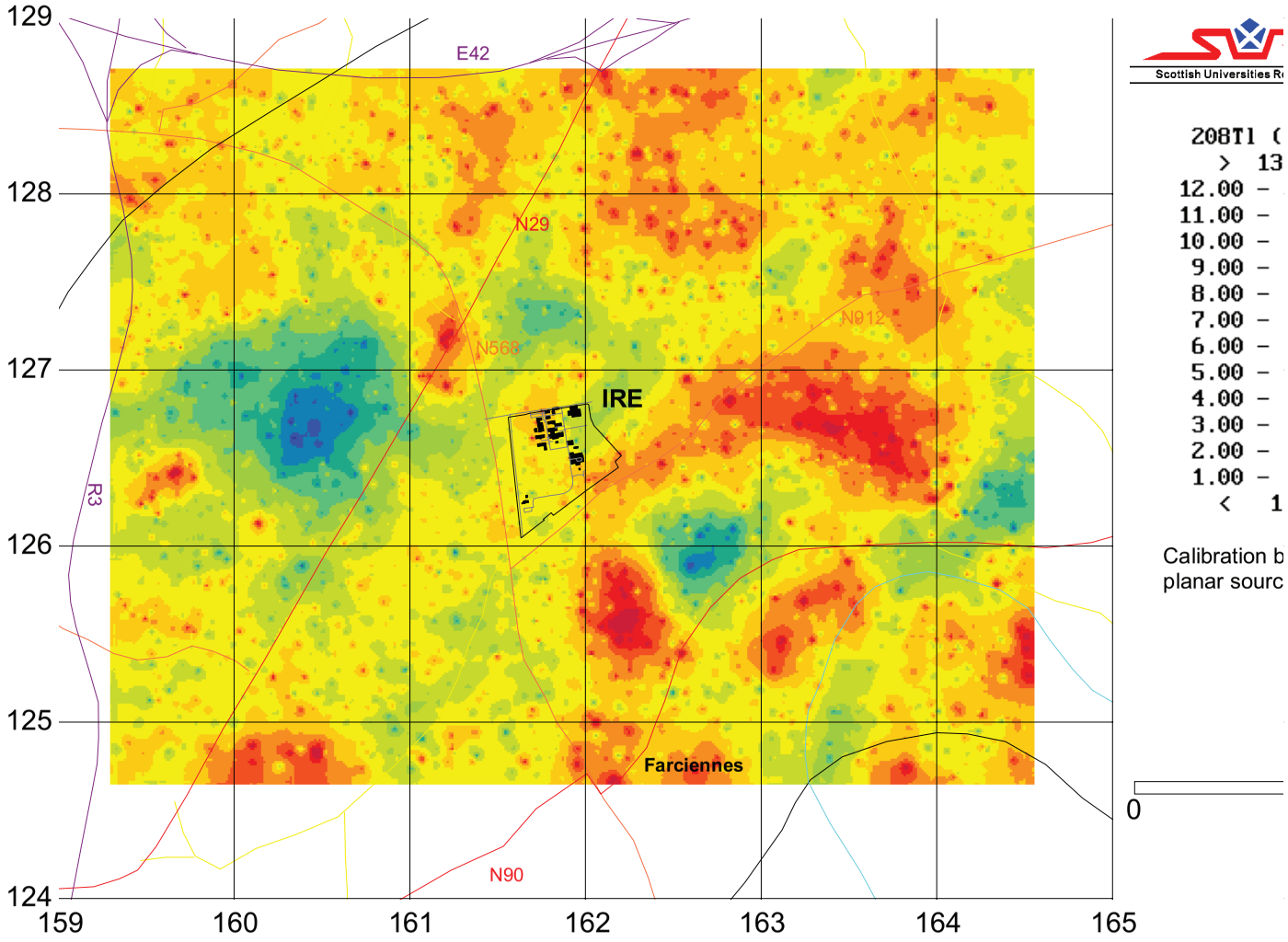

Figure 3.13 The distribution of ^{208}Tl signals (2.6 MeV) in the vicinity of the IRE site.

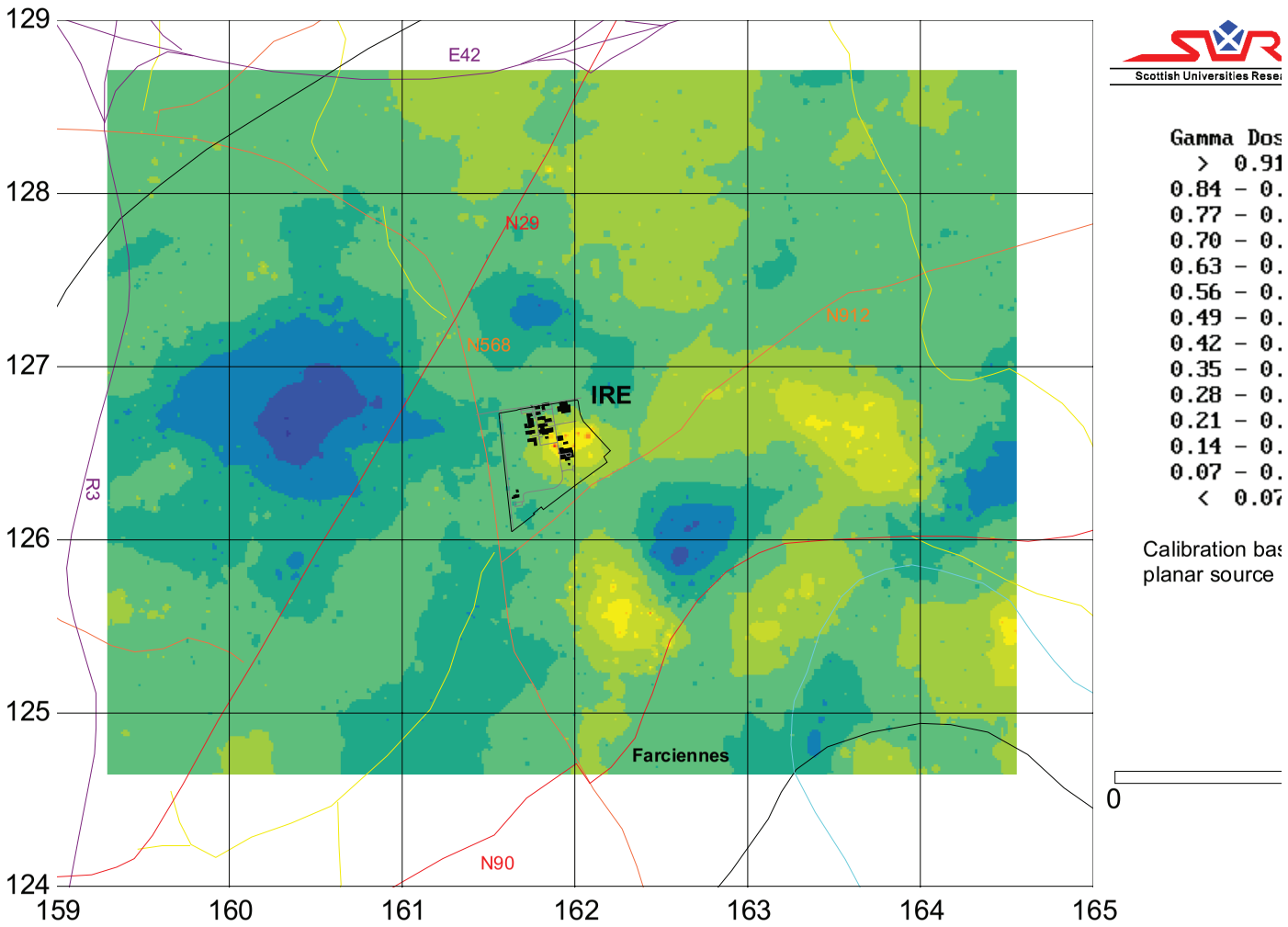

ose

rates after subtraction of cosmic ray and detector background

4. DISCUSSION AND CONCLUSIONS

The Airborne Gamma Spectrometry (AGS) survey was conducted around the vicinity of nuclear sites in two regions of Belgium, near Mol and Fleurus. The sites at Mol were surveyed during the 10th-11th May 2000, with 7500 NaI(Tl) and 3750 GMX spectra recorded during 5½ hours. The IRE site at Fleurus was surveyed on the 12th May 2000, with 5400 NaI(Tl) and 2700 GMX spectra recorded during 4 hours. Spectra were recorded using a 16 litre NaI(Tl) and a 50% efficiency Ge (GMX) spectrometer mounted on the inside of a twin engine Squirrel helicopter. Differential GPS systems were used to aid aircraft navigation and to log the position of each spectrum recorded.

The survey was conducted within one week and was successful, showing that it is feasible to conduct such an operation efficiently using local landing sites and infrastructure support. The technical outputs have confirmed that abundant spectrometric information about the radiation environment of these nuclear sites can be gathered using the airborne survey technique.

The data sets reveal a wide variety of signals associated with the nuclear sites and their facilities, generally confirming the highly localised nature of radiometric anomalies associated with the facilities. The characteristics of the radiometric signals vary in response to the type of operation and radioactivity on each site. Signals observed at IRMM are largely characteristic of machine sources, with high energy components and annihilation radiation present. Those at FBFC by contrast are largely associated with ^{234m}Pa reflecting the uranium distribution around the site, although 662 keV radiation, associated with MOX activities, and ^{214}Bi signals are also present. The SCK-CEN complex produced a range of signals notably including the discharge of ^{41}Ar from the BR1 reactor. It was also possible to observe signals associated with the agricultural research plots to the west of the site. The Belgoprocess sites produced a striking range of signals of which ^{137}Cs and ^{60}Co contributions are associated with nuclear fuel cycle and activated materials, and ^{214}Bi signals are associated with ^{226}Ra and/or uranium series activity. At the IRE site it was possible to see small anomalies associated with short lived nuclides including ^{99}Mo and ^{131}I. The gamma dose rate maps show the relative importance of the anthropogenic radiation fields on the nuclear sites and their surroundings. It is reassuring to note that the spatial distribution and nature of these signals is so highly consistent with expectations based on the types of operation taking place within the sites, and that the signals are so highly localised to the facilities.

The data sets serve as a reference against which future changes can be measured. Whether in response to an internal or external event, or simply as part of a regular series of campaigns to document the changing environments of the sites, as new construction and decommissioning of old plant, or development of new waste-management approaches take place, it would be possible to repeat this survey rapidly to document change.

REFERENCES

Allyson, J.D. & Sanderson, D.C.W. (1998). Monte Carlo Simulation of Environmental Airborne Gamma-Spectrometry, Journal of Environmental Radioactivity, **38**(3), 259-282.

Institut Géographique National (1989). Systèmes de référence et formules de transformation en usage en Belgique. NGI-IGN Report (May 1989), Brussels.

Sanderson, D.C.W. & Scott, E.M. (1989a). An aerial radiometric survey in West Cumbria in 1988, MAFF Food Science Report N611.

Sanderson, D.C.W., East, B.W., Scott, E.M. (1989b). Aerial radiometric survey of parts of North Wales in July 1989, SURRC report 8901.

Sanderson, D.C.W., Scott, E.M., Baxter, M.S. (1990a). Use of Airborne Radiometric Measurements for Monitoring Environmental Radioactive Contamination, IAEA SM-306/138, 411-421, Vienna.

Sanderson, D.C.W, Scott, E.M., Baxter, M.S. (1990b). The use and potential of aerial radiometrics for monitoring environmental radioactivity, in "Nuclear Contamination of Water Resources", Institute of Civil Engineers, pages 99-106.

Sanderson, D.C.W., Allyson, J.D., Martin, E., Tyler, A.N., Scott, E.M. (1990c). An Aerial Gamma-ray Survey of Three Ayrshire Districts. Commissioned by the District Councils of Cunninghame, Kilmarnock and Loudoun, and Kyle and Carrick, SURRC 9001.

Sanderson, D.C.W., Allyson, J.D., Cairns, K.J., MacDonald, P.A. (1990d). A brief aerial survey in the vicinity of Sellafield in September 1990, SURRC report 9101.

Sanderson, D.C.W. and Allyson, J.D. (1991). An aerial gamma ray search for a missing ^{137}Cs source in the Niger Delta, SURRC report.

Sanderson, D.C.W., Allyson, J.D., Tyler, A.N. (1992). An aerial gamma ray survey of Chapelcross and its surroundings in February 1992, SURRC report 9201.

Sanderson D.C.W., Scott E.M., Baxter M.S., Martin E., Ni Riain S. (1993a). The use of aerial radiometrics for epidemiological studies of leukaemia, Scottish Universities Research & Reactor Centre, East Kilbride, 165p.

Sanderson, D.C.W., Allyson, J.D., Tyler, A.N. (1993b). An aerial gamma ray survey of Springfields and the Ribble Estuary in September 1992, SURRC report 9301.

Sanderson, D.C.W., Allyson, J.D., Tyler, A.N., Scott, E.M. (1994a). Environmental Applications of Airborne Gamma Spectrometry. *Application of Uranium Exploration Data and Techniques in Environmental Studies*, IAEA-TECDOC-827, 71-91.

Sanderson, D.C.W., Allyson, J.D., Tyler, A.N. (1994b). Rapid Quantification of Radiometric Data for Anthropogenic and Technologically Enhanced Natural Nuclides. *Application of Uranium Exploration Data and Techniques in Environmental Studies*, IAEA-TECDOC-827, 197-216.

Sanderson D.C.W., Allyson J.D., Tyler A.N., Ni Riain S., Murphy S. (1994c). An Airborne Gamma Ray Survey of parts of SW Scotland, Scottish Universities Research & Reactor Centre, East Kilbride, 118p.

Sanderson, D.C.W., Allyson, J.D., Riain, S. Ni, Gordon, G., Murphy, S., Fisk, S. (1994d). An Aerial Gamma Ray Survey of Torness Nuclear Power Station 27-30 March 1994. SURRC Report.

Sanderson, D.C.W., Allyson, J.D., Gordon, G., Murphy, S., Tyler, A.N., Fisk, S. (1994e). An Aerial Gamma Ray Survey of Hunterston Nuclear Power Station on 14-15th April and 4th May 1994. SURRC Report.

Sanderson, D.C.W., Allyson, J.D., Toivonen, H., Honkamaa, T. (1997a). Gamma Ray Spectrometry Results from Core Samples Collected for RÉSUMÉ 95, September 1995, Scottish Universities Research and Reactor Centre, East Kilbride, 51p.

Sanderson, D.C.W., Allyson, J.D., McConville, P., Murphy, S., Smith, J. (1997b). Airborne Measurements Conducted during an International Trial in Finland. In: RÉSUMÉ 95: ". Published by NKS-Secretariat, FRIT, Denmark. pp237-253.

Sanderson, D.C.W., Cresswell, A.J., McLeod, J., Murphy, S., Tyler,A.N., Atkin,P.A. (2000). Investigation of Spatial and Temporal Aspects of Airborne Gamma Spectrometry. Report on Phase I Survey Conducted April 1999. SURRC Report.

Tyler, A.N., Sanderson, D.C.W., Scott, E.M., Allyson, J.D. (1996a). Accounting for spatial variability and fields of view in environmental gamma-ray spectrometry. Journal of Environmental Radioactivity, **33** (3), 213-235.

Tyler, A.N., Sanderson, D.C.W., Scott, E.M. (1996b). Estimating and accounting for ^{137}Cs source burial through *in-situ* gamma spectrometry in salt marsh environments. Journal of Environmental Radioactivity, **33** (3), 195-212.

APPENDICES

APPENDIX A: SUMMARY OF DETECTOR CALIBRATION AND DATA PROCESSING

1. DESCRIPTION OF DATA PROCESSING ALGORITHMS

Selected windows in the NaI(Tl) spectra are integrated to produce gross count rates for these channels. The standard windows used are given in Table A.1, along with a window around the 1001keV ^{234m}Pa peak which was used for analysis of data recorded around the FBFC International site. Background count rates, recorded over water, are subtracted from the gross count rate data to generate net count rates. The background values used for this survey are given in Table A.2.

Spectral interferences between channels are then stripped from the net count rate data. A stripping matrix, giving the fractional interference for each nuclide window in the other nuclide windows, is formed from data collected from a series of calibration pads with perspex absorber sheets to simulate an air path of several 10s of metres. The stripping matrix used for this work, measured in November 2000 with 7 absorber sheets, equivalent to 70m of air, is given in Table A.3.

The inverse of the stripping matrix is applied to a vector containing the net count rates in each of the five radionuclide channels, producing a vector containing the stripped counts in these channels. This is readily coded as a series of linear equations in which the stripped count rate, Y_s, for channel k is the sum over all channels j of the products of the net count rate, Y_n, for channel j and the element for k, j of the inverted stripping matrix S'.

$$Y_s(k) = \sum_j Y_n(j) S'(k, j)$$

Altitude correction coefficients and sensitivity calibration constants are determined from hover manoeuvres above a calibration site. The calibration site is systematically sampled in a spatially representative expanding hexagonal pattern to give values of activity concentration for anthropogenic ^{137}Cs (kBq m^{-2}) and naturally occurring ^{40}K, ^{214}Bi and ^{208}Tl (Bq kg^{-1}). In most situations the naturally occurring radioisotopes are uniformly distributed with depth, however for ^{137}Cs more complex depth profiles are common and these will affect the calibration.

The altitude correction coefficients normalize the stripped data to a ground clearance of 100m, using an exponential altitude dependence. The altitude corrected count rates, Y_{ac}, are determined from the stripped count rates, Y_s, by:

$$Y_{ac} = Y_s e^{(A-100)a_{cc}}$$

where A is the ground clearance and a_{cc} the altitude correction coefficient. The altitude correction coefficient is determined from the gradient of a plot of the logarithm of stripped count rates against altitude at the calibration site.

The sensitivity calibration constants convert the altitude corrected stripped count rates to calibrated activity concentration units (kBq m^{-2} or Bq kg^{-1}). They are determined by simply dividing the activity concentration on the calibration site found from ground sampling by the stripped altitude corrected count rates from the calibration manoeuvre data. Table A.4 shows the altitude correction and sensitivity calibration constants used for this survey.

The principle source of uncertainties for open field geometries is the statistical counting error in the gross count rate. This could be reduced by using a longer integration time, but at the expense of spatial precision of the reading. Typically in this survey using a 2s integration time these correspond to uncertainties of approximately 5% for ^{137}Cs, 10% for naturals and 2.5% for the dose rate in the predominantly low activity areas outwith the nuclear sites. Within the sites where activity levels are much higher these uncertainties will be significantly reduced.

In situations which closely match the assumed open field geometry with a radiation field consisting of natural components and a small number of anthropogenic nuclides additional small uncertainties will be introduced during spectral stripping and sensitivity calibration. However, in situations where the source geometry and isotopic contribution differs significantly from this these uncertainties may become significant. For example, the presence of other radioisotopes would introduce additional errors in the spectral stripping, and may require the use of a different set of windows and stripping matrix. Highly localised sources and local shielding would introduce errors in the sensitivity calibration.

2. DETECTOR AND DATA COLLECTION SYSTEM

16 litre NaI(Tl) detector array (4 crystal pack):
Serial numbers: IA510, 022100AR, IV43, HR762
EHT: 1000V (nominal)

Single 50% efficiency Ge semiconductor (GMX) detector operated in parallel with scintillation detector:
Serial number: 32-TN30665A (EHT: -3000V)

Window	Radionuclide	Channel range	Energy Range (keV)
1	^{137}Cs (662 keV)	105-136	550-755
2	^{60}Co (1172 keV)	175-210	1015-1250
3	^{40}K (1461 keV)	221-267	1320-1630
4	^{214}Bi (1764 keV)	267-311	1630-1920
5	^{208}Tl (2615 keV)	378-461	2365-2920
6	Total > 350 keV	75-500	350-3180
	^{234m}Pa (1001 keV)	150-185	850-1080

Table A.1 Spectral windows for NaI(Tl) detector

Date	Ch.1	Ch.2	Ch.3	Ch.4	Ch.5	Ch.6
10/5/2000	40.1	17.5	20.7	9.7	7.2	165
11/5/2000	34.4	15.1	17.6	8.6	7.3	145
12/5/2000 (1500)	63.0	25.7	25.3	16.1	8.8	235
12/5/2000 (2015)	52.0	21.9	22.4	13.5	8.6	202

Table A.2 Background count rates (cps) recorded over water

	^{137}Cs	^{60}Co	^{40}K	^{214}Bi	^{208}Tl
^{137}Cs	1	0.005	0	0	0
^{60}Co	0.51	1	0.52	0.037	0.024
^{40}K	0.67	0.49	1	0	0
^{214}Bi	3.37	1.52	0.96	1	0.075
^{208}Tl	2.53	0.69	0.62	0.45	1

Each row indicates the fractional interferences between a nuclide and the other nuclides represented in the columns.

Table A.3 Stripping ratios measured November 2000

Window	Radionuclide	Exponential Altitude Coefficient (m^{-1})	Slope of Calibration Line
1	^{137}Cs	0.0132	0.340
2	^{60}Co	0.011	1.0
3	^{40}K	0.00100	6.817
4	^{214}Bi	0.00661	2.019
5	^{208}Tl	0.00768	0.575
6	gamma dose rate	0.00945	0.0007

Table A.4 Calibration Constants

Date	Resolution at 661 KeV(%)	Gross ^{137}Cs count rate	Net ^{137}Cs count rate
8/5/2000	9.2	2104	1642
10/5/2000	9.1	2106	1649
11/5/2000	9.0	2085	1638
12/5/2000	9.2	2281	1620
13/5/2000	9.4	2239	1626

Table A.5 16 litre Nal(Tl) detector daily performance check

Root file name	Date	Time	Number of files	Comments
MOLA1	10/5/2000	0930-1030	697	Reconnaissance flight
MOLA2	10/5/2000	1105-1150	534	
MOLA3	11/5/2000	0815-0935	966	
MOLA4	11/5/2000	0935-1015	469	
MOLA5	11/5/2000	1105-1250	999	
MOLA6	11/5/2000	1250-1255	60	
MOLA7	11/5/2000	1630-1700	262	
IREA1	12/5/2000	1450-1550	771	
IREA2	12/5/2000	1650-1815	970	
IREA3	12/5/2000	1815-1825	90	
IREA4	12/5/2000	1900-2035	888	

Table A.6 Summary of survey data files

APPENDIX B: COORDINATE TRANSFORMATION

1. INTRODUCTION

Data recorded by the Airborne Gamma Spectrometry system deployed by the SURRC team uses a Navstar GPS to log the position of each measurement. This unit was set to record position as latitude and longitude in the WGS84 datum, although other datums are available this unit can not give the position in a more suitable datum. For the purposes of mapping the data recorded by this system it is necessary to convert the position from WGS84 to the Belgium National Grid. This grid is defined by a latitude and longitude from a Hayford ellipsoid. There are two steps in the conversion from WGS84 to the national grid; conversion to the Hayford ellipsoid, and then to the national grid.

2. WGS84 TO HAYFORD ELLIPSOID

The conversion of latitude and longitude in the WGS84 datum to the Hayford ellipsoid is a three step process; the WGS84 latitude and longitude is converted to a 3D Cartesian coordinate, a Helmert transformation is then applied to convert these 3D Cartesian coordinates to 3D Cartesian coordinates on the Hayford ellipsoid, which are then converted back to latitude and longitude in the Hayford ellipsoid.

For any ellipsoid defined by a semi-major axis length a and eccentricity squared e^2, 3D Cartesian coordinates (X,Y,Z) are obtained from latitude (ϕ) and longitude (λ) by:

$$X = \nu \cos\phi \cos\lambda$$
$$Y = \nu \cos\phi \sin\lambda$$
$$Z = (1 - e^2)\nu \sin\phi$$

where

$$\nu = \frac{a}{\sqrt{1 - e^2 \sin^2\phi}}$$

For the WGS84 datum a=6378138m and e^2=0.006694380.

The Helmert transformation assumes that the rotational parameters r_X, r_Y, r_Z (angles in radians) about the X,Y and Z axes are small. The Cartesian coordinates of a point in system B are derived from Cartesian coordinates in system A by:

$$\begin{bmatrix} x \\ y \\ z \end{bmatrix}^B = \begin{bmatrix} t_x \\ t_y \\ y_z \end{bmatrix} + \begin{bmatrix} 1+s & -r_z & r_y \\ r_z & 1+s & -r_x \\ -r_y & r_x & 1+s \end{bmatrix} \begin{bmatrix} x \\ y \\ z \end{bmatrix}^A$$

where t_X, t_Y and t_Z are translations along the X,Y and Z axes, and s is a scale factor. For the transformation between WGS84 and the Hayford ellipsoid these parameters are:

Parameter	r_x	r_y	r_z	t_x	t_y	t_z	s
Value	-0.419rad	0.830rad	-1.885rad	99.059m	-53.322m	112.486m	0.999999

The 3D Cartesian coordinates in the Hayford ellipsoid produced by this transformation are then converted back into latitude and longitude by:

$$\lambda = \arctan\left(\frac{Y}{X}\right)$$

$$\phi = \arctan\left(\frac{Z\cos\lambda}{(1-e^2)X}\right)$$

where for the Hayford ellipsoid, e^2=0.00672267.

3. HAYFORD ELLIPSOID TO BELGIUM NATIONAL GRID

The algorithm to convert from the Hayford ellipsoid to the Belgium grid was developed from equations given in the report by the Institut Géographique National (1989).

The Hayford ellipsoid is defined by a major axis radius a=6378388 m with a deformation f=1/297. The Belgium grid is based on a Lambert projection, defined by n = 0.7716421928 and K = 11565915.812935 and a reference meridian λ_0 = 4°21'24"983. The rotational transformation parameter α = 29"2985 and translational parameters ΔX = 0.01256 m and ΔY = 88.4378 m.

The transformation from latitude and longitude (ϕ, λ) to the Belgium grid position (X, Y) is given by:

$$X = 150000 + \Delta X + R\sin(\theta - \alpha)$$

$$Y = 5400000 + \Delta Y - R\sin(\theta - \alpha)$$

where

$$R = K\left(\tan\tfrac{z}{2}\right)^n$$

$$\tan\tfrac{z}{2} = \tan\left(\tfrac{\pi}{4} - \tfrac{\phi}{2}\right)\left(\frac{1+e\sin\phi}{1-e\sin\phi}\right)^{\frac{e}{2}}$$

$$b = a(1-f)$$

$$\theta = n(\lambda - \lambda_0)$$

$$e^2 = \frac{a^2 - b^2}{a^2}$$

These equations were encoded in a program which was tested by comparing the results of the resulting code with the output from a website incorporating a Javascript transformation (http://web.inter.nl.net/hcc/Ed.Stevenhagen/groeven/geo/lambert1.htm). The conversion from the Hayford ellipsoid to the Belgian grid using the algorithm above and the website agreed to within 50cm. The conversion between WGS84 and the Hayford ellipsoid and hence to the Belgian national grid were included into the standard analysis program used for AGS data.

APPENDIX C: DETAILED MAPS AND SPECTRA

Appendix C contains detailed maps for each site and a brief discussion of their main features. Each site is represented by a short series of maps. This page lists the site index. The individual maps for each site are listed together with a short discussion at the beginning of each section.

The purpose of these maps is to provide more spatial detail of the configuration of the different sites in relation to the radiation fields observed in the survey. Since the nature and levels of radiation associated with individual sites differ markedly, it is not considered practicable to produce a single set of colour scales appropriate to each nuclide and site. For comparative purposes the general maps in the main report may be of greater interest. The detailed maps produced here attempt to illustrate the local configuration of the most pronounced or relevant features associated with each site. As pointed out in section 2.4 the numerical data set serves as the primary source of further detailed information.

1. BELGIAN NUCLEAR RESEARCH CENTRE (SCK-CEN) SITE

During the morning of the 10th May the BR1 reactor was operating, and as a result was releasing ^{41}Ar into the atmosphere. Spectra recorded down wind of the reactor at that time clearly show the 1293.6 keV ^{41}Ar peak, which produces radiometric signals influencing ^{40}K, ^{60}Co, ^{137}Cs and the gamma dose rate maps. Figure C.1 shows the gamma dose rate map for the site in greater detail. Whereas the largest radiometric feature in this map originates from Belgoprocess site 2, in the vicinity of the BR2 and BR3 reactors; the main signals due to current activities from SCK-CEN are located at the western side of the site. Figure C.2 shows spectra recorded during BR1 operations, with clear registration of ^{41}Ar, and also summed spectra at the plots of land deliberately contaminated by ^{134}Cs and other short lived nuclides for agricultural research purposes. Figures C.3 and C.4 show respectively the area to the west of the site both while the BR1 reactor was operating, and at times when it was not. The first of these shows the ^{41}Ar signal clearly, while the latter shows the signals associated with the agricultural research plots clearly in the absence of ^{41}Ar.

FIGURES

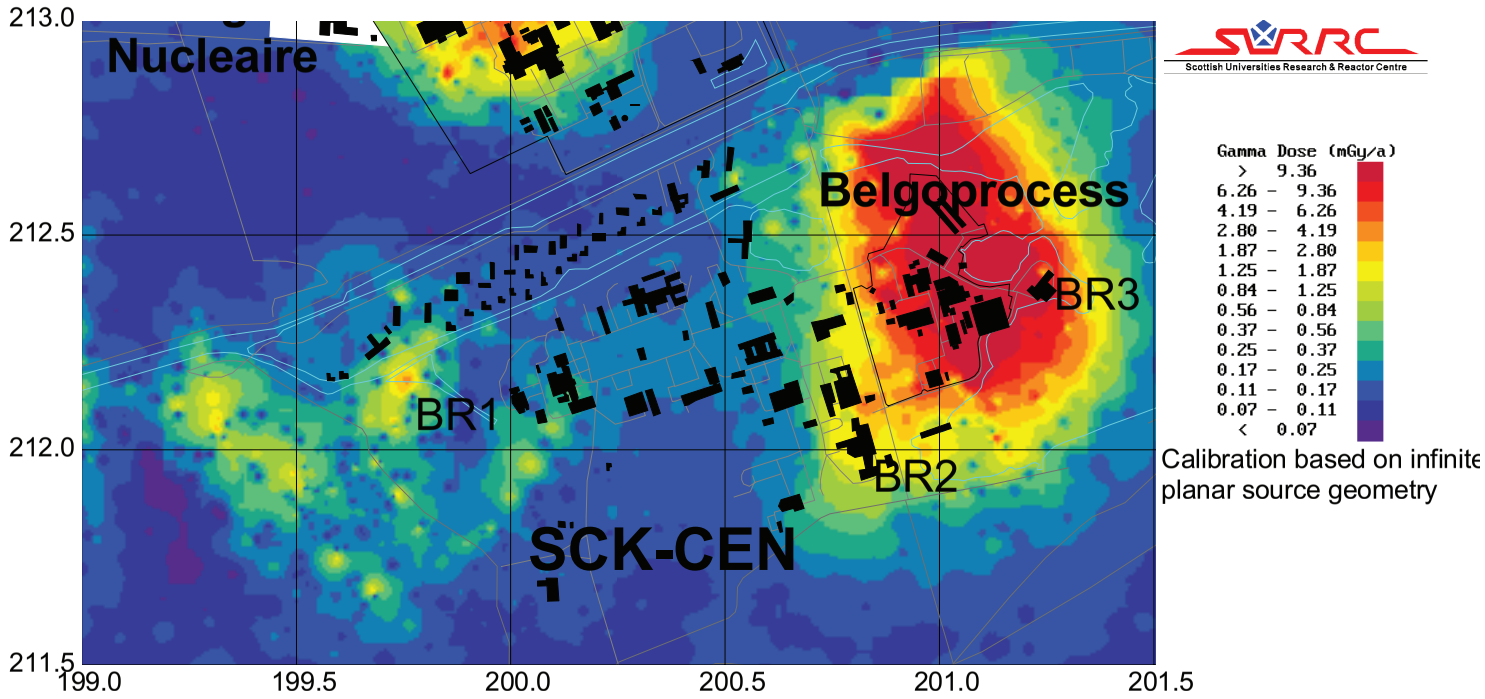

Figure C.1 Gamma-dose rate map for the area surrounding the SCK-CEN site, incorporating observations affected by ^{41}Ar released from BR1

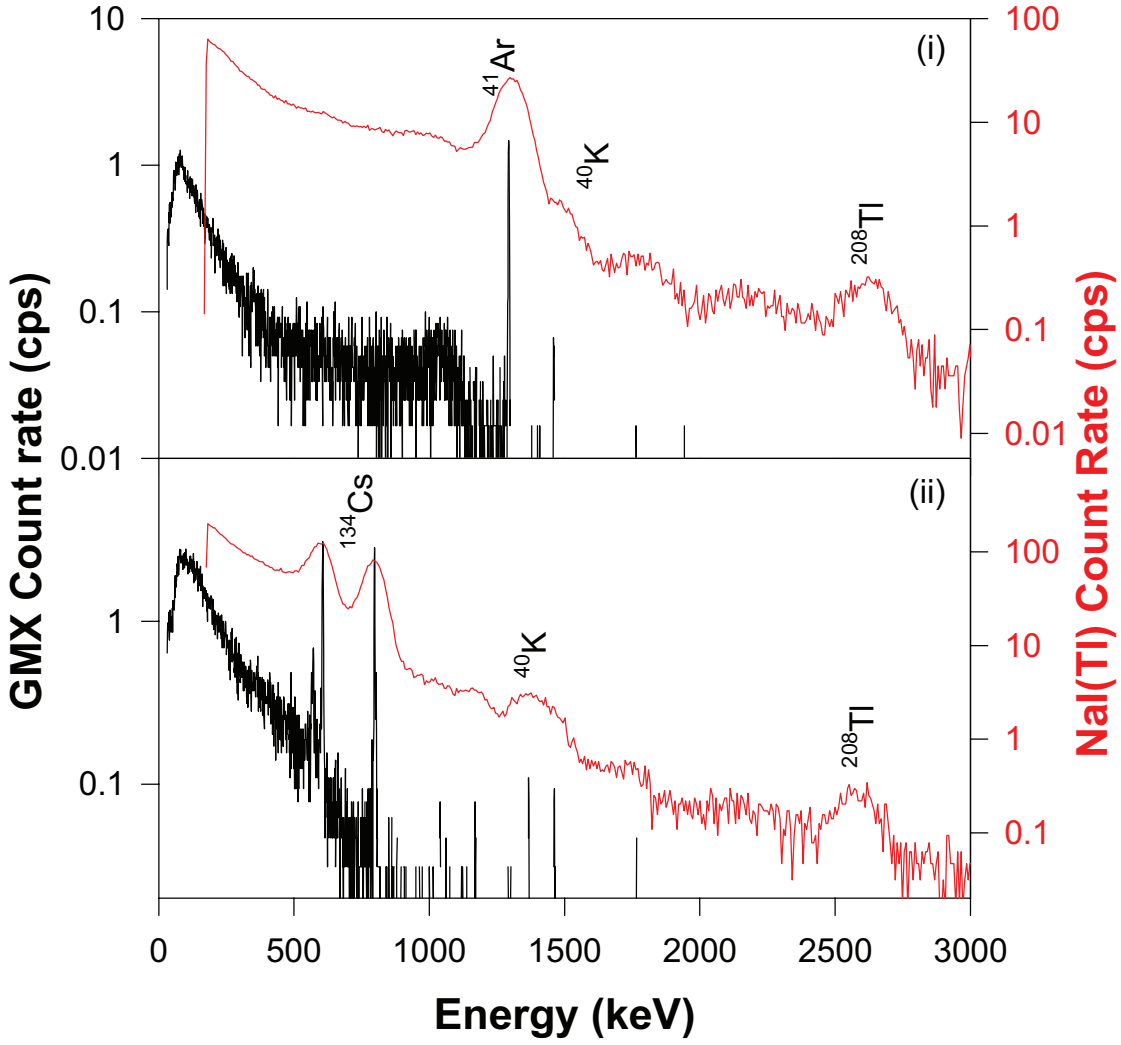

Figure C.2 Gamma-ray spectra in the vicinity of SCK-CEN showing (i) ^{41}Ar from the BR1 reactor, (ii) ^{134}Cs from labelled cultivation plots near the site

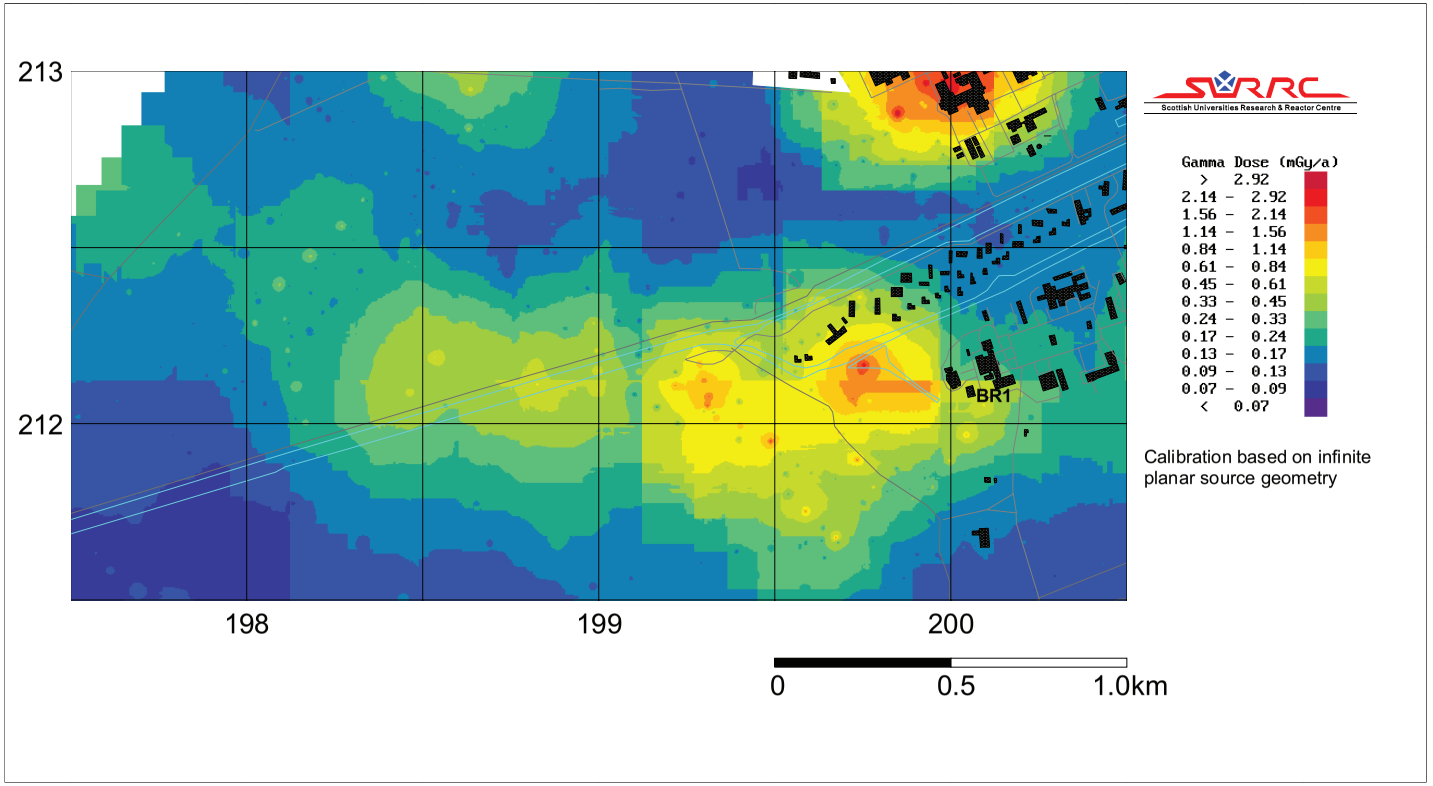

Figure C.3 Gamma-dose rate map showing interference from the ^{41}Ar plume from BR1. Note that the dose rate calibration is based on a terrestrial radionuclide distribution, and therefore does not quantify the dose rate due to ^{41}Ar at ground level

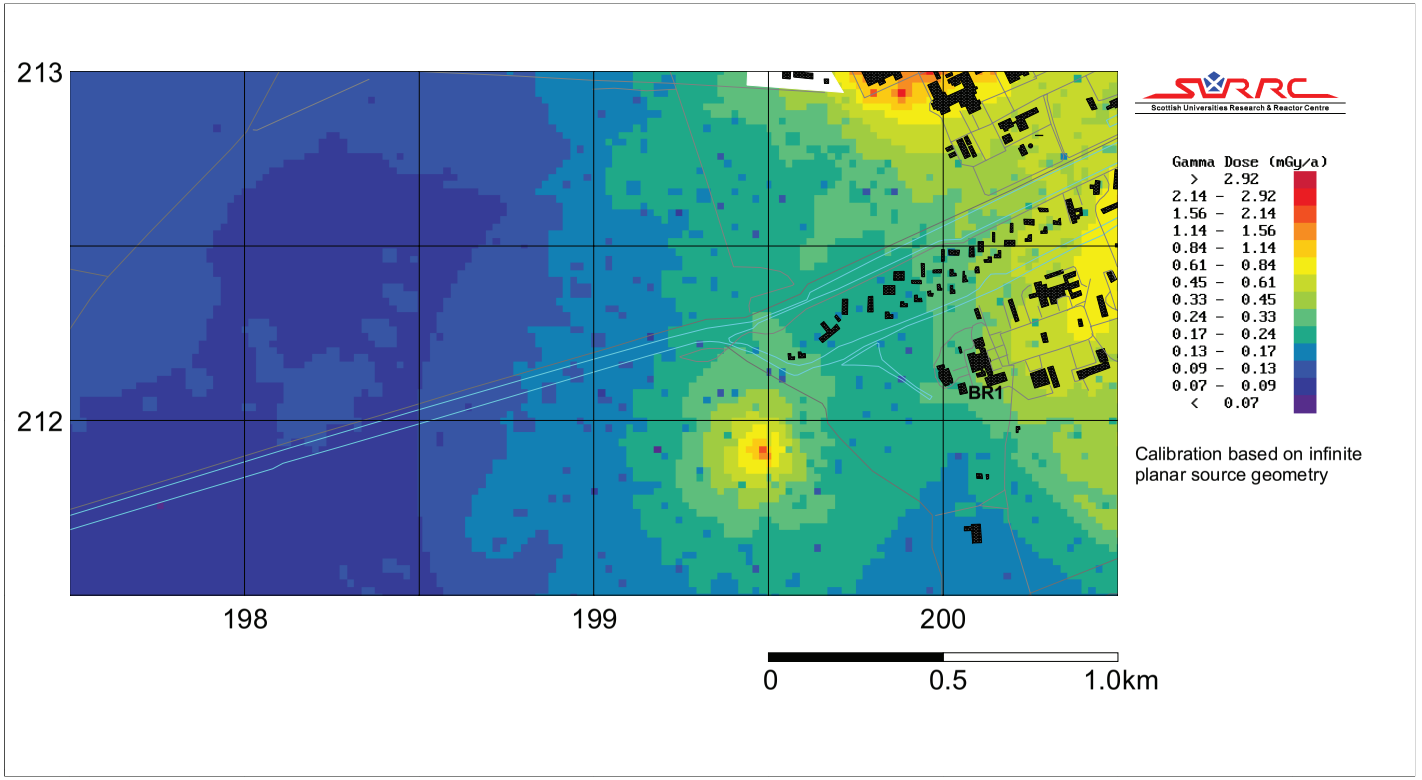

Figure C.4 Gamma-dose rate map in the location of figure C.3, when BR1 is not operating, showing the position of the labelled cultivation plots to the west of the SCK-CEN site.

2. BELGOPROCESS SITE

The two Belgoprocess sites have different radiometric characteristics as shown in the succeeding figures.

Belgoprocess site 1, to the north of the Kanaal Bocholt-Herentals, shows strong signals due to ^{137}Cs, ^{60}Co and U series activity, in proportions which change in different parts of the site. Figure C.5 shows spectra recorded on the western, central and eastern parts of the site; whereas ^{60}Co and uranium derived signals are present in central and western areas, the eastern areas show relatively greater proportions of ^{137}Cs. The extent of shielding of these sources can also be judged by the extent of forward scattering around the ^{137}Cs peaks, indicating the presence of massive shielding in particular in the eastern features. Figures C.6, C.7 and C.8 shows the distribution of ^{137}Cs, ^{60}Co and ^{214}Bi on the site. ^{137}Cs is distributed more evenly across the central and eastern parts of the site than ^{60}Co and ^{214}Bi which mainly occupy central areas. The apparently low level of ^{214}Bi on the western side of the site may be related to the combination of source distribution and radiation scattering in the vicinities of buildings. The possibility that part of this signal is associated with the release of ^{222}Rn from Belgoprocess site 2, and its weather-related entrainment in buildings should also be considered. The dose rate within this site is driven largely by ^{60}Co distribution, which is concentrated around the centre of the site.

Belgoprocess site 2, in the NE areas of the SCK-CEN complex includes facilities for the storage of low level nuclear waste, and shows very strong signals due to ^{137}Cs, ^{60}Co and U and Th series activity. Spectra are shown in figures C.10 which indicate the presence of these nuclides, and also the high intensities of scattered radiation associated with the facilities. Whereas the Ge detectors maintain good spectral performance despite the high radiation levels recorded, there is evidence of spectral distortion, coincidence summing, and high levels of scattered radiation in the NaI detectors. This provides clear confirmation of the value of Ge detectors for work in areas with substantially enhanced radiation fields. The maps in figures C.11 to C.15 show the distributions of ^{137}Cs, ^{60}Co, ^{214}Bi, ^{208}Tl and gamma dose rate respectively at site 2. ^{214}Bi activity is high across the entire site, resulting from continuous discharges of gaseous ^{222}Rn from radium wastes stored in buildings on the site. ^{137}Cs and ^{60}Co activity is more localised around the central and northern parts of the site, with the Co activity relatively higher in the northern part. There is a strong ^{208}Tl signal in the south of the site from a more localised source.

FIGURES

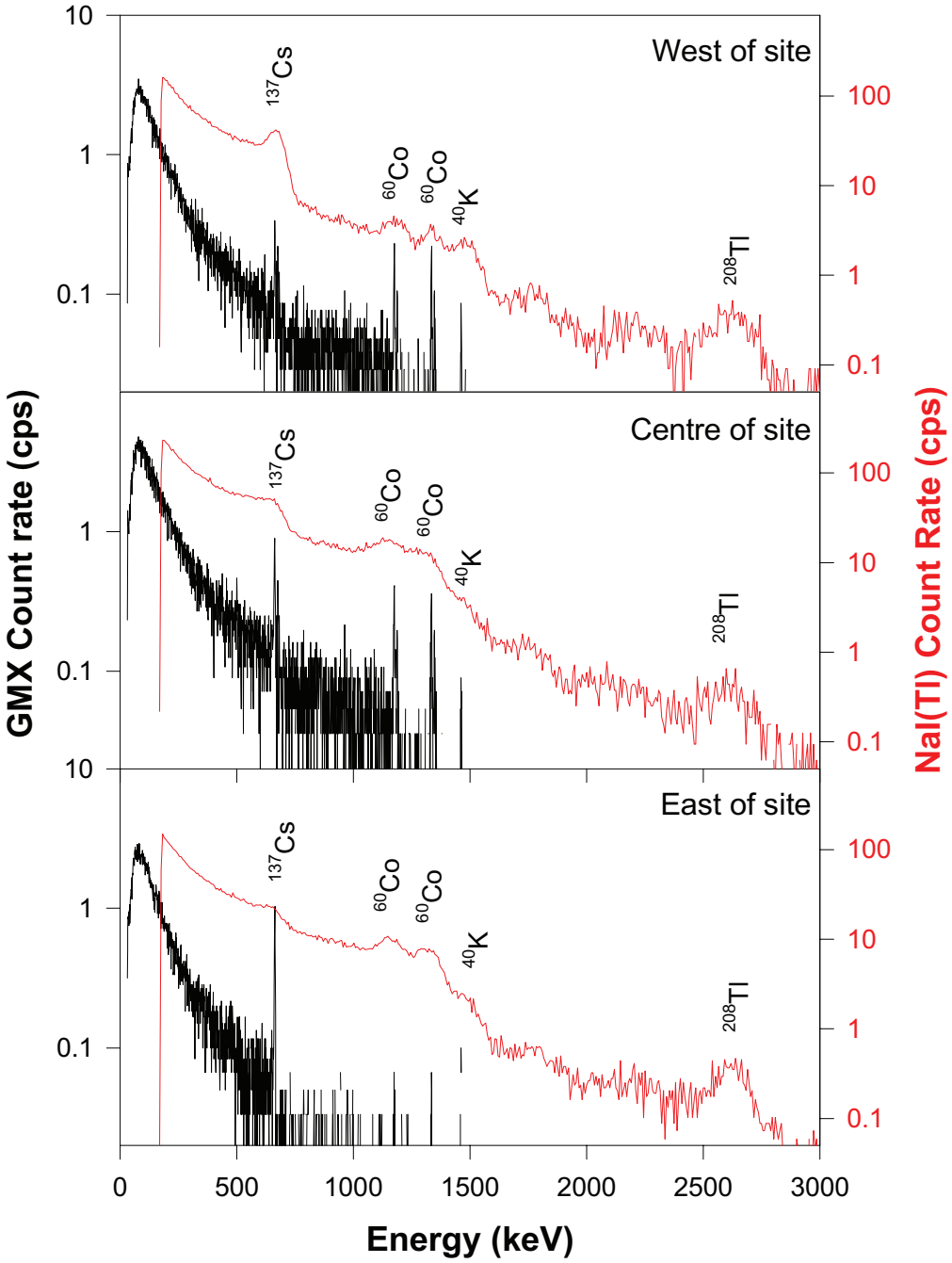

Figure C.5 Gamma-ray spectra for three areas within Belgoprocess site 1

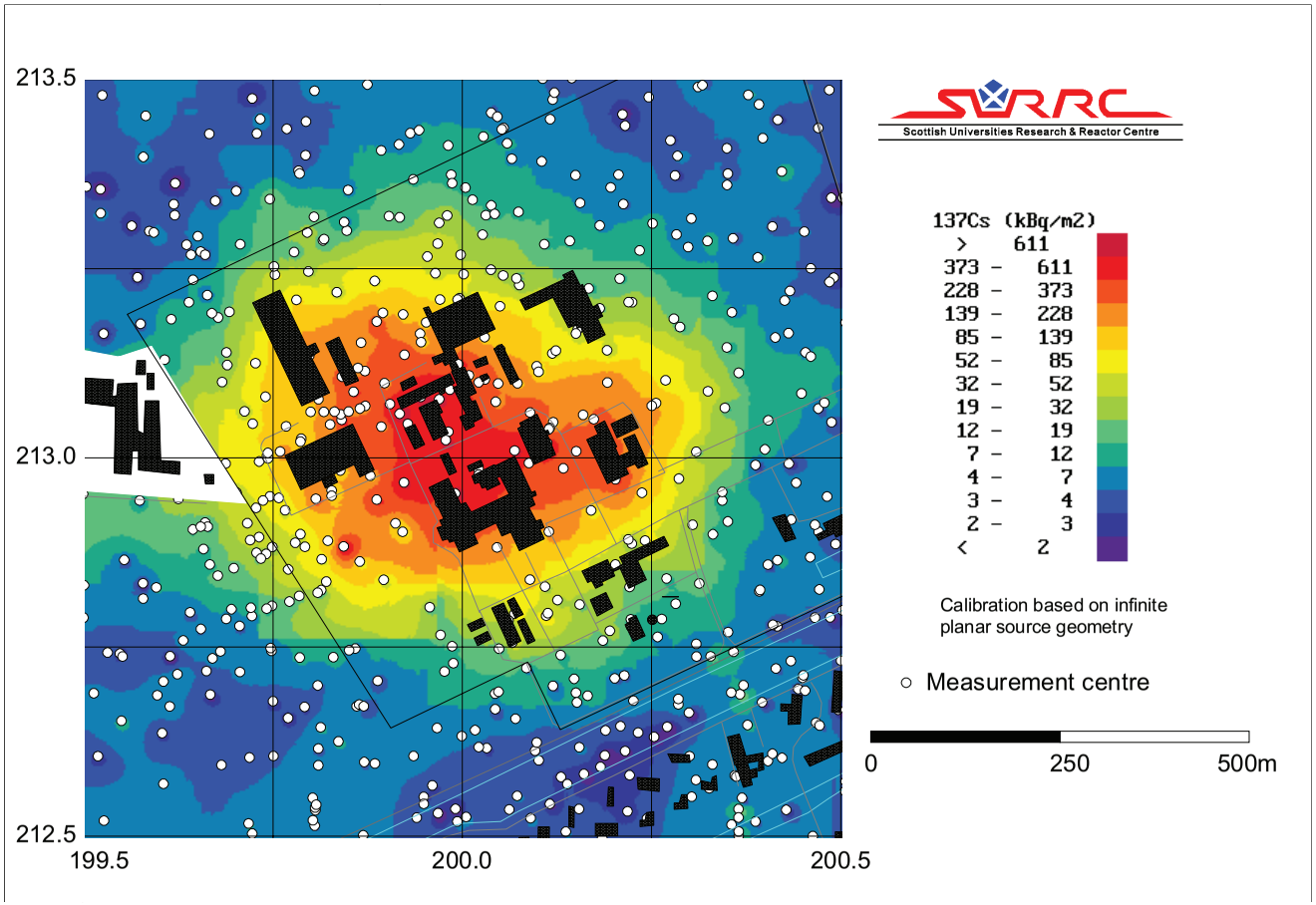

Figure C.6 ^{137}Cs signal distribution around Belgoprocess site 1, as measured from the airborne survey. Note that source geometries, shielding and local configurations are relevant to interpretation.

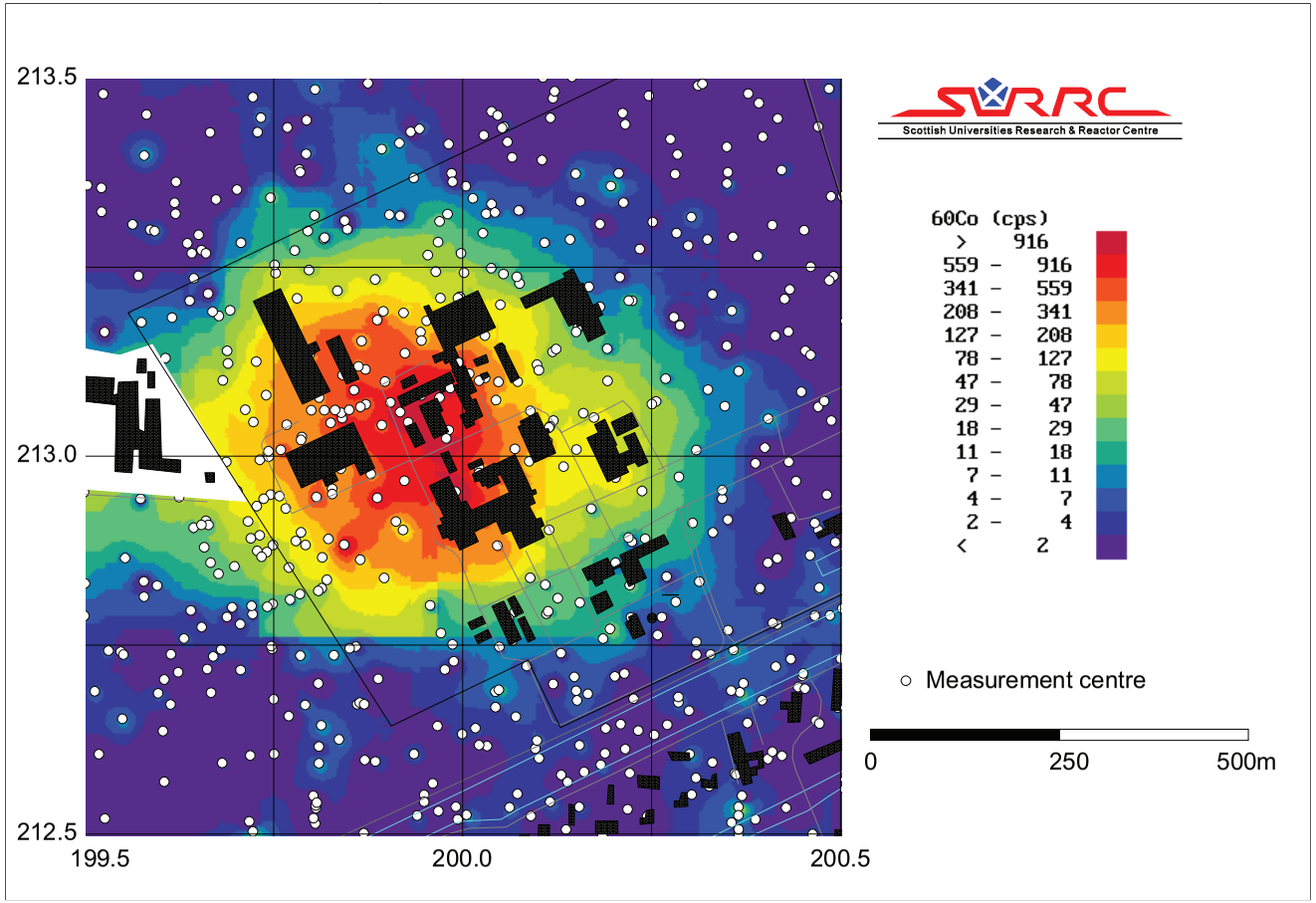

Figure C.7 ^{60}Co signal distribution around Belgoprocess site 1, as measured from the airborne survey. Note that source geometries, shielding and local configurations are relevant to interpretation.

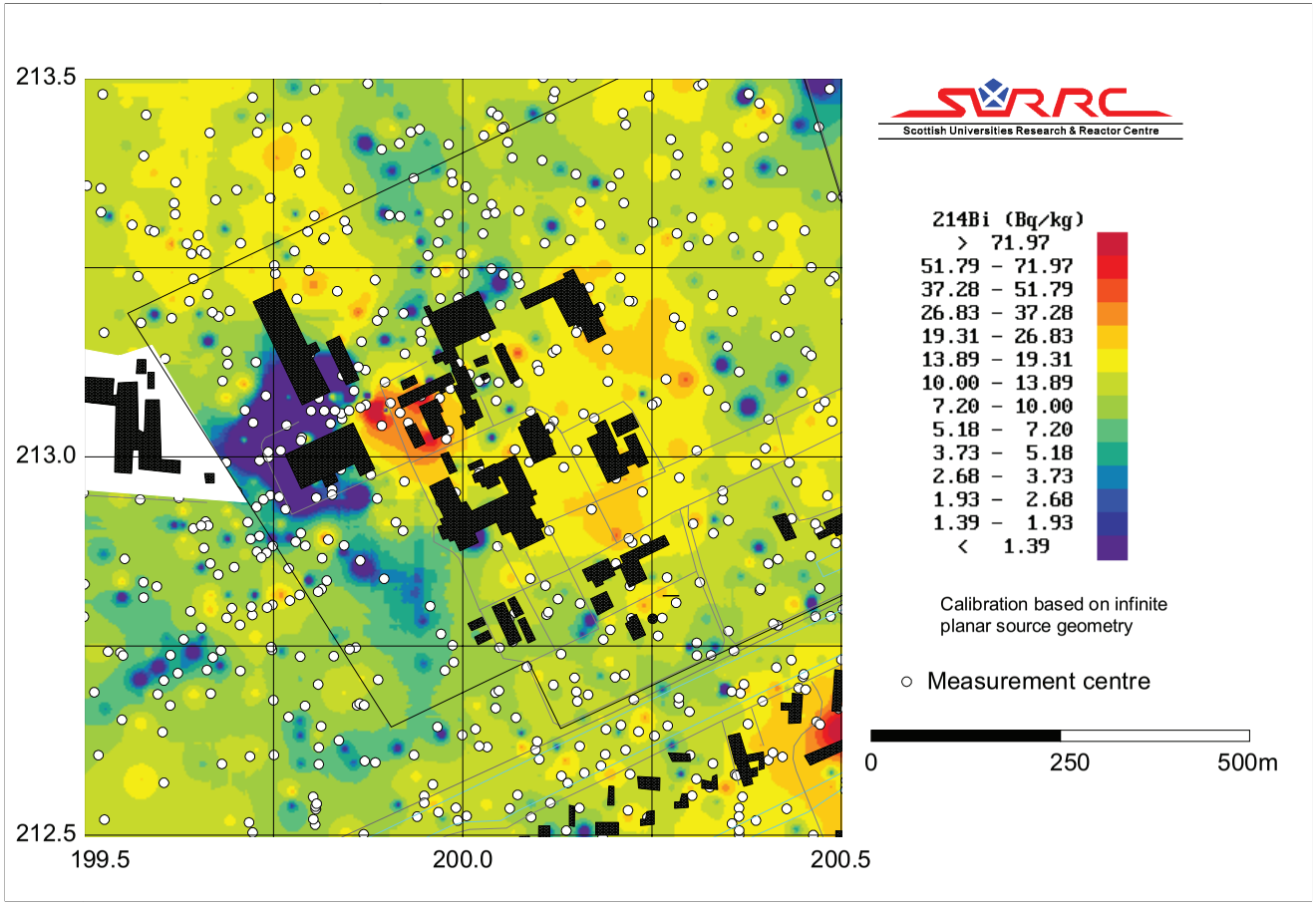

Figure C.8 ^{214}Bi signal distribution around Belgoprocess site 1, as measured from the airborne survey. Note that source geometries, shielding and local configurations are relevant to interpretation.

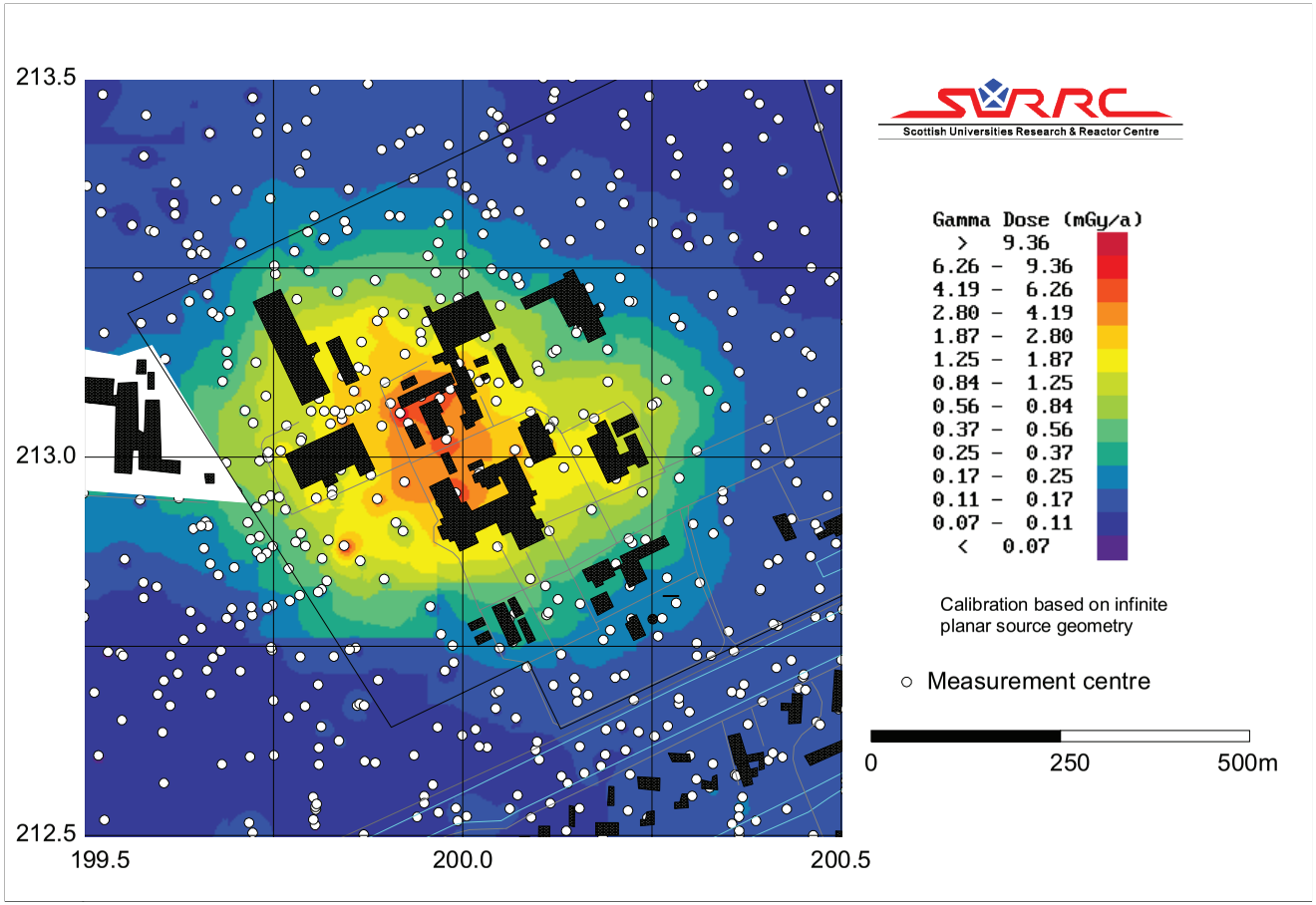

Figure C.9 Gamma-ray dose rate distribution around Belgoprocess site 1, as measured from the airborne survey. Note that source geometries, shielding and local configurations are relevant to interpretation.

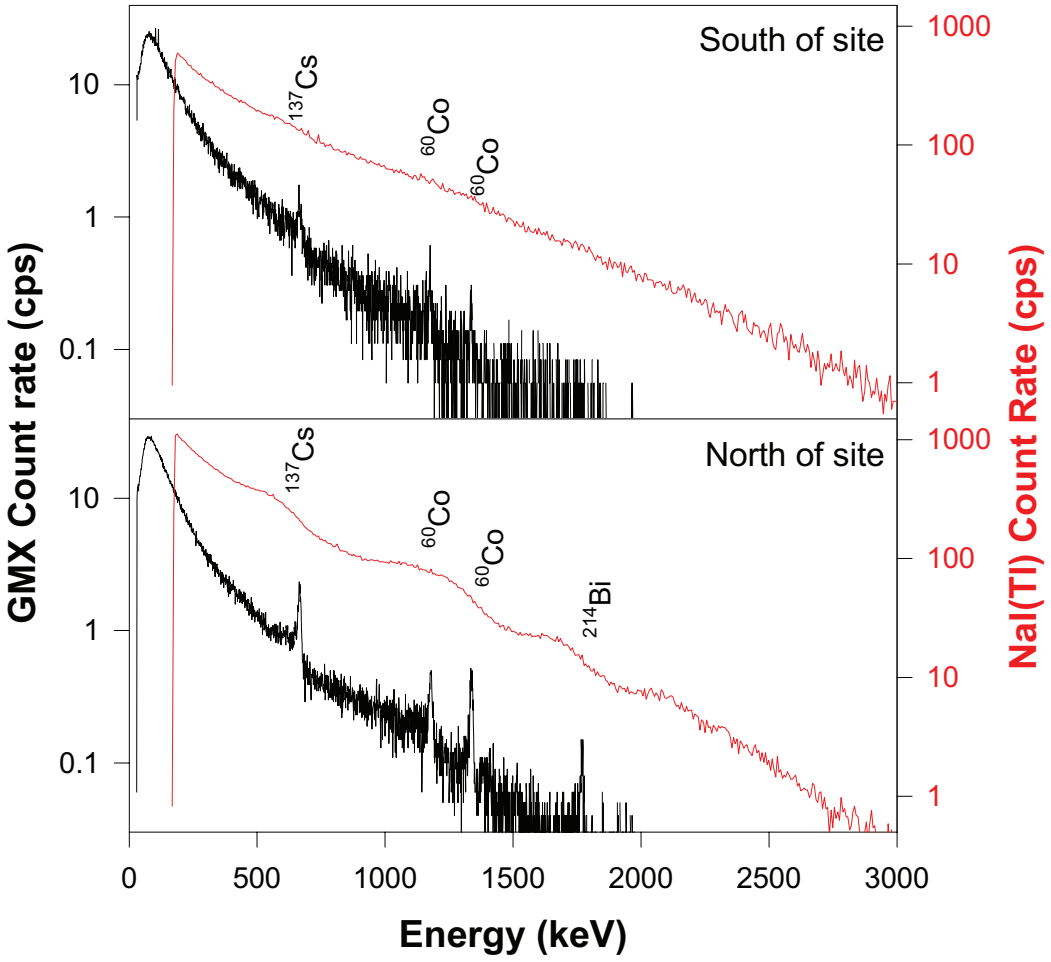

Figure C.10 Gamma-ray spectra for two areas within Belgoprocess site 2

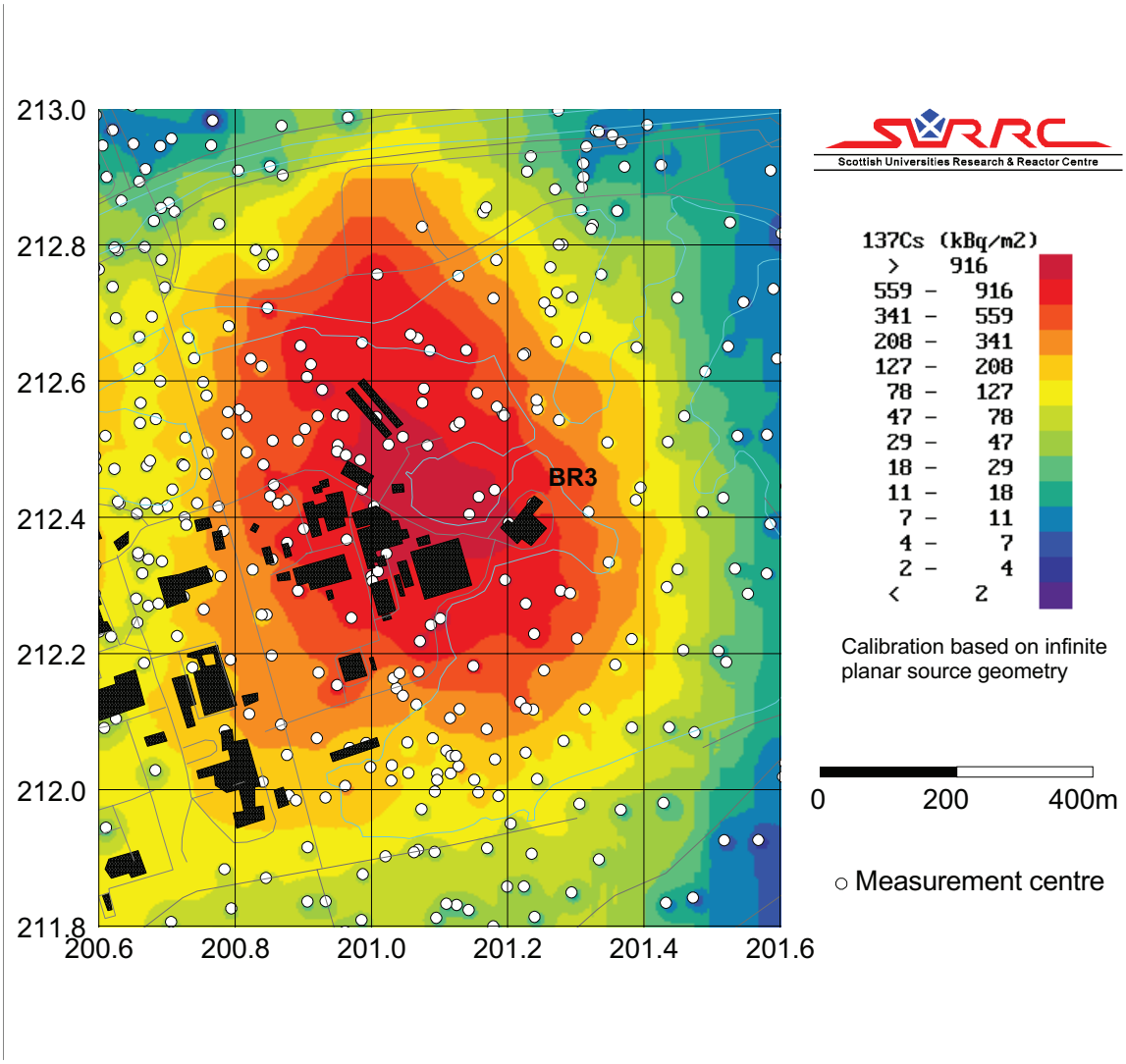

Figure C.11 ^{137}Cs signal distribution around Belgoprocess site 2, as measured from the airborne survey. Note that source geometries, shielding and local configurations are relevant to interpretation.

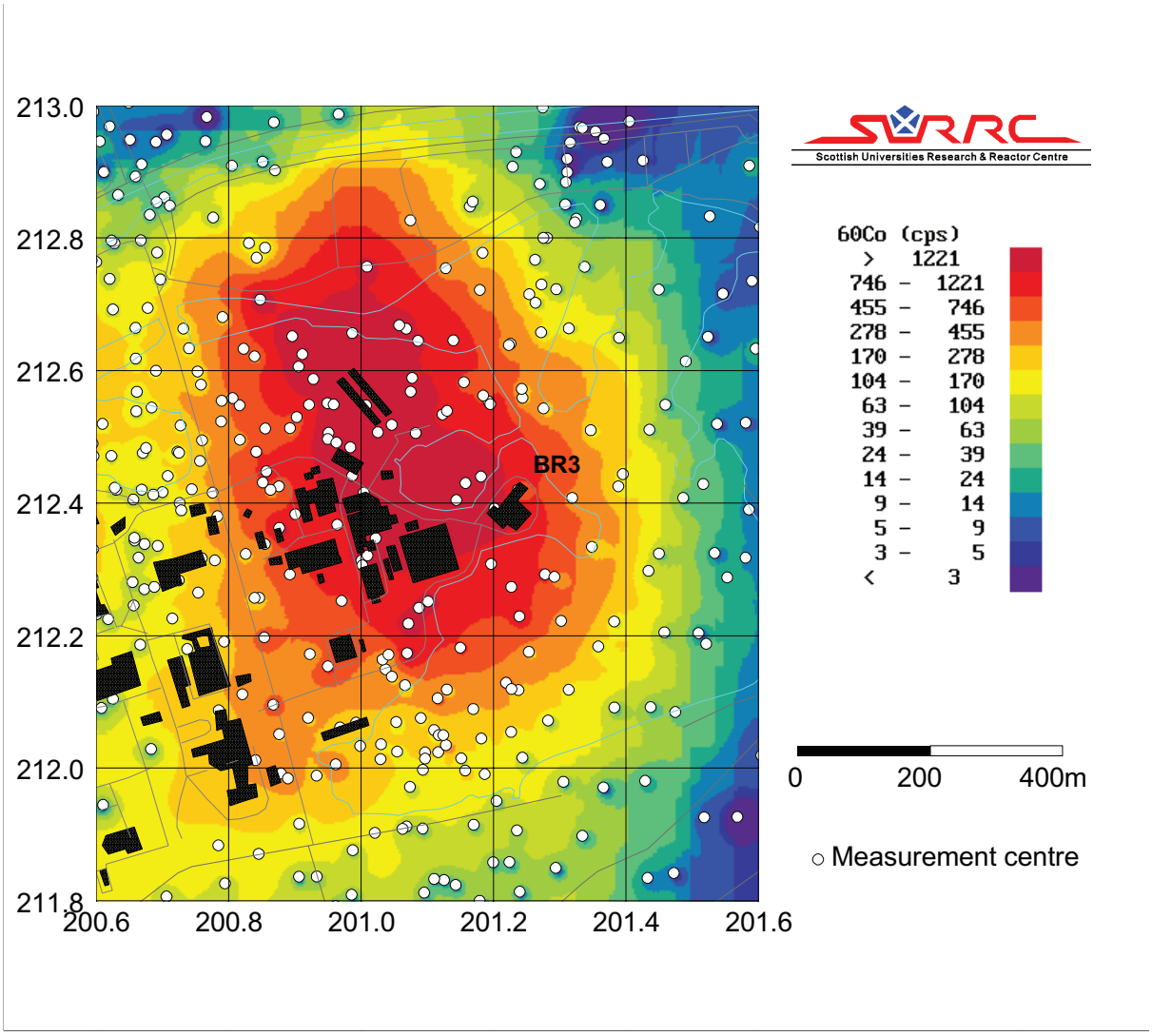

Figure C.12 ^{60}Co signal distribution around Belgoprocess site 2, as measured from the airborne survey. Note that source geometries, shielding and local configurations are relevant to interpretation.

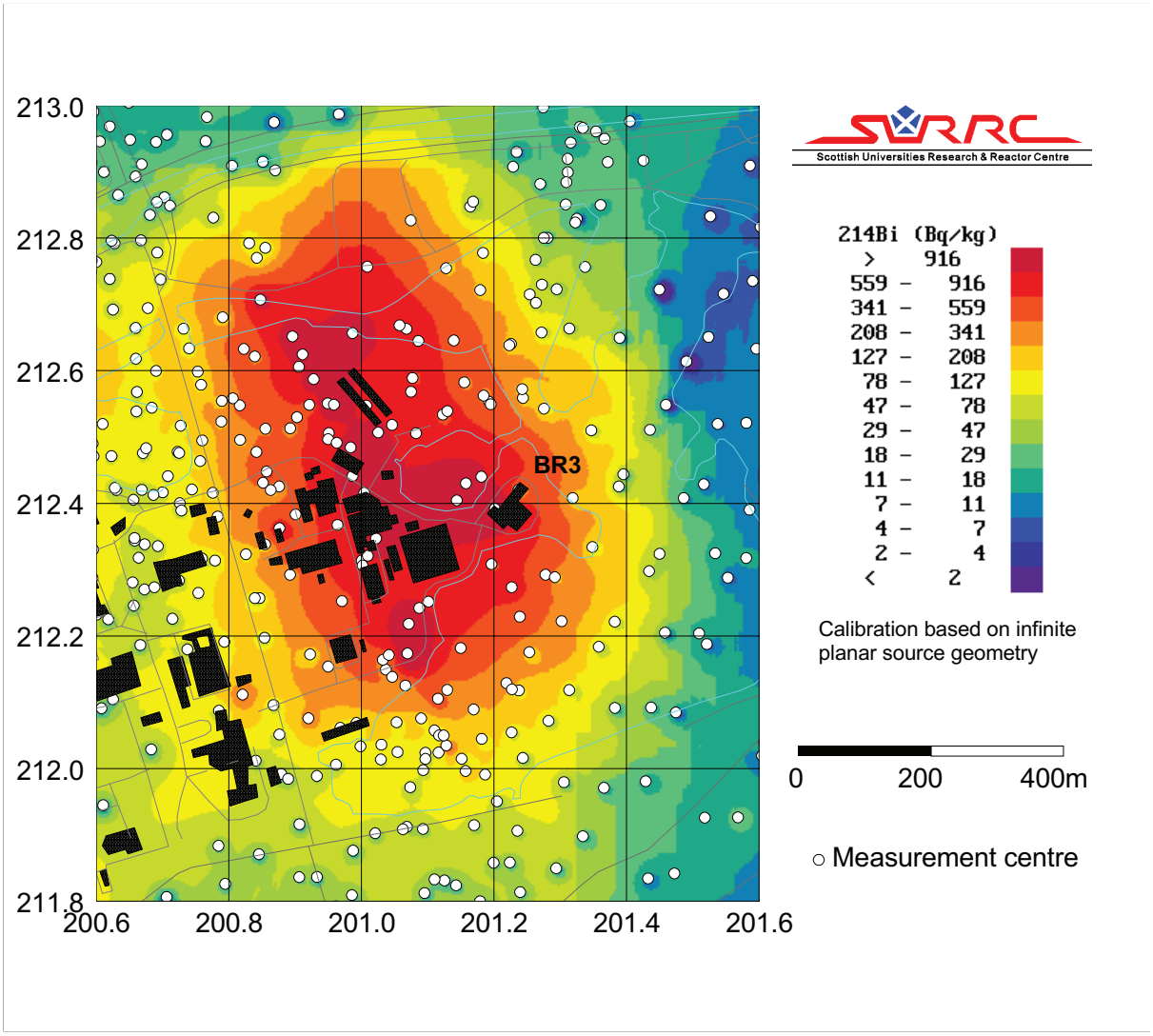

Figure C.13 ^{214}Bi signal distribution around Belgoprocess site 2, as measured from the airborne survey. Note that source geometries, shielding and local configurations are relevant to interpretation.

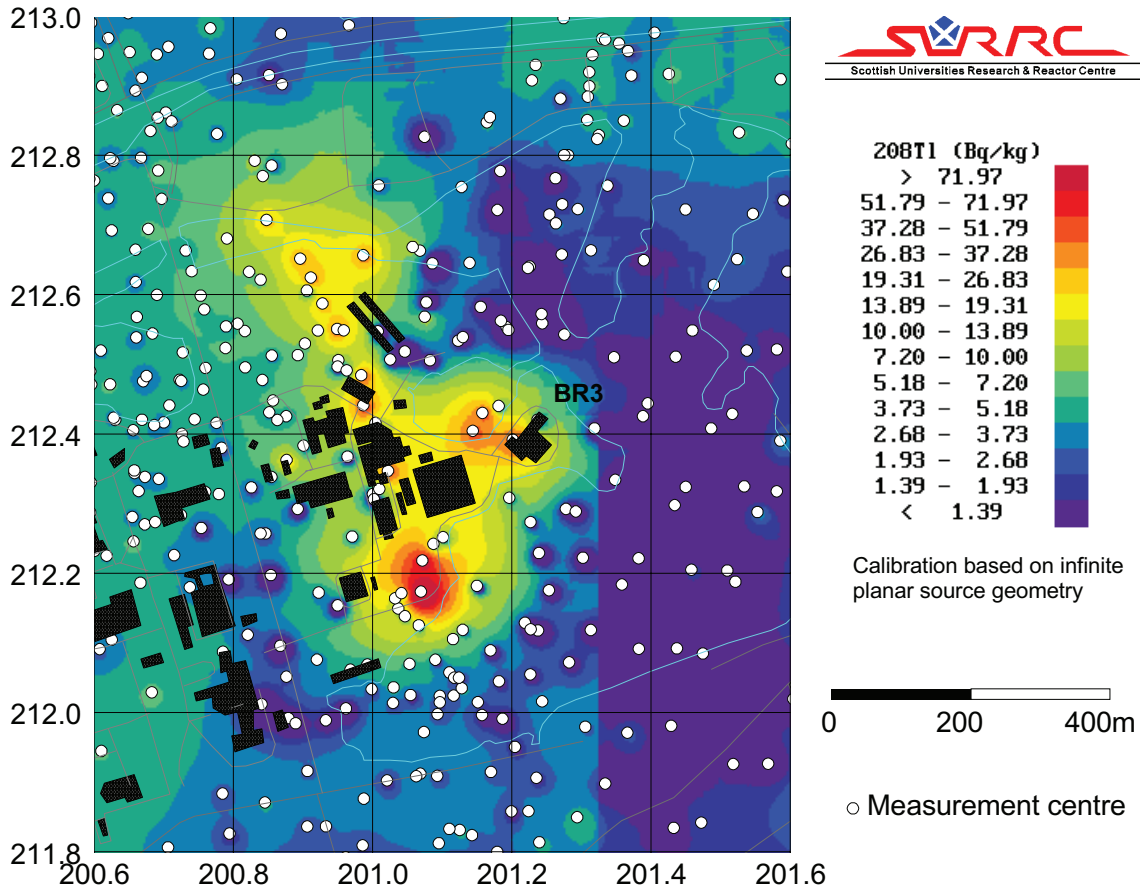

Figure C.14 ^{208}Tl signal distribution around Belgoprocess site 2, as measured from the airborne survey. Note that source geometries, shielding and local configurations are relevant to interpretation.

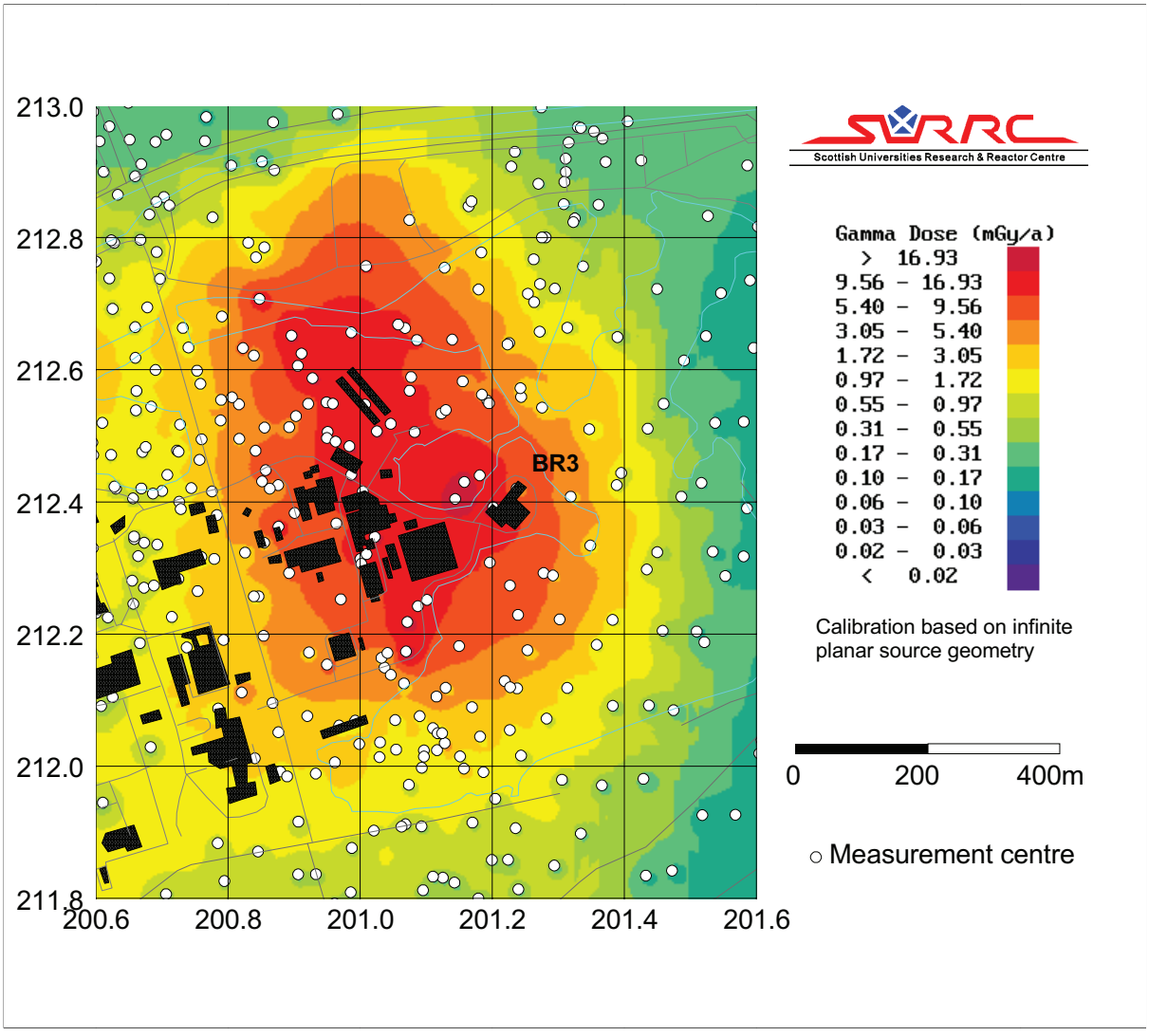

Figure C.15 Gamma-ray dose rate distribution around Belgoprocess site 2, as measured from the airborne survey. Note that source geometries, shielding and local configurations are relevant to interpretation.

3. FBFC SITE

The FBFC fuel fabrication site shows signals due to ^{137}Cs and U series activity and some activity in the spectral window normally associated with ^{60}Co. The spectra recorded over the FBFC do not include any ^{60}Co gamma-ray peaks but do include gamma -rays for ^{234m}Pa at 1001.0 keV from refined uranium, part of this peak is within the window used for ^{60}Co and generates an apparent signal due to ^{60}Co within the FBFC site. Figure C.16 shows spectra from the FBFC site, showing clear evidence of 662 keV radiation, normally attributed to ^{137}Cs, ^{234m}Pa, and enhanced levels of ^{214}Bi relative to normal natural abundances. The data for this site were reanalysed, using a window for ^{234m}Pa instead of ^{60}Co and revised stripping matrix including the ^{234m}Pa interferences. Figure C.17 shows the 662 keV signal distribution after correcting for the presence of ^{234m}Pa, showing low levels of equivalent ^{137}Cs activity(1) on the southern side of the site. The 662 keV signals are most probably associated with MOX materials on site. Figure C.18 shows the ^{234m}Pa signal distribution which is largely associated with the eastern side of the site. The ^{214}Bi signal in figure C.19 is considered to be due to uranium or radium bearing materials associated with past or present activities on site. The gamma dose rate distribution shown in figure C.20 is probably mainly due to the uranium based materials on site.

(1) Equivalent activity of ^{137}Cs (kBq m^{-2}) represents the activity per unit area of ^{137}Cs which would give rise to the observed signal levels under open field conditions.

FIGURES

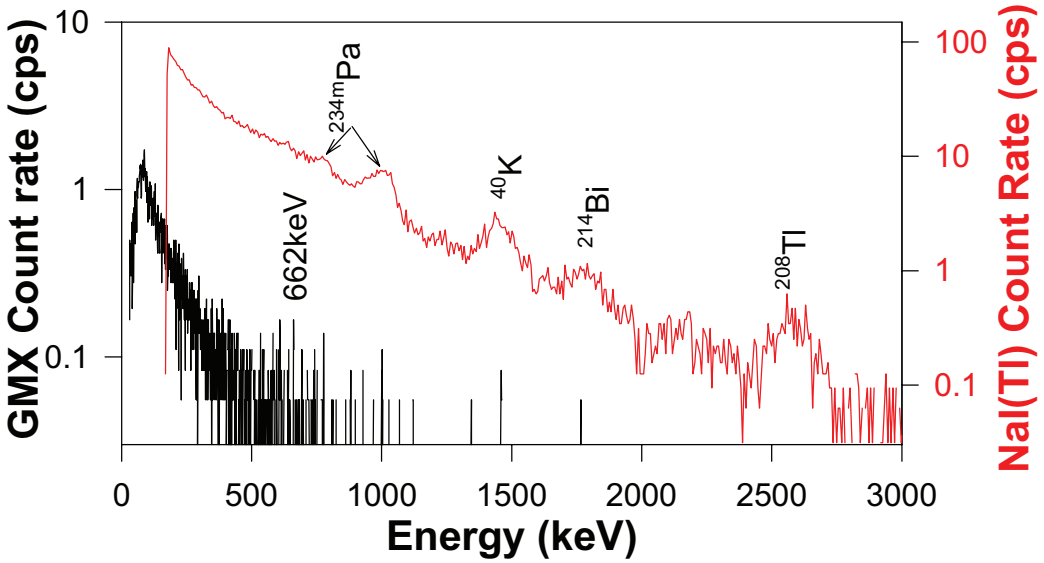

Figure C.16 Gamma-ray spectra from the FBFC site showing evidence of ^{234m}Pa and 662 keV radiation in addition to naturally occuring components

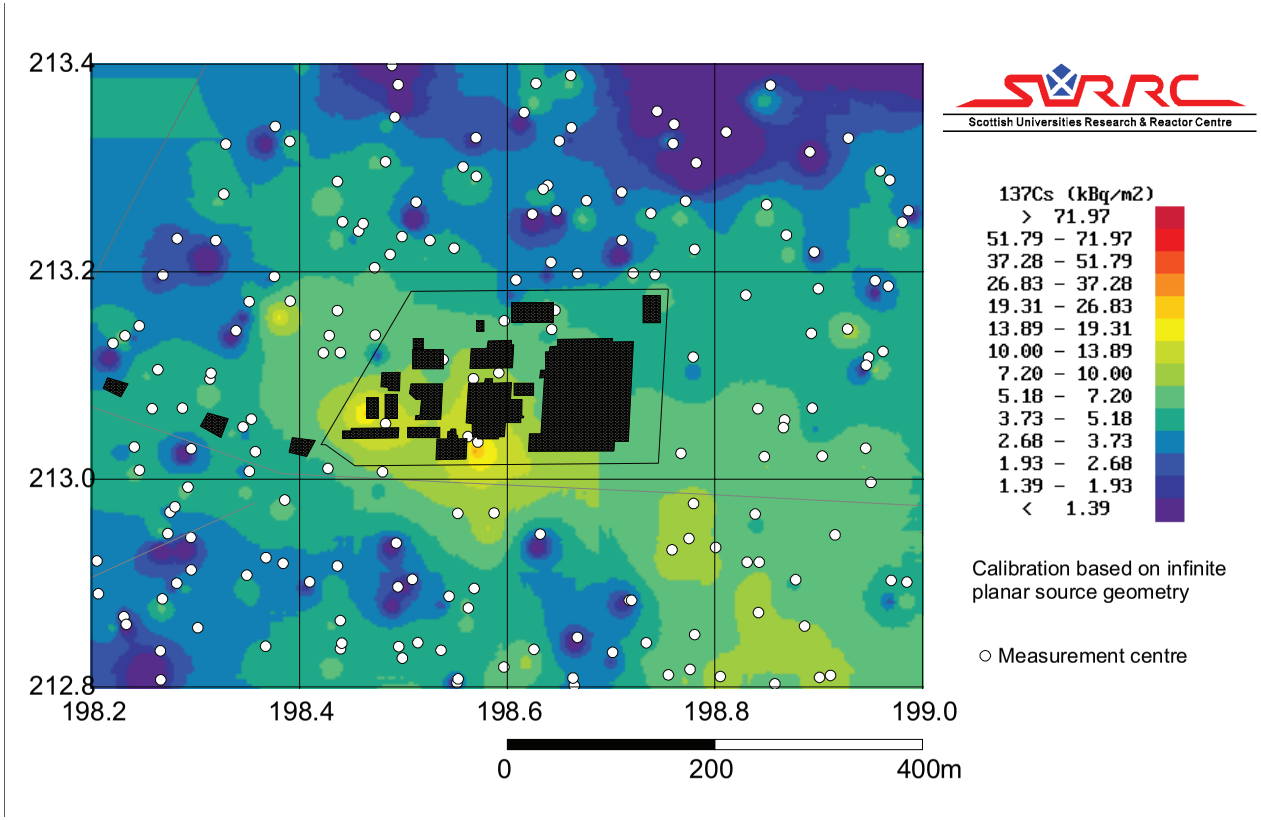

Figure C.17 ^{137}Cs equivalent activity distribution around the FBFC site.

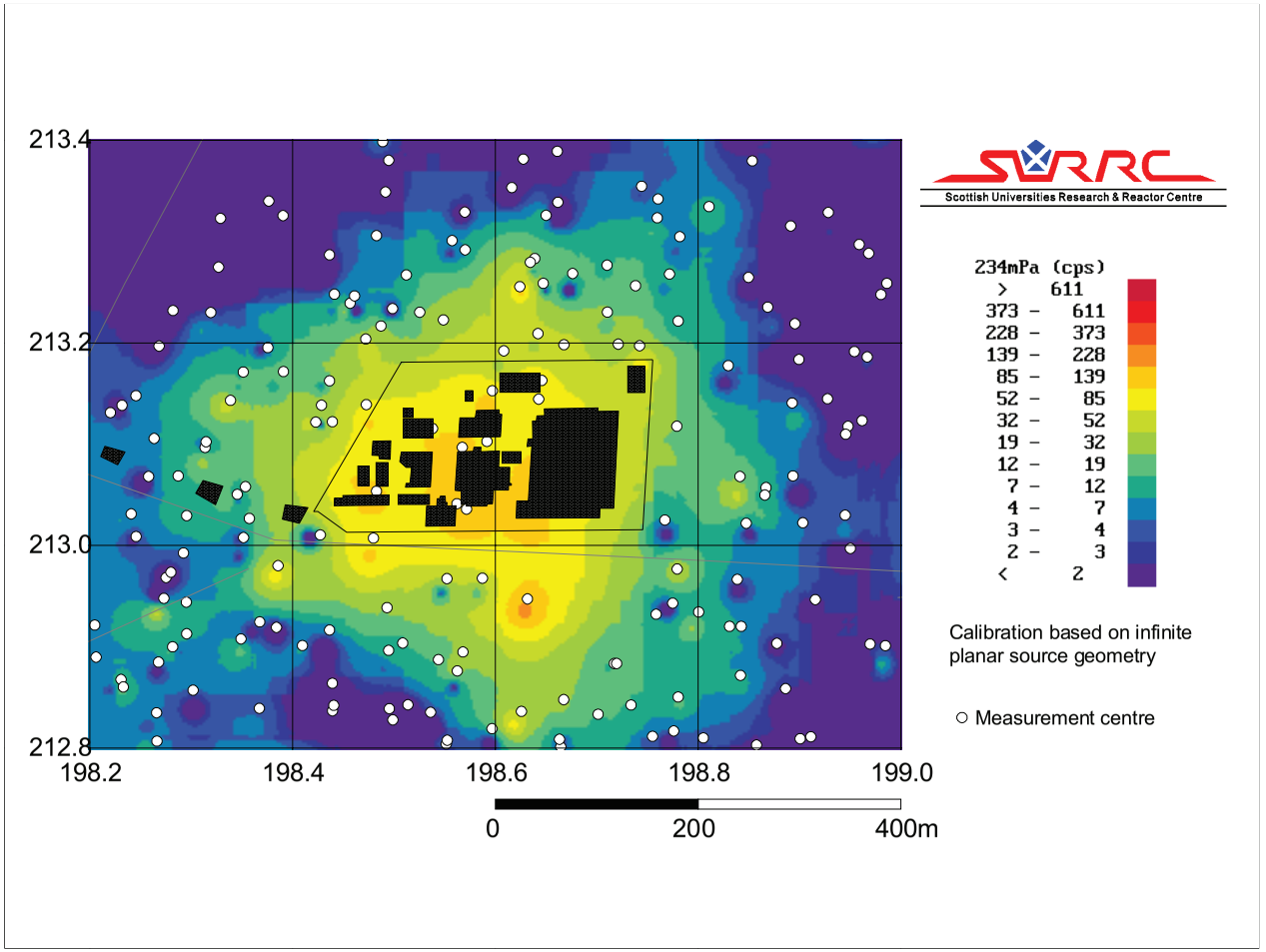

Figure C.18 ^{234m}Pa signal distribution around the FBFC site.

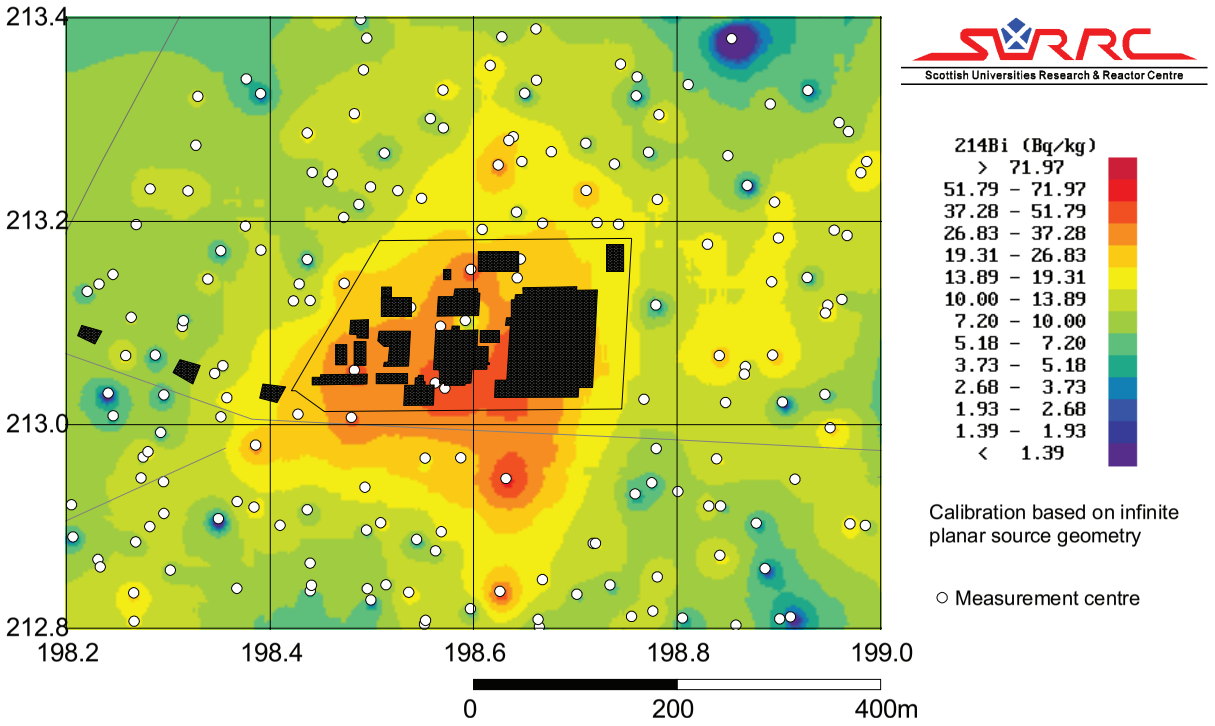

Figure C.19 ^{214}Bi signal distribution around the FBFC site

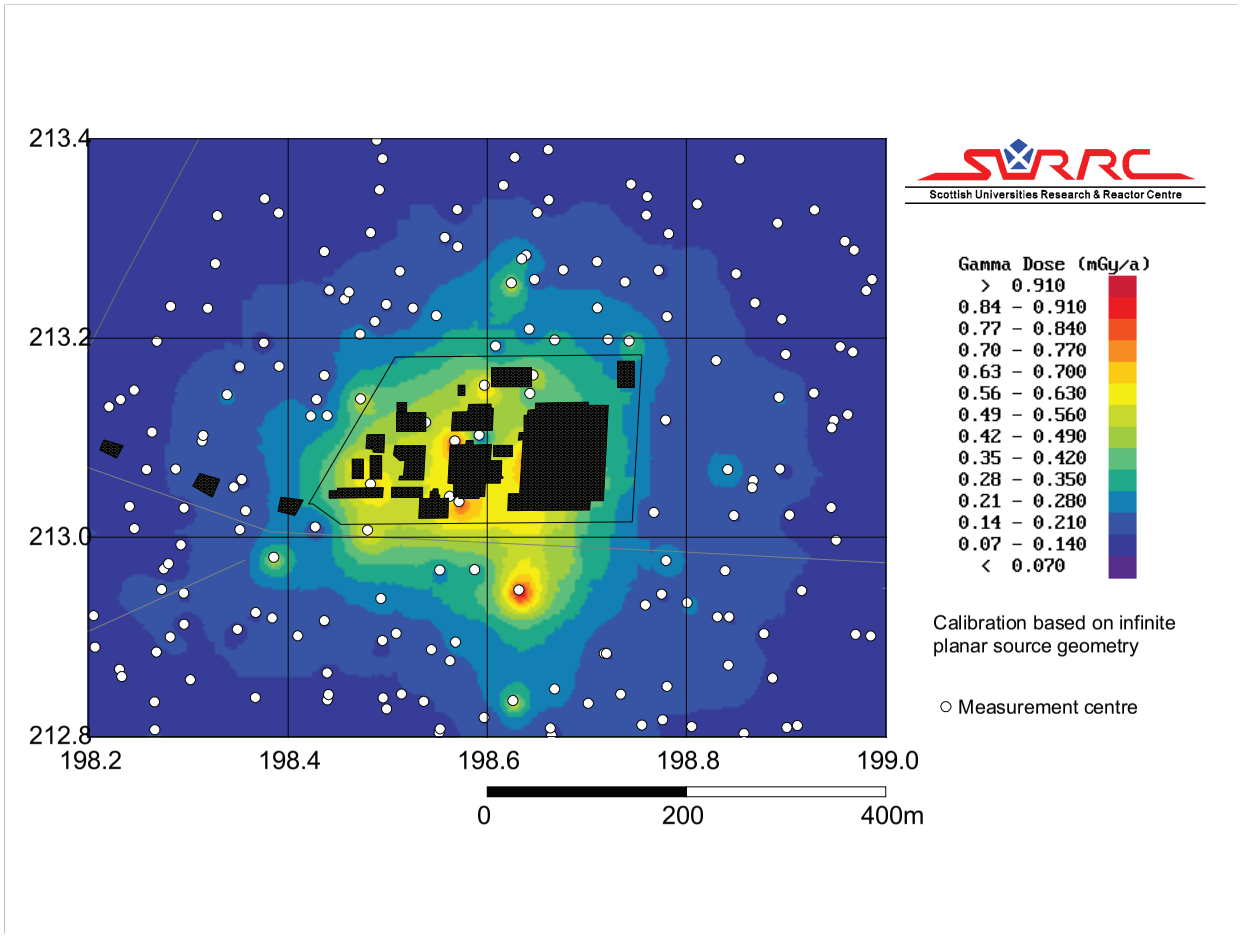

Figure C.20 Gamma-ray dose rate distribution around theFBFC site

4. IRMM SITE

The IRMM site to the south of the survey area contains two accelerators, a LINAC and a Van de Graaff. Slightly enhanced signals in the ^{208}Tl, ^{137}Cs and gamma-dose rate channels were observed associated with the LINAC.

FIGURES

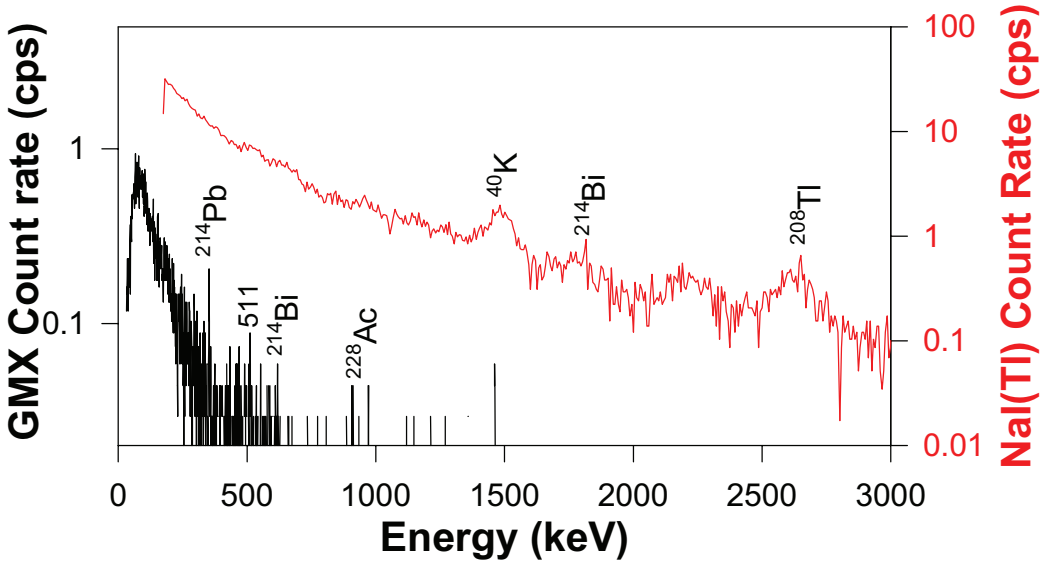

Figure C.21 Gamma-ray spectra recorded in the vicinity of the IRMM LINAC

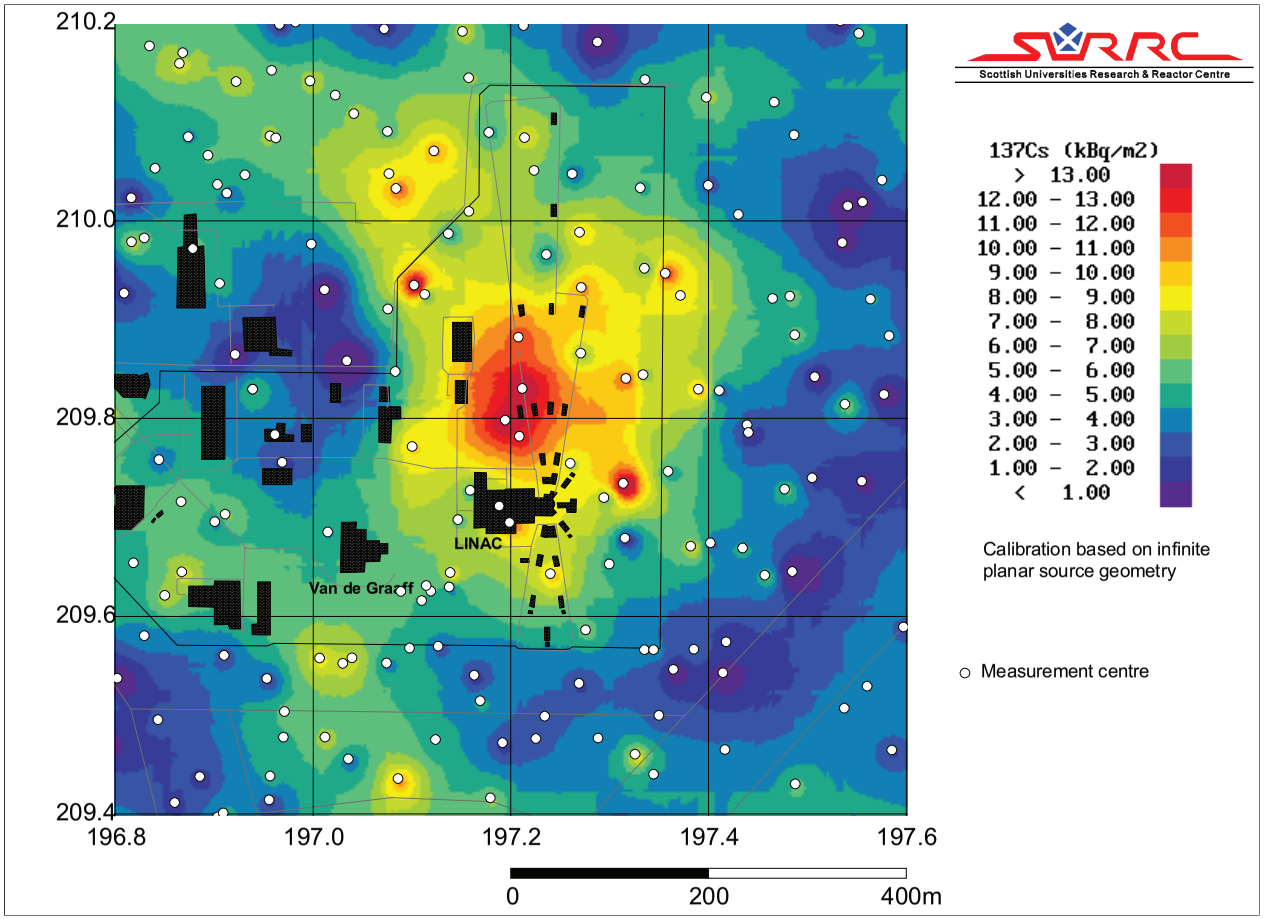

Figure C.22 ^{137}Cs signal distribution around the IRMM site. Note that the low level anomalies are not due to ^{137}Cs, but arise as a consequence of spectral interference from activation products and scattered radiation generated in the vicinity of the LINAC accelerator

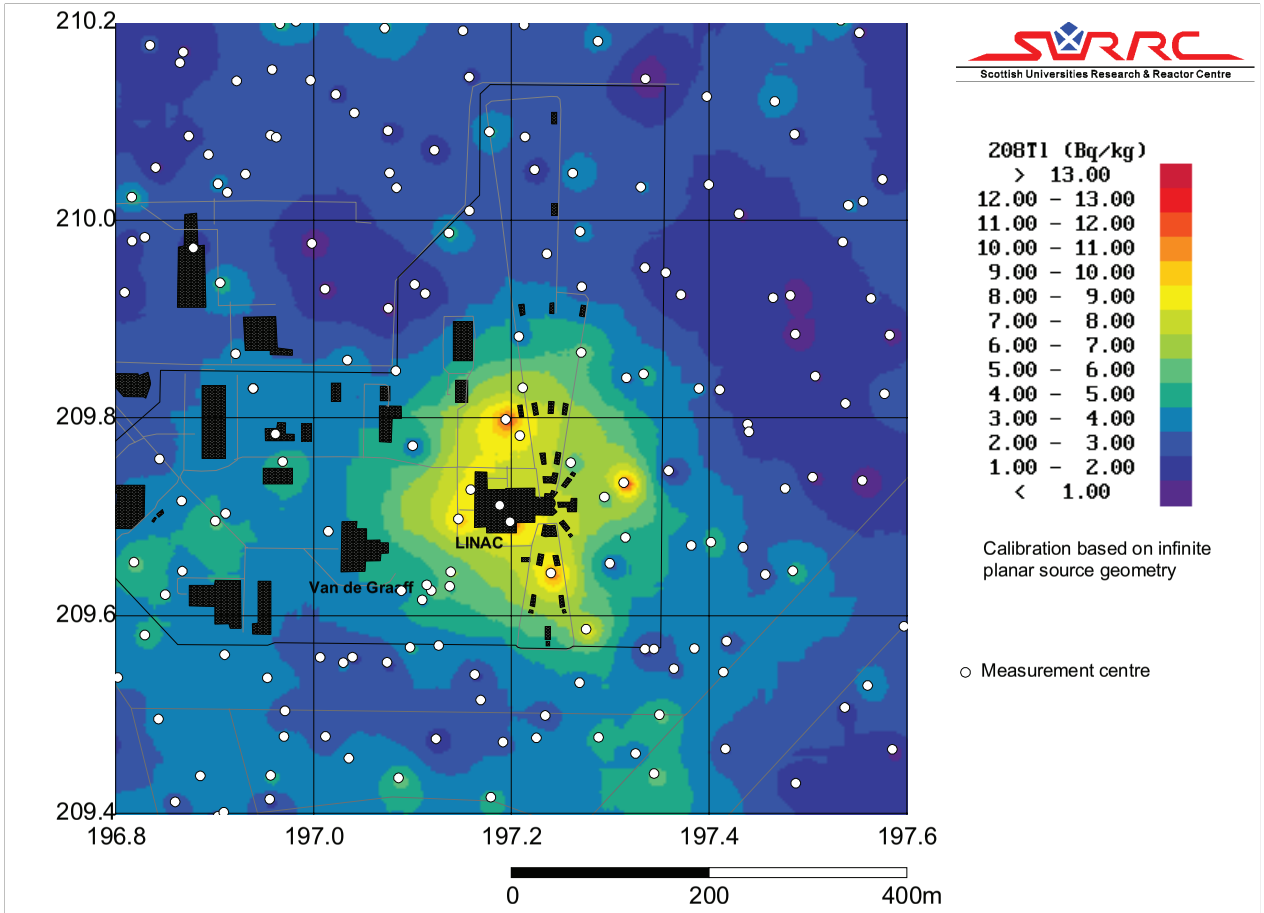

Figure C.23 ^{208}Tl signal distribution around the IRMM site. Note that the anomaly is attributed to the presence of high energy scattered radiation in the vicinity of the LINAC accelerator

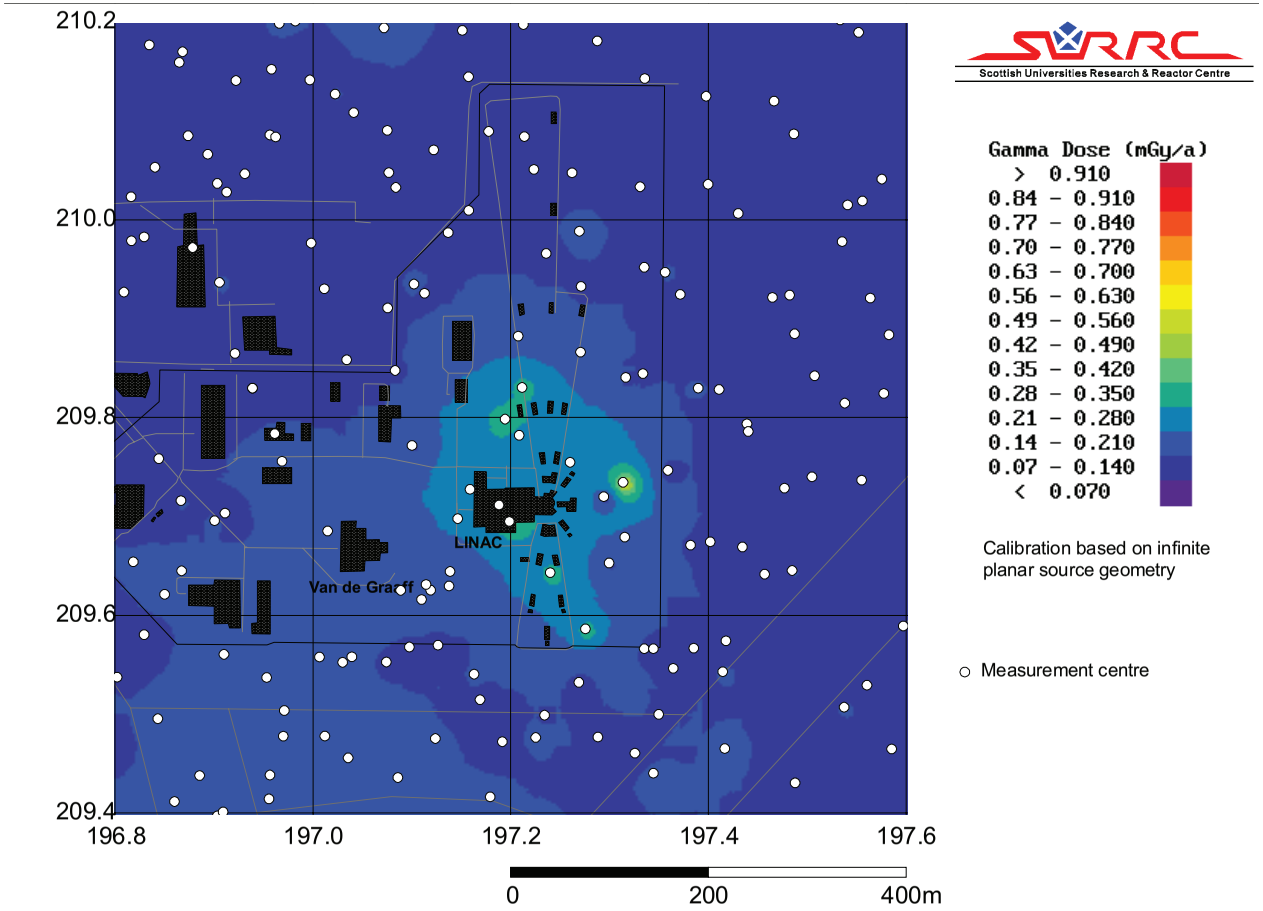

Figure C.24 Gamma-ray dose rate distribution around the IRMM site

5. IRE SITE

The distribution of anthropogenic activity is almost exclusively confined to the IRE site, with a small unidentified ^{137}Cs source to the north of the site. Outside the IRE site the radiation field is almost entirely natural, with a small contribution from ^{137}Cs that could be attributed to weapons testing fallout with a possible contribution from Chernobyl.

Activity on the site is associated with the radiochemistry laboratories and waste stores. Figure C.25 shows spectra. Again the merits of the combined NaI-Ge spectrometer are apparent. The Ge detector shows characteristic lines from ^{133}Xe, ^{131}I and ^{99}Mo at levels which cannot be readily distinguished using the NaI spectra. The anomalies present in the maps of ^{137}Cs and ^{60}Co and gamma dose rate in figures C.26, C.27 and C.28 based on NaI(Tl) spectra include contributions from these isotopes.

The site includes two potentially large radiation sources which do not contribute to the observed activity levels determined by the NaI(Tl) spectrometry system; a 30 MeV cyclotron and a 3 MCi ^{60}Co irradiator. An analysis was made of the low energy (<300 keV) component of the spectra recorded with the GMX spectrometer. Figure C.29 shows the net count rate for this part of the GMX spectra over the IRE site, which does show additional low energy features associated with the cyclotron and ^{60}Co irradiators. These signals are due to scattered radiation from very well shielded sources.

FIGURES

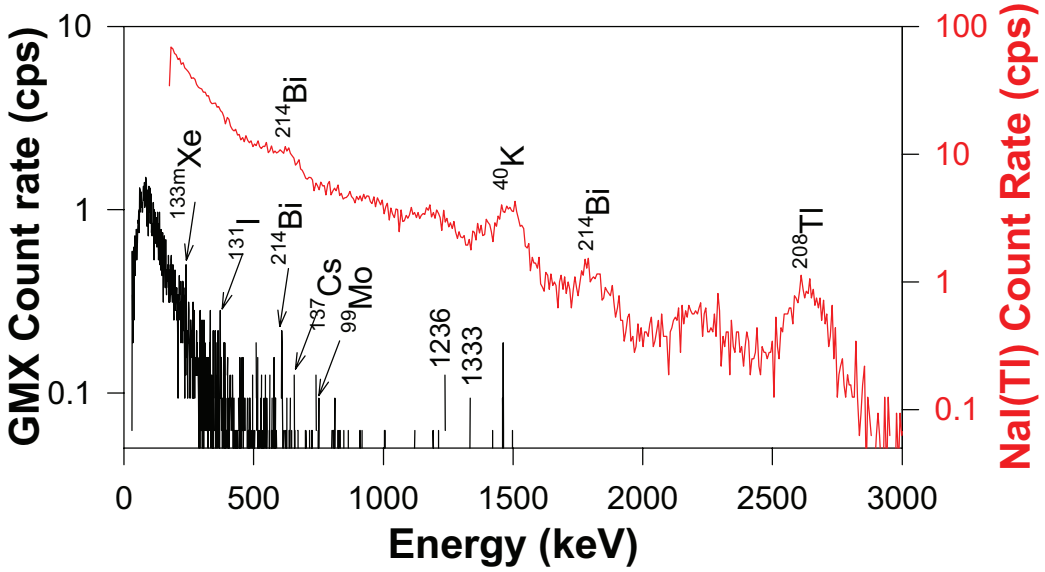

Figure C.25 Gamma-ray spectra from the IRE site

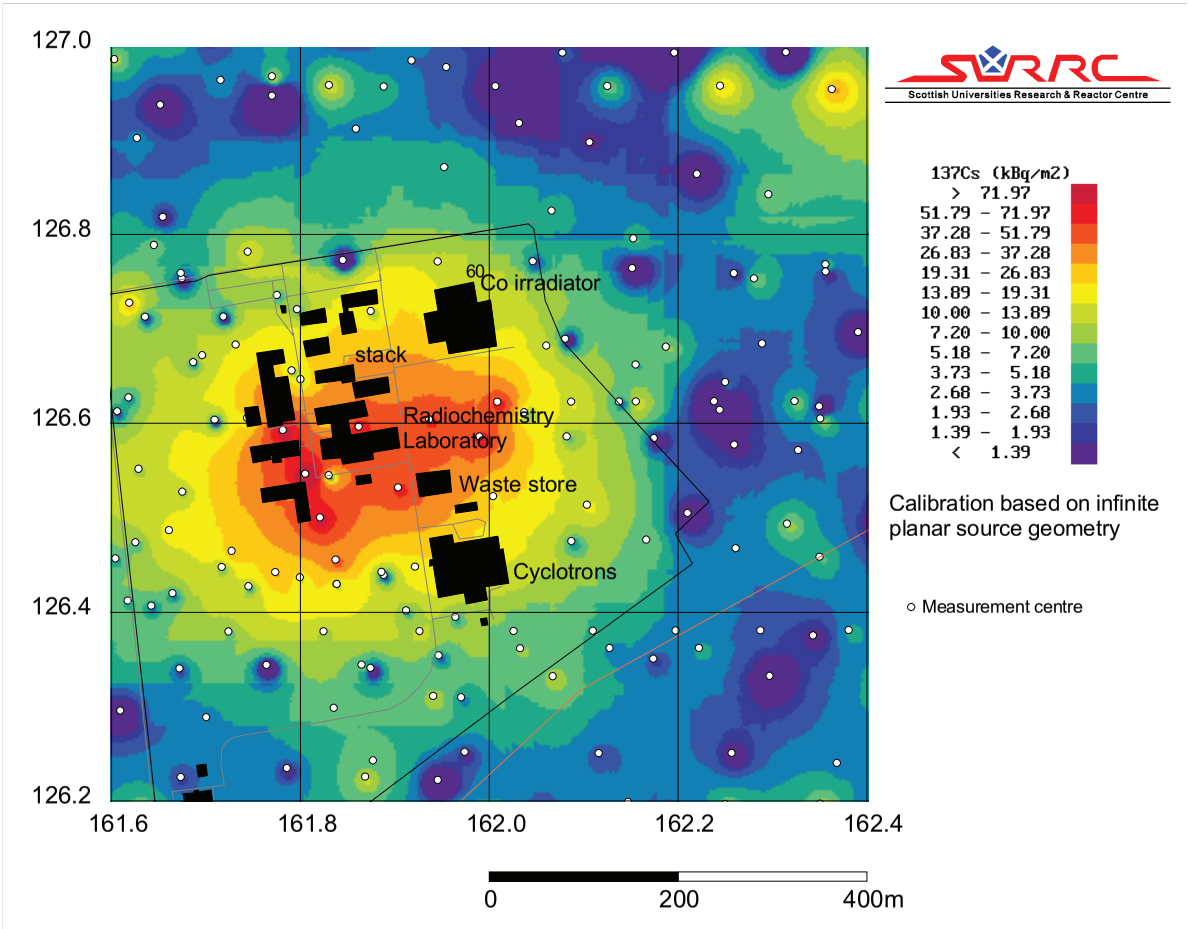

Figure C.26 ^{137}Cs signal distribution within the IRE site

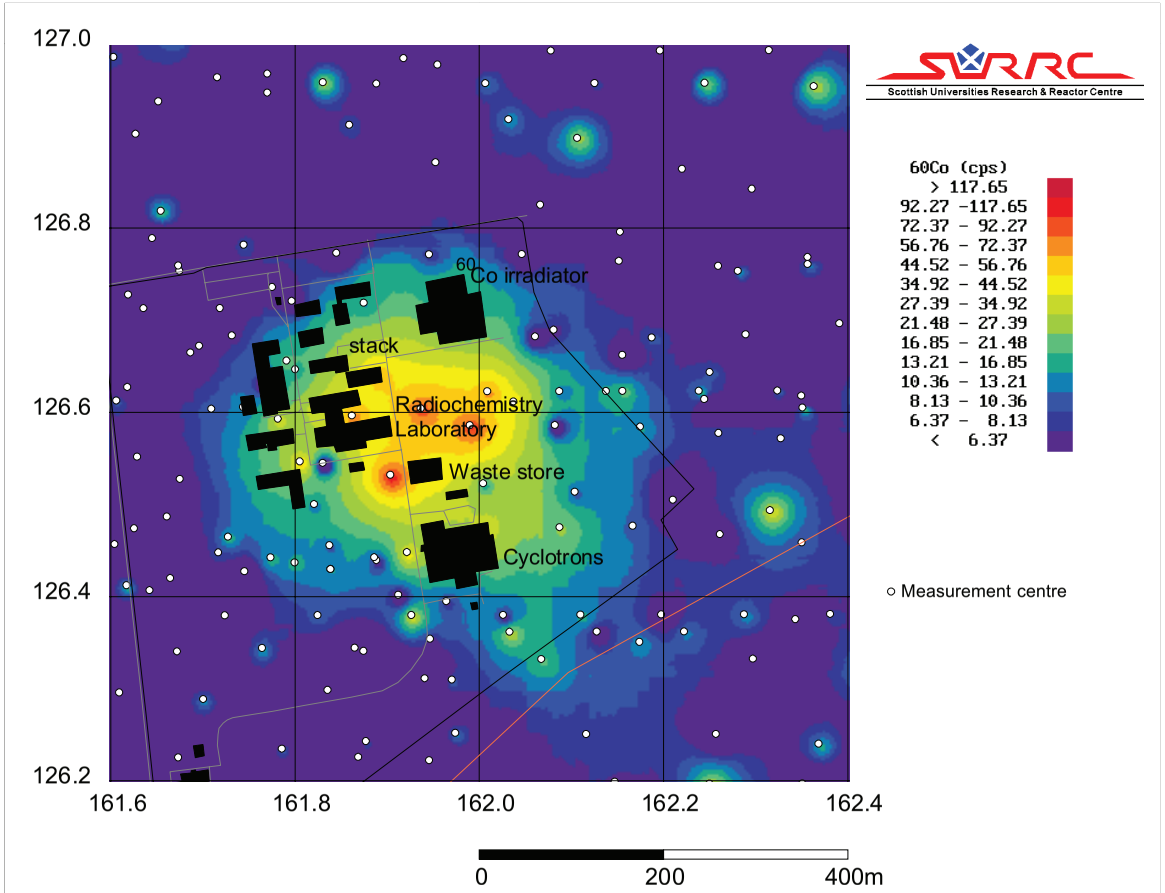

Figure C.27 ^{60}Co signal distribution within the IRE site. Note that the anomaly is not located above the shielded ^{60}Co irradiator. It may reflect the presence of other nuclides with photon emission in the 1-1.5 MeV energy range associated with the radiochemical laboratories or waste stores.

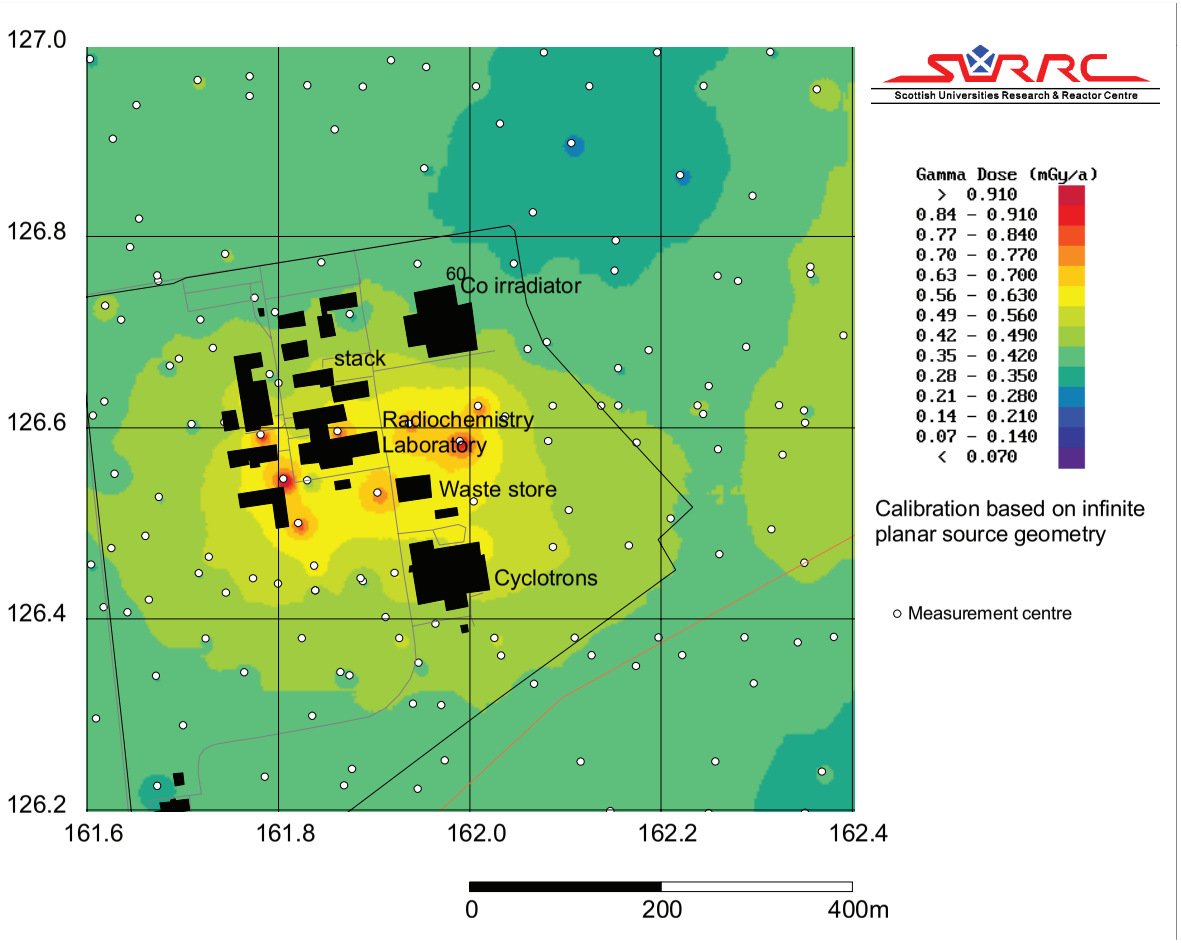

Figure C.28 Gamma-ray dose rate distribution within the IRE site

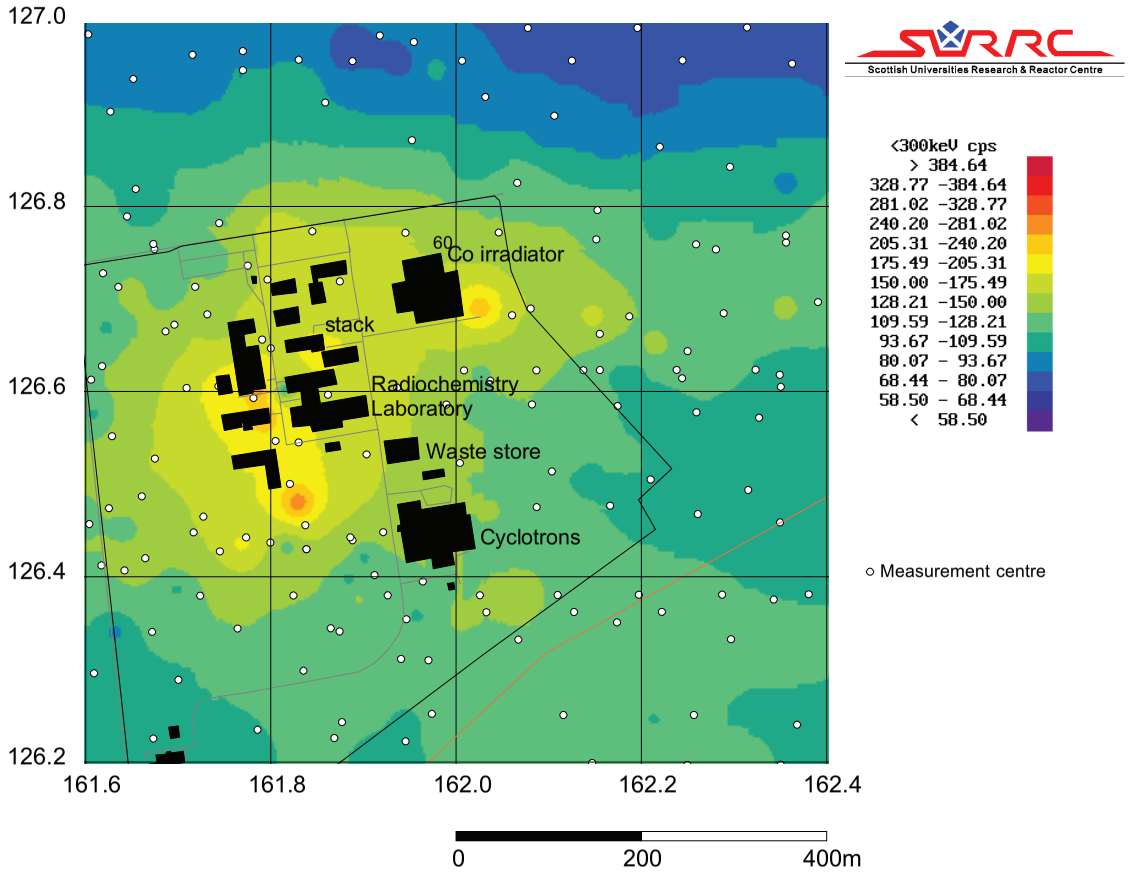

Figure C.29 Net counts in the GMX detector <300 keV within the IRE site